THEORETICAL ANALYSIS OF UNSTEADY SUPERSONIC FLOW AROUND HARMONICALLY OSCILLATING TURBOFAN CASCADES

A THESIS

Presented to

The Faculty of the Division of Graduate

Studies and Research

By

John Everett Caruthers

In Partial Fulfillment

of the Requirements for the Degree

of Doctor of Philosophy in the School of

Aerospace Engineering

Georgia Institute of Technology

September, 1976

THEORETICAL ANALYSIS OF UNSTEADY SUPERSONIC
FLOW AROUND HARMONICALLY OSCILLATING TURBOFAN CASCADES

Approved:

G. Alvin Pierce, Chairman

Warren C. Strahle

Howard M. McMahon

Date approved by Chairman: 8-20-76

ACKNOWLEDGMENTS

To my advisor, Dr. G. Alvin Pierce, I owe special thanks for a variety of reasons. For the many hours he spent in reviewing this thesis and his subsequent contribution to the quality of the work, I am greatly appreciative. Our many private conversations concerning theoretical aspects of aerodynamics have contributed greatly to my understanding and many of the ideas discussed may be found within this thesis. For his counsel and personal concern during my academic career at Georgia Tech I am truly grateful.

I also extend my thanks to the other members of the advisory committee, Dr. Howard M. McMahon and Dr. Warren C. Strahle for their comments and suggestions concerning the thesis.

I am indebted to Mr. Peter C. Tramm of Detroit Diesel Allison who made it possible for me to continue my education. I also gratefully acknowledge the financial assistance given me in support of this work by General Motors Corporation under their Graduate Fellowship program. Thanks are also due Mr. R. R. Allran, also of Detroit Diesel Allison, who supported and helped coordinate this effort.

I would also like to thank Mrs. Harlene Jacobs who typed the final draft of the thesis with a great deal of patience and a high spirit of cooperation. Thanks also to Mrs. Ruth Shaw whose instructions and suggestions concerning the format and typing of the thesis were very helpful.

Throughout my academic career my parents have always been a source of help and encouragement. This endeavor was no different. To my father who graduated from this institution thirty years ago and to my mother who is herself a teacher, and who gave me my first tablet and pencil, this accomplishment has special meaning. I am proud to be able to share it with them.

Lastly, I can here give only a first installment of thanks to my wife, Susan, who provided our primary financial support during this period and who also typed the rough draft of the thesis. If there has been a hardship over these years, it is she who has borne it. Her unfailing love and devotion have given this effort meaning. To our infant son, Brian, whose recent arrival made this task more rewarding yet more difficult, I say we look forward to your education.

I cannot rightfully close without giving considered and prayerful thanks to God upon whom I have called upon frequently for assistance during this pursuit. It is He

who ultimately gives purpose and meaning to all endeavor, including this one.

TABLE OF CONTENTS

LIST OF ILLUSTRATIONS

NOMENCLATURE

Roman Symbols

A	local steady state sound speed
a	local sound speed
a_∞	undisturbed sound speed far upstream
a'	perturbation in sound speed
$\hat{a}$	A/a_∞
a^*	$a' e^{-i\omega t}/a_\infty \delta$
a_j	coefficient defined by Equation (D-10)
B_1, B_2	coefficients in the finite difference system defined by Equations (84) and (85)
b	location of airfoil torsion axis non-dimensionalized with respect to c, positive in x direction
C_1, C_2, C_3	coefficients defined by Equations (60), (61), and (62)
C_ℓ	normalized perturbation lift coefficient
C_{ℓ_α}	complex lift coefficient for torsional oscillation about mid-chord

C_{ℓ_h}	complex lift coefficient for pure translational oscillation normal to the chord
C_{m_α}	complex moment coefficient for torsional oscillation about mid-chord
C_{m_h}	complex moment coefficient about mid-chord for pure translational oscillation normal to the chord
C_{M_α}	$C_{m_\alpha}(8/\pi k^2)$
C_p	normalized pressure coefficient, $(P - P_\infty) / (\frac{1}{2}\rho_\infty U_\infty{}^2 \delta)$
$C_p{}^*$	normalized pressure coefficient amplitude
c	chord
g	damping
h	airfoil translation amplitude
h'	h/c
$\tilde{h}$	unsteady translational displacement normal to airfoil chord = $h e^{i\omega t}$
h_1	$\frac{d\ell}{d\Gamma}$
h_2	$\frac{dn}{dX}$
$I_{m,n}$	integral as defined by Equation (D-2)

i	$\sqrt{-1}$
$\hat{i}$	unit vector in x direction
$\hat{j}$	unit vector in y direction
k	reduced frequency $= \frac{\omega c}{U_\infty}$
L^*	complex lift
ℓ	distance along coordinate Γ
ℓ'	ℓ/c
$\hat{\ell}$	unit vector in Γ direction
M	Mach number
M_∞	Mach number at ∞
M_n	component of Mach number normal to cascade inlet plane
M_Γ	local Mach number in stream direction
M^*	complex moment
N	number of periodicity iterations (or number of blades in the cascade)
N_1	number of the first solution to be used in evaluating $\bar{S}$

n	distance along coordinate χ
n'	n/c
$\hat{n}$	unit vector in χ direction (unit normal)
P	static pressure
$\overline{P}$	local steady value of static pressure
P'	perturbation in static pressure
P'^*	amplitude of perturbation pressure, $P' = P'^* e^{i\omega t}$
P_∞	static pressure at ∞
$\overline{q}$	velocity vector
q_x	velocity in x direction
q_y	velocity in y direction
q_Γ	velocity in Γ direction
q_χ	velocity in χ direction
q_s	steady velocity magnitude
$\overline{q}_r$	velocity relative to a point on moving airfoil surface
$\overline{q}_b$	velocity of airfoil surface

r	radius
S_n	solution at the n^{th} iteration
$\bar{S}$	arithmetic mean of S_n
s	cascade airfoil spacing
s'	normalized spacing = s/c
t	time
U_∞	steady streamwise relative velocity at ∞
U_a	component of upstream velocity normal to the cascade stagger line (along the compressor axis)
U_θ	component of upstream velocity parallel to the cascade stagger line
u	perturbation velocity in x direction
u^*	amplitude of the x component of the complex perturbation velocity
u_R, u_I	real and imaginary parts of u^*
$\bar{V}(\Gamma, \chi)$	steady velocity vector in (Γ,χ) coordinates
V_Γ	steady velocity in Γ direction
V_p	phase speed of cascade wave
v	perturbation velocity in y direction

v^*	amplitude of the y component of the complex perturbation velocity
v_R, v_I	real and imaginary parts of v^*
W_a	aerodynamic work/cycle
(x,y)	rectangular Cartesian coordinates
x'	normalized x coordinate, x/c
$\delta x'$	finite difference x' grid spacing
(x_o,y_o)	point on stationary airfoil surface
y'	normalized y coordinate, y/c
$\delta y'$	finite difference y' grid spacing
y_s	y coordinate of airfoil surface
y_s'	y_s/c

Greek Symbols

α	unsteady rotational amplitude
$\tilde{\alpha}$	unsteady rotational displacement, $\tilde{\alpha} = \alpha e^{i\omega t}$
β	interblade phase angle
γ	specific heat ratio

(Γ, χ)	orthogonal curvilinear coordinates lying along and perpendicular to the steady flow streamlines
$\hat{\gamma}$	airfoil surface point perturbation displacement vector
δ	nondimensional perturbation amplitude of airfoil motion
θ	cascade stagger angle
θ_s	airfoil surface angle measured to horizontal
θ_c	angle between Γ coordinate and horizontal
θ_R	perturbation solid body rotation of the airfoil
θ_b	phase angle between translational and rotational oscillation
λ	finite difference grid ratio
μ	angle between local velocity vector and Mach wave
ρ	density
$\bar{\rho}$	local steady value of density
ρ_∞	density at upstream
$\hat{\rho}$	$\bar{\rho}/\rho_\infty$

σ	cascade solidity c/s
τ	phase angle = ωt
ϕ	total nonlinear potential
ϕ'	perturbation potential
$\bar{\phi}$	complex perturbation potential amplitude
ϕ^*	normalized perturbation potential amplitude, $\bar{\phi}/U_\infty C\delta$
ϕ_R, ϕ_I	real and imaginary parts of ϕ
ϕ_s	steady nonlinear potential function
χ_s	χ coordinate of airfoil surface
ψ_R	real part of C_p^*
ψ_I	imaginary part of C_p^*
ω	frequency
$\bar{\omega}$	$(M_\infty^2/(M_\infty^2 + 1))\,k$

Operators

∇	gradient operation in (x,y) coordinates
∇_c	gradient operator in orthogonal curvilinear coordinates (Γ,χ)

∇^2	Laplacian operator in (x,y) coordinates
∇_c^2	Laplacian operator in orthogonal curvilinear coordinates (Γ, χ)
L	linear operator, $-2(i k + \frac{\partial}{\partial x'})$

SUMMARY

A solution method is developed for the supersonic cascade problem utilizing a finite-difference/pressure-amplitude-function technique. The method developed is valid for both the supersonic and subsonic leading edge problems, although developed specifically for the latter problem. Excellent agreement is obtained with existing solutions in all the limiting cases and the cascade results are compared with some recently published results using other methods. A parametric study is given of a typical supersonic cascade configuration.

The introduction of the pressure amplitude function as the primary independent variable rather than the velocity potential allows the exit region to be solved without explicit consideration of the wake. The objectionable numerical wake reflections of the characteristic discontinuities prevalent in the finite-difference-velocity potential method are shown to be eliminated by the present development.

The iterative technique developed for enforcement of the cascade periodicity conditions is shown to correspond precisely to adding one blade at a time to a finite cascade. The convergence of the method is in doubt at the

resonance points, but appears to converge slowly (at least in the sense of a mean) just away from resonance. Convergence well away from resonance is shown to be much more rapid.

Theoretical considerations are given for the extension of the linearized perturbation method to oscillatory flows under nonuniform steady flow conditions. The perturbation equations and boundary conditions are developed in natural orthogonal curvilinear coordinates yielding an equation very similar in form to the previous uniform steady flow case. Physical interpretations are given for the modified equation and boundary conditions.

CHAPTER I

INTRODUCTION

One of the most serious problems associated with the design of turbomachine compressors and fans has been that of self-excited blade vibration (i.e., flutter). This flutter may fall into three basic categories, stall or positive incidence flutter, choke or negative incidence flutter, and unstalled flutter. Stall flutter, as the name implies, occurs under conditions of partial or full flow separation over the low pressure surface of each airfoil. This happens under high loading conditions when the cascade of rotor airfoils is at high positive incidence or angle of attack (i.e., near the compressor steady state "surge" or stall line). Choke flutter, on the other hand, occurs at very low pressure ratios near the compressor "choke line" where the airfoils are operating at negative incidence thereby causing stream tube convergence and local sonic or choked flow.

Both stall and choke flutter occur at so called "off design" conditions away from the normal operating line or design point for the compressor and generally are only encountered during excursions near the steady operational limits of the compressor. Unstalled flutter,

however, may occur anywhere within the normal operational envelope of the compressor and indeed even at the design point itself. For this reason it is of utmost importance to know the unstalled flutter susceptibility of a given compressor blade row design as early as possible in the design process. Adjustments may then be made to the design (e.g., the addition of part span shrouds or use of composite materials) before the final design and testing stage after which such major redesign is prohibitively time consuming and expensive.

Although it has been shown both theoretically[1,2,3] and experimentally[4] that unstalled cascade flutter is possible in incompressible and subsonic compressible flow, Snyder[5] shows why it has not been a significant design problem for modern turbofans. However, the trend toward lighter weight, high stage pressure ratios, and greater efficiency has, from performance considerations, dictated higher rotational speeds with accompanying supersonic rotor tip Mach numbers and thin lower frequency supersonic blading. This has resulted in compressor/turbofan designs which are susceptible to supersonic unstalled flutter[5,6,7] thereby prompting a concerted effort toward the analysis of supersonic unsteady cascade flows.

The first such supersonic cascade analysis is due to Lane[8] who applied a Laplace transform method to the

case with supersonic axial flow (referred to as the supersonic leading edge locus case). The same problem was more recently solved by Platzer and Chalkley[9] who extended a method of characteristics procedure previously developed by Platzer and Pierce [10] for the purpose of studying supersonic wind tunnel wall interference. Unfortunately, the restriction of the above analyses to supersonic axial flow precludes its use in the analysis of present day compressors and turbofans where the condition exists of supersonic rotor relative flow with subsonic axial component. This condition gravely complicates the formulation and solution of the problem by requiring consideration of the infinity of cascade blades along with their inlet and exit flow fields, whereas only one blade channel need be considered in the former case.

Verdon [11] (1973) gave the first significant analytical treatment of the subsonic leading edge problem (i.e., supersonic relative flow with a subsonic axial component). The analysis is based on the linearized small disturbance velocity potential equations and considers the cascade of airfoils to be a cascade of flat plates. It also introduces the idea of an infinite cascade as the asymptotic limit of a finite cascade by considering the flow around only a finite number of blades. The solution

procedure used is a mixed analytical/finite-difference method. A Laplace transform solution is used in the inlet flow region and a finite difference technique is used in the interblade and exit flow regions. The results of this analysis show considerable irregularity in the pressure distribution over the aft portion of the blade pressure surface. The behavior of the solution near the acoustic cutoff or resonance [12,13] conditions is not discussed. More recently, Verdon and McCune [14] (1975) presented a more rigorous analytical treatment of this problem which eliminated the previous pressure irregularities but which failed to converge over the range of interblade phase angles lying between the acoustic resonance points.

Kurosaka [15] (1974) obtained a closed form solution of the same linearized flat plate problem by expanding the velocity potential in a power series of the frequency parameter and neglecting all terms above first order. Although mathematically appealing, the limitation of this approach to small frequency parameters severely restricts its applicability to typical high frequency turbofan blading.

Nagashima and Whitehead [16] have also published a solution of this problem obtained by a method of distributed pressure dipoles. The results show fair agreement

with other published results for particular cases, however, the analysis is restricted to very simple cascade flows which have at most one bow wave reflection within the blade channel.

Brix and Platzer [17] (1974) have extended the earlier work of Platzer and Chalkley[9] to the case of subsonic axial flow using Verdon's idea of a finite cascade simulation of an infinite cascade. Again no mention is made of the solution behavior near the acoustic cutoff conditions and no results are shown to illustrate the convergence of the method.

An inadequacy common to all the above mentioned analyses is the failure to consider potentially important steady field effects (e.g., the effect of finite blade camber, thickness, and back pressure). Even though typical supersonic fan blades are thin and of small camber, they may, nonetheless, possess a significant expansion and/or shock compression system. This, of course, is inconsistent with the assumption of uniform undisturbed steady flow used in the above analyses and none of these analyses may be easily extended to consider such effects. A good experimental example of the important effects of blade shape and back pressure on the supersonic unstalled flutter of a cascade is presented by Snyder[5] . Other recent experimental evidence [18] has indicated that in

certain cases these steady field effects may be of critical importance in determining the aerodynamic stability of the cascade. Ni [19] abandons this assumption of uniform undisturbed steady flow and attempts to solve the cascade problem for thick cambered airfoils with back pressure by applying a time marching finite difference method to the modified small perturbation equations. Although this analysis represents a reasonable approach to the totally subsonic problem, other critical considerations (e.g., shock translation and acoustic-disturbance/shock-wave interaction) must be made before such an analysis can be properly applied to the subsonic case with finite strength shock-expansion systems.

Another serious problem may also be encountered in the practical application of these two-dimensional flow analyses along the rotor blade span. At some point along the blade span it is possible, indeed even likely, that conditions exist which are at or near the previously mentioned (resonance) conditions. Under these conditions, the idea of the infinite cascade as the asymptotic limit of a finite cascade is subject to serious doubt and the convergence of the method in this region is not assured.

The purpose of this investigation is to develop a new solution procedure for the unsteady flat plate cascade problem under conditions of supersonic relative flow and

subsonic flow perpendicular to cascade stagger line. The finite difference solution procedure is developed in a form which might be readily adapted to the more complex problem of unsteady perturbation from a nonuniform flow. Theoretical consideration is given this problem with the equations and boundary conditions developed in a form most suitable for physical interpretation as well as numerical calculation.

CHAPTER II

THEORY

The Linearized Problem

The ultimate intent for the analysis presented herein is to provide aerodynamic force and moment coefficients for the supersonic outer span portion of a fan or compressor rotor. These coefficients, along with estimated structural damping and calculated or estimated aerodynamic damping for the remaining span of the rotor, are required for the determination of the flutter stability of the rotor dynamic system. The first assumption needed to reduce this problem to a tractable model relates to replacing the three dimensional flow field in the rotor by a series of two dimensional sections for which the aerodynamic properties are calculated independently. Considering the lack of a rigorous justification of this process, (sometimes referred to as "strip analysis"), confidence to proceed on the basis of this assumption derives from its successful application to high aspect ratio wings in aircraft wing flutter theory [20] and to the calculation of steady fan/compressor rotor flows. The two dimensional sections to be analyzed are also assumed to lie on cylindrical stream surfaces which

intersect the annular rotor cascade at the desired radial locations. This assumption allows the problem to be cast in a coordinate system rotating with the blades without having to allow for centrifugal and Coriolis effects. The next assumption, which shall be reconsidered in a later section, is that the supersonic rotor airfoil sections which are very thin and have little camber, may be replaced by flat plates at the same cascade stagger angle (θ as shown in Figure 1) and chord-to-spacing ratio, σ.

The problem has now been reduced, under the above assumptions, to the two-dimensional problem depicted in Figure 1 where the cylindrical surface has been "unwrapped" into an infinite cascade by requiring periodicity over intervals containing the same number of blades as is in the annular rotor. The inlet relative Mach number to the cascade for the flow regime under investigation is supersonic while the component of velocity in the direction of the compressor axis is less than sonic. This condition constitutes the so-called subsonic leading edge locus problem in analogy to the three-dimensional supersonic wing problem when the leading edge is swept behind the leading edge Mach cone.

Before proceeding with the development of the equations and boundary conditions governing the unsteady

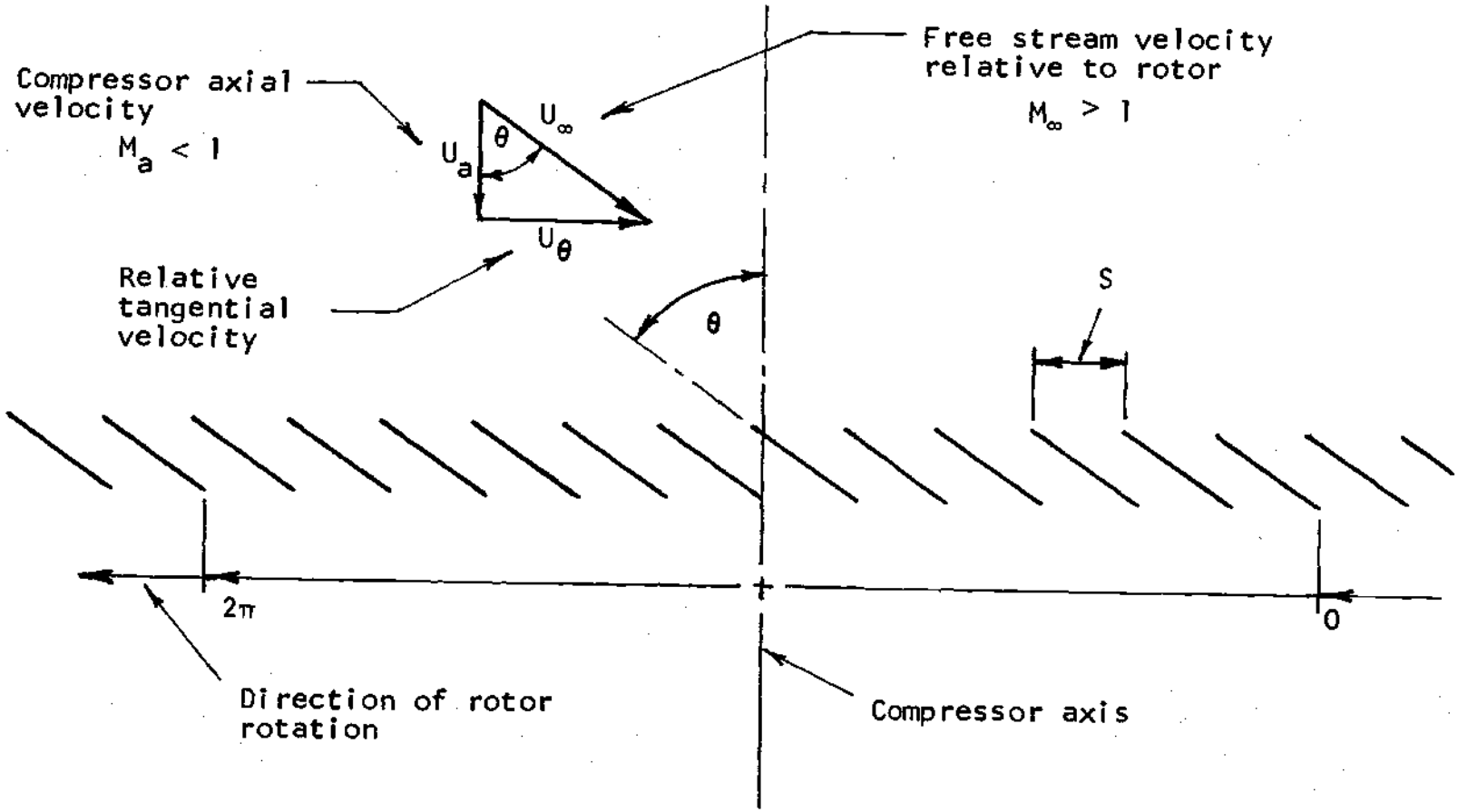

Figure 1. Schematic of an Infinite Flat Plate Cascade

cascade flow, it is convenient to list the assumptions which shall be used in the derivation including the assumptions used in reducing the problem thus far.

(1) The flow at any section is two-dimensional and lies entirely in a cylindrical stream surface.

(2) The blades are flat plates of zero thickness.

(3) The flow is inviscid, isentropic, and irrotational.

(4) The steady relative flow is uniform throughout the blade passage, which implies that the cascade has a pressure ratio of one. This assumption will be reconsidered later.

(5) The flow is supersonic.

(6) The blades are oscillating simple harmonically at small amplitude with a constant phasing between blades, β, such that $\beta N = 2n\pi$ where N is the number of blades in the rotor and n is an integer.

Assumption (3) allows the momentum and continuity equations to be combined in terms of a velocity potential, ϕ, and the local sound speed, a, as [21]

$$\nabla^2\phi = \frac{1}{a^2}\left[\frac{\partial^2\phi}{\partial t^2} + \frac{\partial}{\partial t}\left|\nabla\phi\right|^2 + \nabla\phi \cdot \nabla\left|\nabla\phi\right|^2/2\right] \qquad (1)$$

where

$$\nabla\phi = \bar{q} \tag{2}$$

now, under assumptions 4 and 6, let

$$\bar{q} = \nabla\phi = U_\infty \hat{i} + \nabla\phi' \quad \text{where} \quad |\nabla\phi'| \ll U_\infty \tag{3}$$

it is shown in Appendix A that the above small perturbation assumption along with the assumption that $\frac{\partial\phi'}{\partial t}$ and $\nabla\phi'$ are of the same order of magnitude implies that

$$a = a_\infty + a'$$

where

$$|a'| \ll a_\infty$$

In fact, a' may be written in terms of the velocity potential to first order (Appendix A) as

$$a' = -\frac{\gamma-1}{2a_\infty}\left[\frac{\partial\phi'}{\partial t} + U_\infty \frac{\partial\phi'}{\partial x}\right] \tag{4}$$

Substituting for ϕ and a in Equation (1) gives

$$\left(1 + \frac{2a'}{a_\infty} + \frac{a'^2}{a_\infty^2}\right) \nabla^2\phi' = \frac{1}{a_\infty^2}\left\{\frac{\partial^2\phi'}{\partial t^2} + \frac{\partial}{\partial t}\left[(U_\infty\hat{i} + \nabla\phi') \right.\right. \tag{5}$$

$$\left.\left. \cdot (U_\infty\hat{i} + \nabla\phi')\right] + \frac{(U_\infty\hat{i} + \nabla\phi')}{2} \cdot \nabla\left[(U_\infty\hat{i} + \nabla\phi') \cdot (U_\infty\hat{i} + \nabla\phi')\right]\right\}$$

or

$$\left(1 + \frac{2a'}{a_\infty} + \frac{a'^2}{a_\infty^2}\right)\nabla^2\phi' = \frac{1}{a_\infty^2}\left\{\frac{\partial^2\phi'}{\partial t^2}\ \frac{\partial}{\partial t}\ \left[\ 2U_\infty\ \frac{\partial\phi'}{\partial x} + \left(\frac{\partial\phi'}{\partial x}\right)^2 \right.\right. \tag{6}$$

$$\left. + \left(\frac{\partial\phi'}{\partial y}\right)^2\right] + (U_\infty\hat{i} + \nabla\phi') \cdot \left[U_\infty\ \frac{\partial^2\phi'}{\partial x^2}\ \hat{i} + U_\infty\ \frac{\partial^2\phi'}{\partial x\partial y}\ \hat{j}\right.$$

$$\left.\left. + \left(\frac{\partial\phi'}{\partial x}\ \frac{\partial^2\phi'}{\partial x^2} + \frac{\partial\phi'}{\partial y}\ \frac{\partial^2\phi'}{\partial x\partial y}\right)\hat{i} + \left(\frac{\partial\phi'}{\partial x}\ \frac{\partial^2\phi'}{\partial x\partial y} + \frac{\partial\phi'}{\partial y}\ \frac{\partial^2\phi'}{\partial y^2}\right)\hat{j}\right]\right\}$$

Neglecting only the third order terms in the perturbation quantities and collecting terms gives

$$\left[(1 - M_\infty^2) + \left(\frac{2a'}{a_\infty} - \frac{2M_\infty^2}{U_\infty}\ \frac{\partial\phi'}{\partial x}\right)\right]\frac{\partial^2\phi'}{\partial x^2} + \frac{\partial^2\phi'}{\partial y^2} = \tag{7}$$

$$\frac{1}{a_\infty^2}\left[\frac{\partial^2\phi'}{\partial t^2} + 2\left(U_\infty + \frac{\partial\phi'}{\partial x}\right)\frac{\partial^2\phi'}{\partial t\partial x} + 2U_\infty\ \frac{\partial\phi'}{\partial y}\ \frac{\partial^2\phi'}{\partial x\partial y} + 2\ \frac{\partial\phi'}{\partial y}\ \frac{\partial^2\phi'}{\partial t\partial y}\right.$$

$$\left. - 2a'a_\infty\ \frac{\partial^2\phi'}{\partial y^2}\right]$$

The second order terms on the right hand side are now neglected relative to the retained first order terms to give

$$\left[(1 - M_\infty^2) + \left(\frac{2a'}{a_\infty} - \frac{2M_\infty^2}{U_\infty}\frac{\partial\phi'}{\partial x}\right)\right]\frac{\partial^2\phi'}{\partial x^2} + \frac{\partial\phi'}{\partial y^2} \qquad (8)$$

$$= \frac{1}{a_\infty^2}\left(\frac{\partial^2\phi'}{\partial t^2} + 2U_\infty\frac{\partial^2\phi'}{\partial x\partial t}\right)$$

Equation (4) may be used to put Equation (8) in the more familiar "transonic" form

$$\left[(1 - M_\infty^2) - \left(\frac{\gamma-1}{a_\infty^2}\frac{\partial\phi'}{\partial t} + (\gamma + 1)\frac{M_\infty^2}{U_\infty}\frac{\partial\phi'}{\partial x}\right)\right]\frac{\partial^2\phi'}{\partial x^2} + \frac{\partial^2\phi'}{\partial y^2} \qquad (9)$$

$$= \frac{1}{a_\infty^2}\left(\frac{\partial^2\phi'}{\partial t^2} + 2U_\infty\frac{\partial^2\phi'}{\partial x\partial t}\right)$$

In order to neglect the remaining second order non-linear terms in Equation (9), it is necessary that the flow regime of interest be restricted such that

$$\left|1 - M_\infty^2\right| >> \left|\nabla\phi'\right|$$

This implies that the Mach number of the flow must not be too close to unity. Under this condition the governing equation takes the well known form

$$(1 - M_\infty^2)\frac{\partial^2\phi'}{\partial x^2} + \frac{\partial^2\phi'}{\partial y^2} - \frac{1}{a_\infty^2}\left(\frac{\partial^2\phi'}{\partial t^2} + 2U_\infty\frac{\partial^2\phi'}{\partial x\partial t}\right) = 0 \qquad (10)$$

Assuming a simple harmonic time variation

$$\phi'(x,y,t) = \bar{\phi}(x,y)\, e^{i\omega t}$$

where $\bar{\phi}(x,y)$ is the complex amplitude of the perturbation velocity potential, and using the following normalizations

$$x' = x/c$$
$$y' = y/c$$
$$\phi^* = \bar{\phi}/U_\infty c\,\delta$$
$$k = \omega c/U_\infty$$

where δ is the nondimensional perturbation amplitude, the linearized potential flow equation for $\phi^*(x',y')$ becomes

$$(1 - M_\infty^2)\frac{\partial^2\phi^*}{\partial x'^2} + \frac{\partial^2\phi^*}{\partial y'^2} - 2i M_\infty^2 k \frac{\partial\phi^*}{\partial x'} + M_\infty^2 k^2\phi^* = 0 \qquad (11)$$

As discussed previously the actual rotor section has been modeled in two dimensions by requiring that the entire flow field repeat after each section containing N blades. In other words, the N + 1 blade and the first blade are actually the same blade in the rotor so that the equivalent two-dimensional flow field is periodic. Since all the cascade blades are assumed to oscillate in simple harmonic fashion with a constant phase angle relative to the adjacent blade then the blade motion and

associated flow field are identical to the adjacent blade except that they are shifted in phase by the inter-blade phase angle, β. This allows consideration of a single blade channel such as shown in Figure 2 which consists of an upper and lower blade and hypothetical boundaries extended toward upstream and downstream infinity. The boundary conditions along the hypothetical boundaries are thus obtained from the periodicity condition which may be stated in terms of the complex amplitude of the nondimensional perturbation velocity potential as

$$\phi^*(x',y') = e^{i\beta}\phi^*(x' + s'\sin\theta, y' + s'\cos\theta) \quad (12)$$

The boundary condition for the airfoil surface is stated most simply by the condition that the component of the relative velocity vector, $\bar{q}_r$, normal to airfoil surface must vanish.

$$\bar{q}_r \cdot \hat{n} = 0 \quad (13)$$

where $\hat{n}$ is a unit vector normal to the airfoil surface. Now let a blade surface be described by

$$f(x,y,z,t) = 0 \quad (14)$$

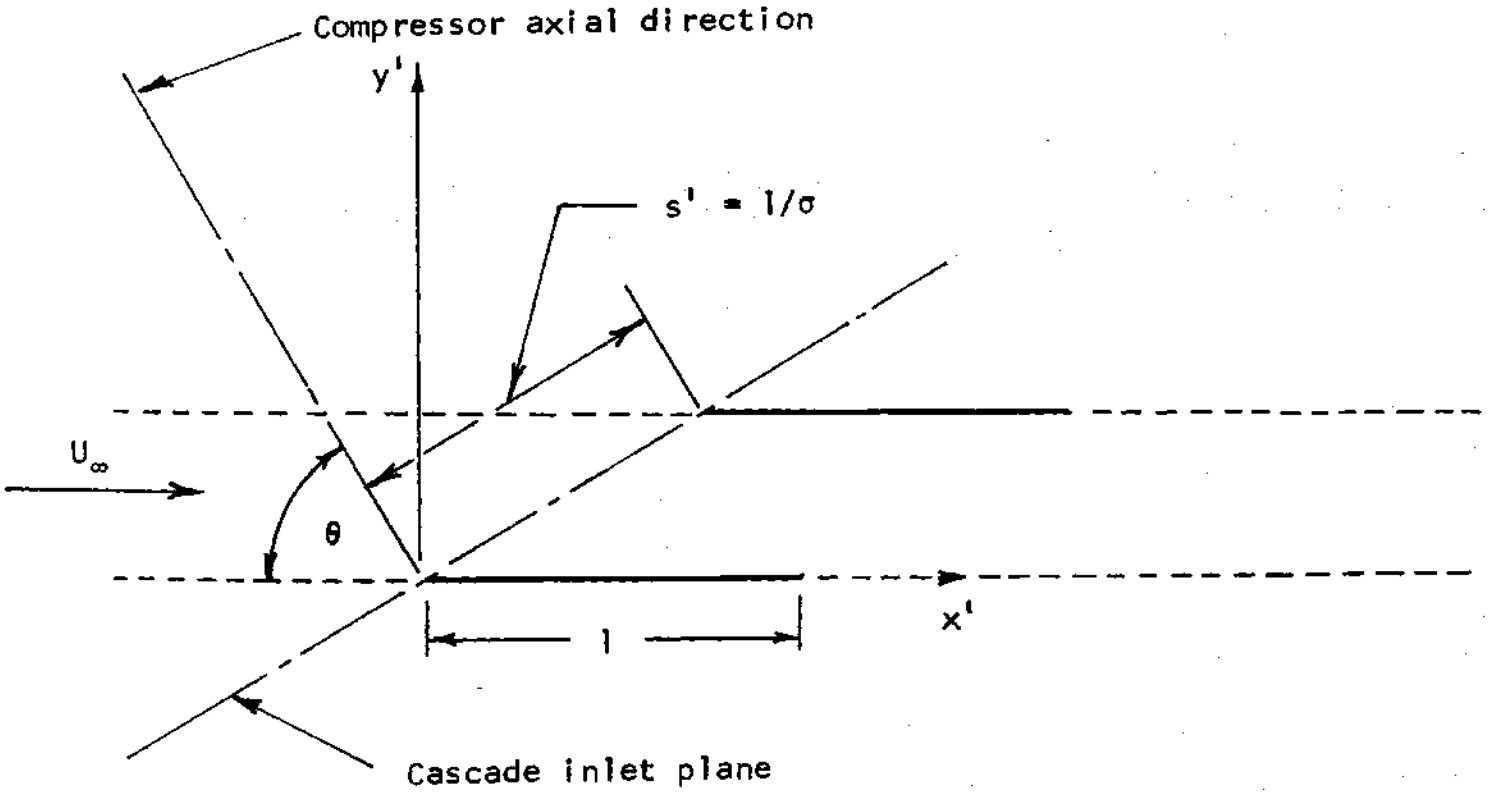

Figure 2. Isolated Blade Channel

where for two-dimensional flow $\frac{\partial f}{\partial z} = 0$. Equation (14) then implicitly defines

$$y = y_s(x,z,t) \tag{15}$$

or

$$f(x,y,z,t) = y - y_s(x,z,t) = 0 \tag{16}$$

Now

$$\hat{n} = \nabla f / |\nabla f|$$

and

$$\bar{q}_r = \bar{q} - \bar{q}_b$$

where $\bar{q}_b$ is the velocity of the airfoil surface, so that Equation (13) can be written as

$$(\bar{q} - \bar{q}_b) \cdot \nabla f = 0 \tag{17}$$

but

$$\frac{df}{dt} = \frac{\partial f}{\partial t} + \frac{\partial f}{\partial x}\frac{dx}{dt} + \frac{\partial f}{\partial y}\frac{dy}{dt} + \frac{\partial f}{\partial z}\frac{dz}{dt} = 0$$

or

$$\frac{\partial f}{\partial t} = - \bar{q}_b \cdot \nabla f \tag{18}$$

so that Equation (17) becomes

$$\frac{\partial f}{\partial t} + \bar{q} \cdot \nabla f = \frac{df}{dt} = 0 \tag{19}$$

which is the form given by Lamb [22].

Using Equation (16) the boundary condition for two-dimensional flow is written as

$$q_y(x,y_s) = \frac{\partial y_s}{\partial t} + q_x \frac{\partial y_s}{\partial x} \tag{20}$$

Note that this is the exact boundary condition which is to be applied at the airfoil surface which is assumed to be undergoing some unsteady motion at small amplitude. It is shown, however, that to first order approximation this boundary condition may be applied at the mean surface position. Expanding q_y in a double Taylor's series

$$q_y(x,y_s) = q_y(x_o,y_o) + \frac{\partial q_y}{\partial y}(y_s-y_o) + \frac{\partial q_y}{\partial x}(x-x_o) + \ldots \tag{21}$$

$$+ \left[0\right] \Delta x^2,\ \Delta y^2,\ \Delta x \Delta y$$

Since

$$q_x = U_\infty + \frac{\partial \phi'}{\partial x}$$

$$q_y = \frac{\partial \phi'}{\partial y}$$

then to second order in perturbation quantities

$$\left.\frac{\partial \phi'}{\partial y}\right|_{x,y_s} = \left.\frac{\partial \phi'}{\partial y}\right|_{x_o,y_o} + \frac{\partial^2 \phi'}{\partial y^2}(y_s - y_o) + \frac{\partial^2 \phi'}{\partial x \partial y}(x - x_o) \qquad (22)$$

but since

$$\Delta y = y_s - y_o$$

$$\Delta x = x - x_o$$

are themselves perturbation quantities, then to first order

$$\left.\frac{\partial \phi'}{\partial y}\right|_{x,y_s} = \left.\frac{\partial \phi'}{\partial y}\right|_{x,y_o} \qquad (23)$$

Substituting Equation (3) into the right hand side of Equation (20) and dropping second order terms in the perturbation quantities the linearized boundary condition for the airfoil surface becomes

$$\left.\frac{\partial \phi'}{\partial y}\right|_{x,y_o} = \frac{\partial y_s}{\partial t} + U_\infty \frac{\partial y_s}{\partial x} \qquad (24)$$

Assuming simple harmonic motion so that

$$y_s(x,t) = cy_s'(x,t) = c\bar{y}_s' e^{i\omega t} \tag{25}$$

the normalized boundary condition on the upper surface of the lower airfoil is

$$\left.\frac{\partial \phi^*}{\partial y'}\right|_{x',o} = \left(ik\bar{y}_s' + \frac{d\bar{y}_s'}{dx'} \right) \Big/ \delta \tag{26}$$

From the periodicity condition of Equation (12)

$$\left.\frac{\partial \phi^*}{\partial y'}\right|_{x',y'} = e^{i\beta} \left.\frac{\partial \phi^*}{\partial y'}\right|_{x'+s'\sin\theta,\, y'+s'\cos\theta} \tag{27}$$

thus the boundary condition on the lower surface of the upper airfoil is

$$\left.\frac{\partial \phi^*}{\partial y'}\right|_{x',s'\cos\theta} = e^{-i\beta} \left[ik\bar{y}_s' (x'-s'\sin\theta) + \frac{d\bar{y}_s'(x-s'\sin\theta)}{dx'} \right] \Big/ \delta \tag{28}$$

Although the airfoil surface boundary conditions of Equations (26) and (28) are applicable for any prescribed $\bar{y}_s'(x)$, only rigid body rotation and translation normal to the chord line (see Figure 3) will be considered here.

For this type of airfoil motion y_s' is given by

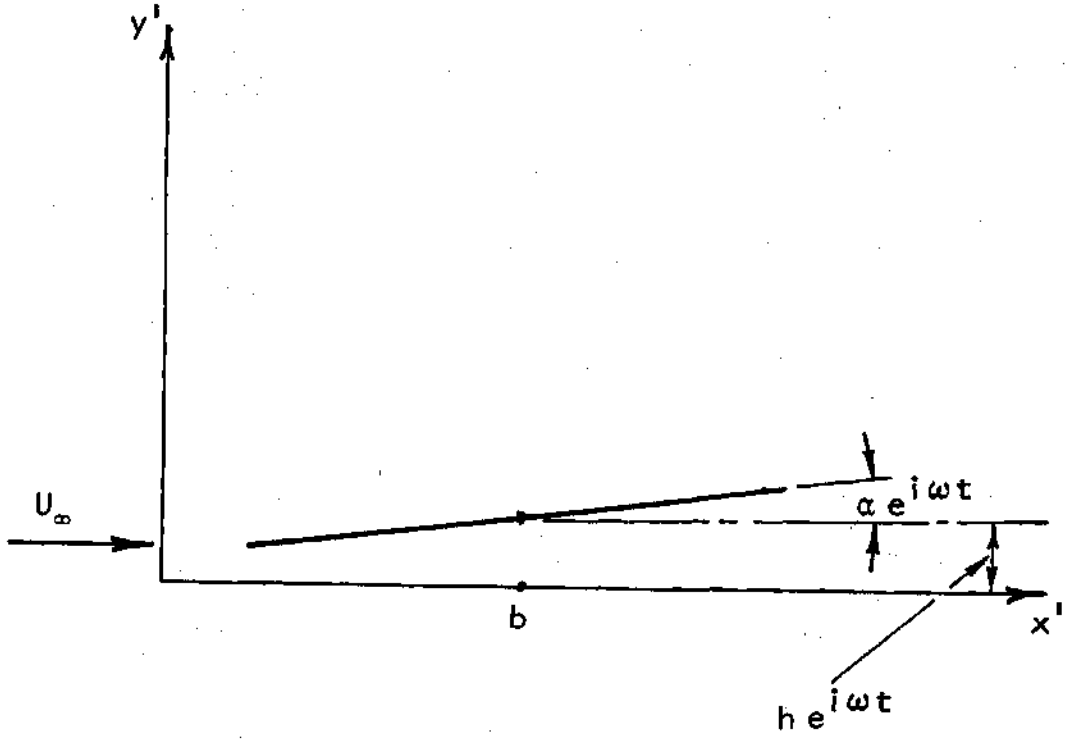

Figure 3. Rigid Body Motion of a Flat Plate

$$y_s'(x', t) = \left[\alpha(x' - b) + h'\right] e^{i\omega t} \tag{29}$$

where α is assumed to be small and $h' = h/c$ may be complex so that rotation and translation are not necessarily in phase. This slight complication in the boundary conditions may be avoided, however, without any loss in generality because the linearity of the governing equation and boundary conditions allow superposition of separate solutions for rotation and translation at any desired phase relationship. The boundary condition of the lower airfoil for rotation is then

$$\left.\frac{\partial \phi^*}{\partial y'}\right|_{x',o} = ik(x' - b) + 1 \tag{30}$$

where $\delta = \alpha$. For translation the boundary condition is

$$\left.\frac{\partial \phi^*}{\partial y'}\right|_{x',o} = ik \tag{31}$$

where $\delta = h'$. The boundary conditions for the upper airfoil surface are obtained through Equation (28) as

$$\left.\frac{\partial \phi^*}{\partial y'}\right|_{x',s'\cos\theta} = e^{-i\beta}\left[ik(x' - s'\sin\theta - b)\right] + 1 \tag{32}$$

for rotation and

$$\left.\frac{\partial \phi^*}{\partial y'}\right|_{x',s'\cos\theta} = ike^{-i\beta} \tag{33}$$

for translation.

Turning now to the consideration of the boundaries at infinity of Figure 2, it is not clear what conditions, if any, are appropriate and it is here that some attention must be devoted to the peculiar properties of the infinite supersonic cascade mathematical model. It is not appropriate to assume that the unsteady disturbances vanish at infinity since beyond the acoustic cutoff points (see Chapter III) these disturbances may appear at infinity even for supersonic relative flow. Notice that the domain of influence of a point lying at the cascade inlet bounded by its right and left running characteristics, includes the infinity of cascade blades lying above it. This situation is illustrated in Figure 4 and occurs whenever $M_n < 1$ while $M_\infty > 1$. It is clear that disturbances originating in the cascade inlet region may propagate infinitely far in front of the cascade while remaining within their characteristic or Mach wedges. It is therefore apparent that some form of radiation condition must be specified at infinity or some acoustic impedance distribution must be given at boundaries far upstream and downstream which would allow transmission of all the

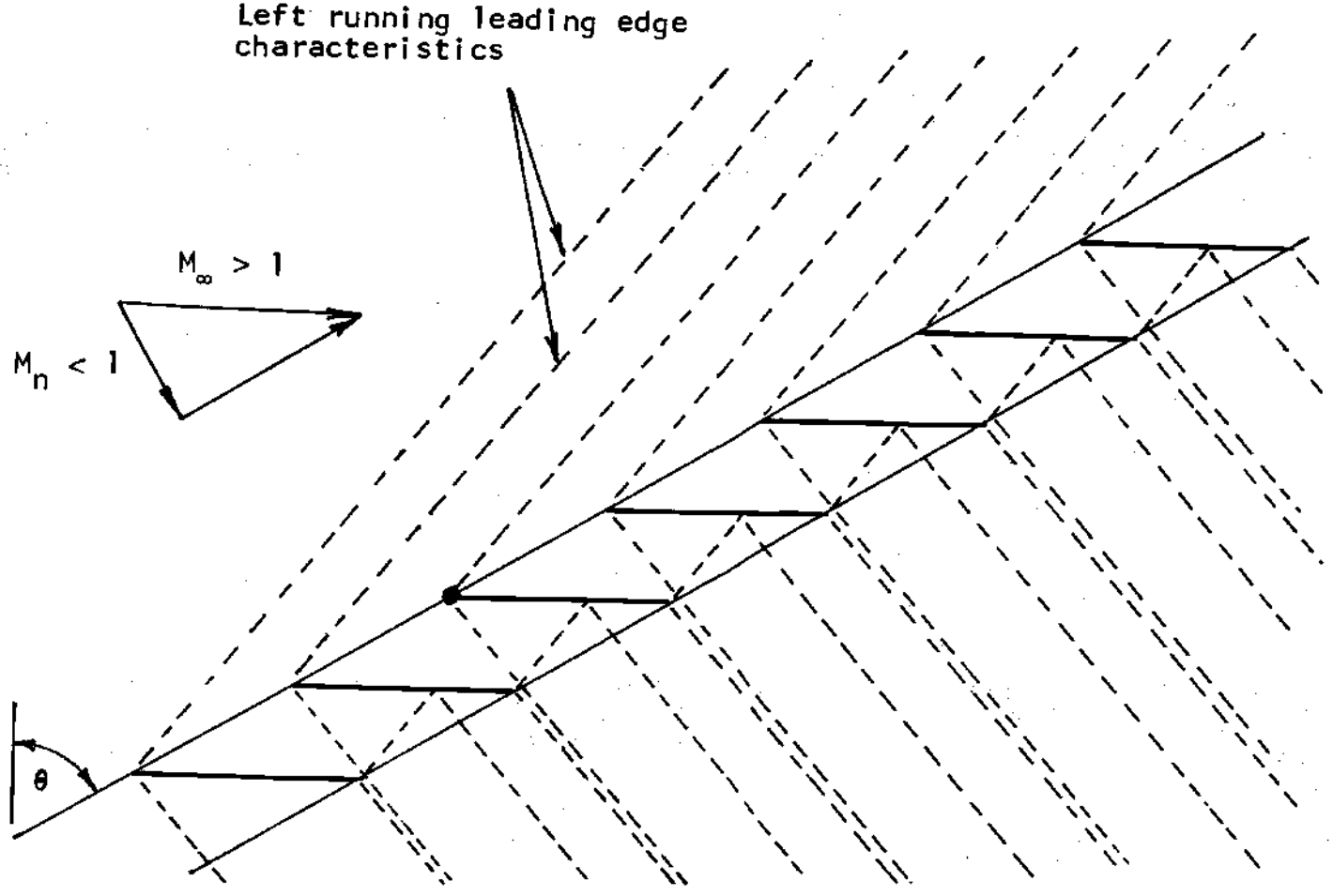

Figure 4. Supersonic Cascade with $M_n < 1$

incident waves.

The radiation condition at the far upstream and downstream boundaries and the periodicity condition, Equation (12), are thus necessary for the physical compatibility of the model and the original rotor problem. A difficulty arises here, however, since for $M_\infty > 1$ Equation (11) is hyperbolic in the entire domain and specification of upstream and downstream boundary conditions would now enclose this entire domain. This represents an improper mathematical specification [23] for equations of this type. One proper posing of this problem might be specification of Cauchy type data [23] along an upstream initial data line and removal of the downstream boundary condition while maintaining the same side boundary conditions. Although this now appears to represent a proper mathematical specification, there are two serious difficulties. First, from a practical point of view, no such initial data is known at any location since all of infinity is influenced by the cascade. Second, the existence of a periodic solution is not assured for arbitrary data given along the initial data line. This difficulty has not been totally resolved, however, it is believed that a relationship exists between the allowable upstream conditions and the existence of periodic solutions to the infinite cascade problem. This

situation has an analogy in steady supersonic cascade flow theory known as the unique incidence requirement [24]. It will be shown in Chapter III how this consideration leads naturally to the finite cascade simulation of the infinite cascade.

In addition to the difficulty described above, there are two other complications which are unique to unsteady cascade flows of this type and which require special considerations in the formulation of the solution procedure. The first is that the physical domain contains an infinite number of characteristics across which the perturbation velocities as well as the velocity derivatives are discontinuous. These lines of finite discontinuities originate at the leading and trailing edges of the airfoils and extend through all of space. The second complication arises from the fact that the unsteady convected vortex wakes which originate at the airfoil trailing edges influence every blade above them in the cascade. This is in contrast with the supersonic isolated airfoil where the wake cannot influence the upstream airfoil. As a result, the wakes must be considered in the calculation of the exit flow field which now contains an infinite number of lines across which the velocity potential itself is discontinuous. The condition of pressure continuity across the wake allows

this discontinuity to be calculated as follows.

The normalized pressure coefficient (Appendix B) may be written for uniform flow in terms of ϕ^* as

$$C_p^* = -2\left(ik\phi^* + \frac{\partial\phi^*}{\partial x'}\right) \tag{34}$$

Differencing Equation (34) above and below a wake yields

$$\Delta C_p^* = -2\left(ik\,\Delta\phi^* + \frac{\partial\,\Delta\phi^*}{\partial x'}\right) = 0 \tag{35}$$

Now along a wake at constant y' Equation (35) may be integrated to give

$$\Delta\phi^*_{wake} = e^{-ikx'}\,\Delta\phi^*_{trailing\ edge} \tag{36}$$

These wake discontinuities require explicit consideration in the velocity potential formulation and solution of the cascade problem. A more convenient formulation for this problem which does not require explicit handling of the wake discontinuities may be obtained in terms of the pressure amplitude function, C_p^*, which is equivalent to a pressure or acceleration potential. The governing equation for C_p^* may be obtained by direct application of the linear operator

$$L(\phi^*) = -2\left(ik + \frac{\partial}{\partial x'}\right)\phi^* = C_p^* \tag{37}$$

to the potential flow relation of Equation (11) and interchanging the order of the linear operators. The equation for C_p^* is obtained as

$$(1-M_\infty^2)\frac{\partial^2 C_p^*}{\partial x'^2} + \frac{\partial^2 C_p^*}{\partial y'^2} - 2iM_\infty^2 k \frac{\partial C_p^*}{\partial x'} + M_\infty^2 k^2 C_p^* = 0 \qquad (38)$$

The periodicity condition of Equation (12) yields

$$C_p^*(x',y') = e^{i\beta} Cp^*(x' + s'\sin\theta, y' + s'\cos\theta) \qquad (39)$$

The airfoil surface boundary conditions are obtained similarly by operating on Equations (30), (31), (32), and (33).

For rotation

$$\left.\frac{\partial C_p^*}{\partial y'}\right|_{x',o} = 2k^2(x' - b) - 4ik \qquad (40)$$

and

$$\left.\frac{\partial C_p^*}{\partial y'}\right|_{x',s'\cos\theta} = e^{-i\beta}\,(2k^2(x' - s'\sin\theta - b) - 4ik) \qquad (41)$$

For translation

$$\left.\frac{\partial C_p^*}{\partial y'}\right|_{x',o} = 2k^2 \tag{42}$$

and

$$\left.\frac{\partial C_p^*}{\partial y'}\right|_{x',s'\cos\theta} = 2k^2 e^{-i\beta} \tag{43}$$

Linearization for Non-Uniform Steady Flow

In the previous derivation, the steady flow field consisted of a constant uniform stream and the blades were approximated by flat plates (assumptions 2 and 4). The governing equations and boundary conditions are now derived for the velocity potential without resorting to these assumptions. Although shock waves are now allowed, they must still be sufficiently weak or straight enough so that assumption (3) applies.

Considerable simplification in the governing equations and boundary conditions can be achieved through transformation to an orthogonal curvilinear coordinate system (Γ, χ) with one set of coordinates lying along the steady flow streamlines as indicated in Figure 5. The full nonlinear potential equation in this system as derived in Appendix C can be written as

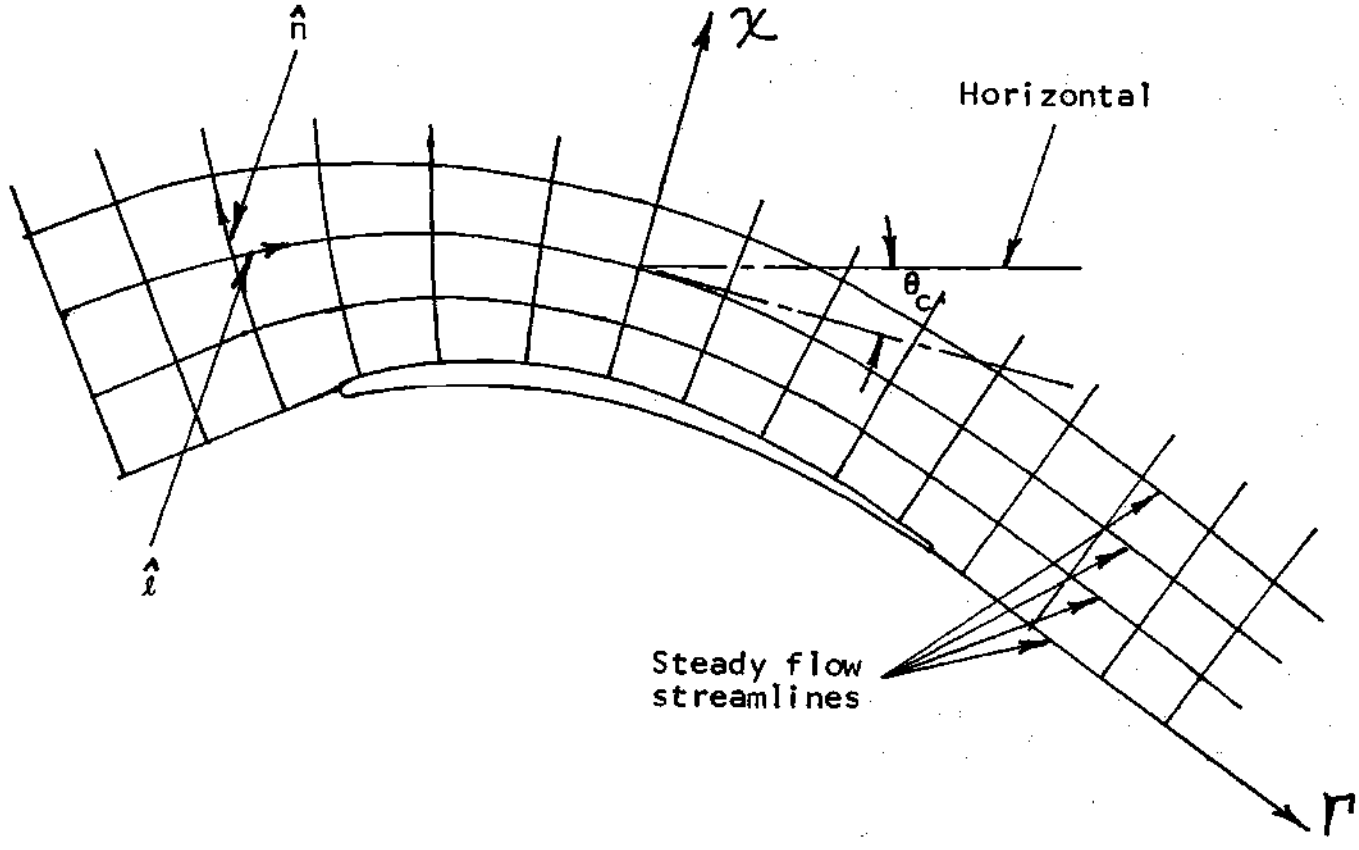

Figure 5. Natural Orthogonal Curvilinear Coordinates

$$\frac{\bar{\partial}^2\phi}{\bar{\partial}\ell^2} + \frac{\bar{\partial}^2\phi}{\bar{\partial}n^2} + \frac{\bar{\partial}\phi}{\bar{\partial}\ell}\frac{\bar{\partial}\theta_c}{\bar{\partial}n} - \frac{\bar{\partial}\phi}{\bar{\partial}n}\frac{\bar{\partial}\theta_c}{\bar{\partial}\ell} \tag{44}$$

$$= \frac{1}{a^2}\left[\frac{\partial^2\phi}{\partial t^2} + \frac{\partial q^2}{\partial t} + \bar{q} \cdot \nabla_c\,(q^2/2)\right]$$

where

$$\frac{\bar{\partial}}{\bar{\partial}\ell} = \frac{d\Gamma}{d\ell}\frac{\partial}{\partial\Gamma} \tag{45}$$

$$\frac{\bar{\partial}}{\bar{\partial}n} = \frac{d\chi}{dn}\frac{\partial}{\partial\chi} \tag{46}$$

$$\nabla_c = \hat{\ell}\frac{\partial}{\partial\ell} + \hat{n}\frac{\partial}{\partial n} \tag{47}$$

Also note that

$$\nabla_c{}^2 = \frac{\bar{\partial}^2}{\bar{\partial}\ell^2} + \frac{\bar{\partial}^2}{\bar{\partial}n^2} + \frac{\bar{\partial}\theta_c}{\bar{\partial}n}\frac{\bar{\partial}}{\bar{\partial}\ell} - \frac{\bar{\partial}\theta_c}{\bar{\partial}\ell}\frac{\bar{\partial}}{\bar{\partial}n} \tag{48}$$

As before, let the unsteady part of the potential be a small perturbation from the steady part, but let the steady part be a general nonlinear steady flow. Then

$$\bar{q} = \nabla_c\phi = \bar{V}(\Gamma,\chi) + \nabla_c\phi'(\Gamma,\chi,t) \tag{49}$$

where

$$\left| \nabla_c \phi' \right| << \left| \bar{V}(\Gamma,\chi) \right|$$

Since one coordinate lies in the steady stream direction

$$\bar{V}(\Gamma,\chi) = V_\Gamma \hat{\ell} \tag{50}$$

Also let a' be a small perturbation of the local sound speed so that

$$a(\Gamma,\chi,t) = A(\Gamma,\chi) + a'(\Gamma,\chi,t) \tag{51}$$

where

$$\left| a' \right| << \left| A \right|$$

Using Equations (49) and (51) in Equation (44) gives

$$(A^2 + 2Aa' + a'^2)\,(\nabla_c \cdot \bar{V} + \nabla_c{}^2\phi') = \frac{\partial \phi'}{\partial t^2} \tag{52}$$

$$+ \frac{\partial}{\partial t}\left(2V_\Gamma \frac{\bar{\partial}\phi'}{\bar{\partial}\ell} + \left| \nabla_c \phi' \right|^2 \right) + \frac{1}{2}(V_\Gamma \ell + \nabla_c \phi')$$

$$\cdot \nabla_c \left[V_\Gamma{}^2 + 2V_\Gamma \frac{\bar{\partial}\phi'}{\bar{\partial}\ell} + \left| \nabla_c \phi' \right|^2 \right]$$

Again restricting consideration to flows for which

$$\left| 1 - M_\Gamma{}^2 \right| >> \left| \nabla_c \phi' \right|$$

all second order terms in the perturbation quantities are neglected relative to the retained terms to give

$$A^2(\nabla_c \cdot \bar{V}) + (A^2 \nabla_c{}^2 \phi' + 2A(\nabla_c \cdot \bar{V})a') = \frac{\partial^2 \phi'}{\partial t^2} \tag{53}$$

$$+ 2V_\Gamma \frac{\partial}{\partial t}\left(\frac{\bar{\partial}\phi'}{\bar{\partial}\ell}\right) + V_\Gamma{}^2 \frac{\bar{\partial} V_\Gamma}{\bar{\partial}\ell} + V_\Gamma \frac{\bar{\partial} V_\Gamma}{\bar{\partial}\ell}\frac{\bar{\partial}\phi'}{\bar{\partial}\ell} + V_\Gamma{}^2 \frac{\bar{\partial}^2\phi'}{\bar{\partial}\ell^2}$$

$$+ \frac{1}{2} \nabla_c V_\Gamma{}^2 \cdot \nabla_c \phi'$$

Since ϕ' is a function of t and V_Γ is not, Equation (53) may be split into two parts with a separation function.

$$\nabla_c \cdot \bar{V} - V_\Gamma{}^2/A^2 \frac{\bar{\partial} V_\Gamma}{\bar{\partial}\ell} = f(\Gamma,\chi) \tag{54}$$

and

$$\nabla_c{}^2\phi' - M_\Gamma{}^2 \frac{\bar{\partial}^2\phi'}{\bar{\partial}\ell^2} + 2(\nabla_c \cdot \bar{V})\, a'/A = \frac{1}{A^2}\left[\frac{\partial^2\phi'}{\partial t^2}\right. \tag{55}$$

$$\left. + 2V_\Gamma \frac{\partial}{\partial t}\left(\frac{\bar{\partial}\phi'}{\bar{\partial}\ell}\right) + \frac{1}{2}\frac{\partial V_\Gamma{}^2}{\bar{\partial}\ell}\frac{\partial\phi'}{\bar{\partial}\ell} + \frac{1}{2}\nabla_c V_\Gamma{}^2 \cdot \nabla_c\phi'\right] - f(\Gamma,\chi)$$

However $f(\Gamma,\chi)$ is equal to zero since Equation (54) is the steady flow equation in the natural coordinate system for V_Γ which is completely uncoupled from the unsteady equation. Replacing a' is Equation (55) from Equation

(A-5) of Appendix A the perturbation potential equation becomes

$$\nabla_c^2\phi' - M_T^2 \frac{\bar{\partial}^2\phi'}{\bar{\partial}\ell^2} - 1/A^2\left[\frac{\partial^2\phi'}{\partial t^2} + 2V_T \frac{\partial}{\partial t}\left(\frac{\bar{\partial}\phi'}{\bar{\partial}\ell}\right)\right] = \tag{56}$$

$$1/A^2\left[\frac{1}{2}\frac{\bar{\partial}V_T^2}{\bar{\partial}\ell}\frac{\bar{\partial}\phi'}{\bar{\partial}\ell} + \frac{1}{2}\nabla_c V_T^2 \cdot \nabla_c\phi' + (\gamma-1)(\nabla_c\cdot\bar{V})\left(\frac{\partial\phi'}{\partial t} + V_T\frac{\bar{\partial}\phi'}{\bar{\partial}\ell}\right)\right]$$

Again assuming a simple harmonic time variation, the equation for the normalized perturbation potential amplitude is

$$(1-M_T^2)\frac{\bar{\partial}^2\phi^*}{\bar{\partial}\ell'^2} + \frac{\bar{\partial}^2\phi^*}{\bar{\partial}n'^2} + \frac{\bar{\partial}\theta_c}{\bar{\partial}n'}\frac{\bar{\partial}\phi^*}{\bar{\partial}\ell'} - \frac{\bar{\partial}\theta_c}{\partial\ell'}\frac{\partial\phi^*}{\partial n'} \tag{57}$$

$$+ k^2M_\infty^2\phi^* - 2ik\frac{M_T M_\infty}{\hat{a}}\frac{\bar{\partial}\phi^*}{\partial\ell'} = \frac{1}{A^2}\left[\frac{1}{2}\frac{\bar{\partial}V_T^2}{\bar{\partial}\ell'}\frac{\bar{\partial}\phi^*}{\bar{\partial}\ell'}\right.$$

$$\left. + \frac{1}{2}\nabla_c' V_T^2 \cdot \nabla_c'\phi^* + (\gamma-1)(\nabla_c'\cdot\bar{V})\left(iU_\infty k\phi^* + V_T\frac{\bar{\partial}\phi^*}{\bar{\partial}\ell'}\right)\right]$$

where

$$\nabla_c' \equiv \hat{\ell}\frac{\bar{\partial}}{\bar{\partial}\ell'} + \hat{n}\frac{\bar{\partial}}{\bar{\partial}n'} \tag{58}$$

Collecting terms, the equation may be rewritten as

$$(1-M_\Gamma^2)\frac{\bar{\partial}^2\phi^*}{\bar{\partial}\ell'^2}+\frac{\bar{\partial}^2\phi^*}{\bar{\partial}n'^2}+C_1(\Gamma,\chi)\frac{\bar{\partial}\phi^*}{\bar{\partial}\ell'}+C_2(\Gamma,\chi)\frac{\bar{\partial}\phi^*}{\bar{\partial}n'} \tag{59}$$

$$+C_3(\Gamma,\chi)\phi^*=0$$

where

$$C_1(\Gamma,\chi)=-\frac{2ikM_\infty M_\Gamma}{\hat{a}}+\frac{\bar{\partial}\theta_c}{\bar{\partial}n'}-\frac{1}{A^2}\frac{\bar{\partial}V_\Gamma^2}{\bar{\partial}\ell'}-(\gamma-1)V_\Gamma(\nabla_c'\cdot\bar{V}) \tag{60}$$

$$C_2(\Gamma,\chi)=-\frac{\bar{\partial}\theta_c}{\bar{\partial}\ell'}-\frac{1}{2A^2}\frac{\bar{\partial}V_\Gamma^2}{\bar{\partial}n'} \tag{61}$$

$$C_3(\Gamma,\chi)=\frac{M_\infty^2k^2}{\hat{a}^2}-ik(\gamma-1)(\nabla_c'\cdot\bar{V})\frac{U_\infty}{A^2} \tag{62}$$

are considered known functions of the steady nonlinear velocity field.

Notice the similarity of Equation (59) to the previous form, Equation (11). The equation remains linear, but now the coefficients are variable. If

$$\bar{V}=U_\infty\hat{i}$$

then Equation (59) reduces identically to Equation (11). Physically the variations of local Mach number, sound speed, and flow direction alter the speed, direction, shape, and intensity of the spreading acoustic disturbances.

This is reflected in the solution for ϕ^* through the dependence of the coefficients of the governing equation on the steady flow field. Examination of Equation (59) for the presently considered hyperbolic case ($M_T > 1$) reveals that its physical characteristics [25] are identical with those of the steady flow being inclined at $\pm \mu$ relative to the steady flow velocity vector where

$$\mu = \mathrm{Sin}^{-1} 1/M_T$$

This verifies the physically expected result that the acoustic disturbances are confined to the same domains of influence as are the steady flow disturbances. The hodograph characteristics, on the other hand, are determined by both the coefficients of the higher order derivatives and by the remaining lower order terms. These terms prevent "simple wave" solutions of Equation (59) or Equation (11) for that matter, and are responsible for the wave like variation and decay of the disturbances along and behind the physical characteristics.

One of the most significant of the nonuniform steady field effects is also the most subtle. The effect is introduced through the appearance of an extra term in the unsteady boundary conditions which may be thought of as serving to translate the steady field with the moving airfoil surfaces.

For the development of the boundary conditions, consider a general motion of an arbitrarily shaped airfoil surface in the previously described (Γ,χ) coordinate system (See Figure 6). Let the airfoil surface be described by

$$f(\Gamma,\chi,t) = 0 \tag{63}$$

which implicity gives

$$f(\Gamma,\chi,t) = \chi - \chi_s(\Gamma,t) = 0 \tag{64}$$

and the boundary condition from Equation (20) is

$$\frac{df}{dt} = 0$$

which expanded in these coordinates gives

$$\frac{\partial f}{\partial t} + \frac{1}{h_1} q_\Gamma \frac{\partial f}{\partial \Gamma} + \frac{1}{h_2} q_\chi \frac{\partial f}{\partial \chi} = 0 \tag{65}$$

or, using Equation (64)

$$- \frac{\partial \chi_s}{\partial t} - \frac{q_\Gamma}{h_1} \frac{\partial \chi_s}{\partial \Gamma} + \frac{q_\chi}{h_1} = 0 \tag{66}$$

Rearranging gives

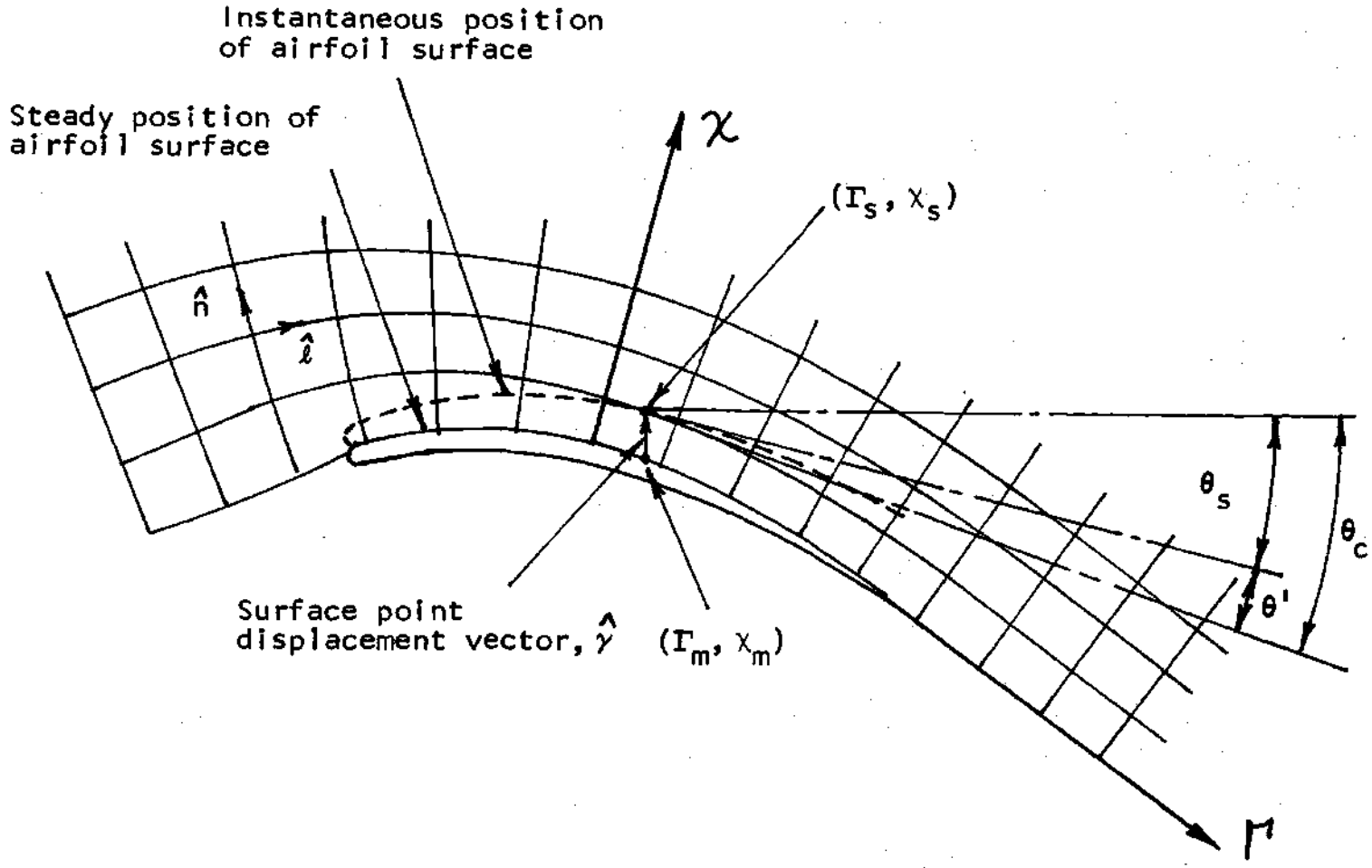

Figure 6. Displacement of Airfoil Surface in (Γ, χ) Coordinates

$$q_\chi = h_2\left(\frac{\partial \chi_s}{\partial t} + \frac{1}{h_1} q_\Gamma \frac{\partial \chi_s}{\partial \Gamma}\right) = h_2\left(\frac{\partial \chi_s}{\partial t} + q_\Gamma \frac{\bar{\partial} \chi_s}{\partial \ell}\right) \quad (67)$$

Referring to Figure 6 the angle between the instantaneous surface and coordinate directions, θ', is given by

$$\theta' = \theta_s - \theta_c = \mathrm{Tan}^{-1}\left(h_2 \frac{\bar{\partial} \chi_s}{\partial \ell}\right) \quad (68)$$

so the exact boundary condition to be applied at the moving airfoil surface is

$$q_\chi = h_2 \frac{\partial \chi_s}{\partial t} + q_\Gamma \tan \theta' \quad (69)$$

With the small perturbation assumption

$$\theta' \simeq \tan \theta' = h_2 \frac{\bar{\partial} \chi_s}{\bar{\partial} \ell} \quad (70)$$

Since

$$V_\chi \equiv 0$$

then

$$q_\chi = V_\chi + \frac{\bar{\partial} \phi'}{\bar{\partial} n} = \frac{\bar{\partial} \phi'}{\bar{\partial} n} \quad (71)$$

and also

$$q_\Gamma = V_\Gamma + \frac{\partial \bar{\phi}'}{\partial \ell} \tag{72}$$

so that to first order approximation in perturbation quantities the boundary condition at the airfoil surface becomes

$$\left.\frac{\partial \phi'}{\partial n}\right|_{\Gamma_s, \chi_s} = h_2 \frac{\partial \chi_s}{\partial t} + V_\Gamma(\theta_s - \theta_c)\Big|_{\Gamma_s, \chi_s} \tag{73}$$

Now for rigid body motion the instantaneous surface angle,

$$\theta_s \Big|_{\Gamma_{s,t}}$$

may be given as the sum of the unperturbed steady surface angle,

$$\theta_c \Big|_{\Gamma_m, \chi_m}$$

plus an unsteady angle perturbation, $\theta_R(t)$, so that

$$\theta_s(\Gamma,t)\Big|_{\Gamma_s} = \theta_c(\Gamma,\chi)\Big|_{\Gamma_m,\chi_m} + \theta_R(t) \tag{74}$$

It is desirable to apply the boundary condition along a fixed boundary in (Γ,χ) rather than on a surface in (Γ,χ,t).

This is accomplished by substituting Equation (74) into the boundary condition, Equation (73), and expanding the remaining terms in a double Taylor's series from the unperturbed steady surface position. To first order in $(\Delta\Gamma, \Delta\chi)$ the result is

$$\left.\frac{\partial\bar{\phi}'}{\partial n}\right|_{\Gamma_m,\chi_m} + \frac{\partial}{\partial\Gamma}\left(\left.\frac{\partial\bar{\phi}'}{\partial n}\right|_{\Gamma_m,\chi_m}\right)\Delta\Gamma + \frac{\partial}{\partial\chi}\left(\left.\frac{\partial\bar{\phi}'}{\partial n}\right|_{\Gamma_m,\chi_m}\right)\Delta\chi \qquad (75)$$

$$= h_2\left.\frac{\partial\chi_s}{\partial t}\right|_{\Gamma_m,\chi_m} + \frac{\partial}{\partial\Gamma}\left(h_2\frac{\partial\chi_s}{\partial t}\right)\Big|_{\Gamma_m,\chi_m}\Delta\Gamma + \frac{\partial}{\partial\chi}\left(h_2\frac{\partial\chi_s}{\partial t}\right)\Big|_{\Gamma_m,\chi_m}\Delta\chi$$

$$+\left[\left.V_\Gamma\right|_{\Gamma_m,\chi_m} + \left.\frac{\partial V_\Gamma}{\partial\Gamma}\right|_{\Gamma_m,\chi_m}\Delta\Gamma + \left.\frac{\partial V_\Gamma}{\partial\chi}\right|_{\Gamma_m,\chi_m}\Delta\chi\right]\left[\left.\theta_c\right|_{\Gamma_m,\chi_m} +\right.$$

$$\left.\theta_R - \left(\left.\theta_c\right|_{\Gamma_m,\chi_m} + \left.\frac{\partial\theta_c}{\partial\Gamma}\right|_{\Gamma_m,\chi_m}\Delta\Gamma + \left.\frac{\partial\theta_c}{\partial\chi}\right|_{\Gamma_m,\chi_m}\Delta\chi\right)\right]$$

Dropping second order terms in perturbation quantities and simplifying gives

$$\left.\frac{\partial\bar{\phi}'}{\partial n}\right|_{\Gamma_m,\chi_m} = h_2\left.\frac{\partial\chi_s}{\partial t}\right|_{\Gamma_m,\chi_m} + V_\Gamma\,\theta_R(t)\Big|_{\Gamma_m,\chi_m} + V_\Gamma\frac{d\theta_c}{d\gamma}\Delta\gamma\Big|_{\Gamma_m,\chi_m} \qquad (76)$$

where the last term is expressed in terms of the total derivative in the direction of the surface perturbation displacement (Figure 6) as

$$\frac{d\theta_c}{d\gamma}\Delta\gamma = \frac{\partial\theta_c}{\partial\Gamma}\Delta\Gamma + \frac{\partial\theta_c}{\partial\chi}\Delta\chi \qquad (77)$$

The first two terms on the right hand side of Equation (76) are familiar and are completely analogous to the corresponding terms in the unsteady boundary condition with uniform steady flow, Equation (24). The first term is simply the component of the airfoil velocity normal to its surface. The second term is the induced normal velocity due to a change in surface angle. The third term, which did not appear in the former case, is due to unsteady translation of the airfoil surface through the steady vector field, $\bar{V}(\Gamma,\chi)$.

CHAPTER III

THE SOLUTION METHOD

The Numerical Procedure

The choice of the solution method for the supersonic flat plate cascade model is influenced by a desire to choose a method which might be readily extended to treat the more general perturbation problem developed in the last section. Since finite difference methods are ideally suited to treatment of equations of this type, this method was chosen.

Consider the governing equation for the complex pressure amplitude function C_p^* which can be split into real and imaginary parts as

$$C_p^* = \psi_R + i\psi_I \tag{78}$$

Then Equation (38) may be split into the coupled equations

$$(1-M_\infty^2)\frac{\partial^2\psi_R}{\partial x'^2} + \frac{\partial^2\psi_R}{\partial y'^2} + 2M_\infty^2 k\frac{\partial\psi_I}{\partial x'} + M_\infty^2 k^2\psi_R = 0 \tag{79}$$

and

$$(1-M_\infty^2)\frac{\partial^2\psi_I}{\partial x'^2} + \frac{\partial^2\psi_I}{\partial y'^2} - 2M_\infty^2 k\frac{\partial\psi_R}{\partial x'} + M_\infty^2 k^2\psi_I = 0 \tag{80}$$

The second order finite difference approximations of these equations at a point (m,n) in the grid network of Figure (7) are obtained by substituting the appropriate difference representations of the derivatives. These difference equations are

$$(1-M_\infty^2)\left(\psi_{R_{m+1,n}} - 2\psi_{R_{m,n}} + \psi_{R_{m-1,n}}\right) \tag{81}$$

$$+\left(\frac{\delta x'}{\delta y'}\right)^2\left(\psi_{R_{m,n+1}} - 2\psi_{R_{m,n}} + \psi_{R_{m,n-1}}\right)$$

$$+ M_\infty^2\, k\,\delta x'\left(\psi_{I_{m+1,n}} - \psi_{I_{m-1,n}}\right) + M_\infty^2 k^2\,\delta x'^2\,\psi_{R_{m,n}} = 0$$

and

$$(1-M_\infty^2)\left(\psi_{I_{m+1,n}} - 2\psi_{I_{m,n}} + \psi_{I_{m-1,n}}\right) \tag{82}$$

$$+\left(\frac{\delta x'}{\delta y'}\right)^2\left(\psi_{I_{m,n+1}} - 2\psi_{I_{m,n}} + \psi_{I_{m,n-1}}\right)$$

$$- M_\infty^2\, k\,\delta x'\left(\psi_{R_{m+1,n}} - \psi_{R_{m-1,n}}\right) + M_\infty^2\, k^2\,\delta x'^2\,\psi_{I_{m,n}} = 0$$

Since for supersonic flow the system of governing equations is hyperbolic, then the appropriate finite difference procedure for the resulting initial value problem is to solve for point (m+1,n) in terms of data along m and m-1. The

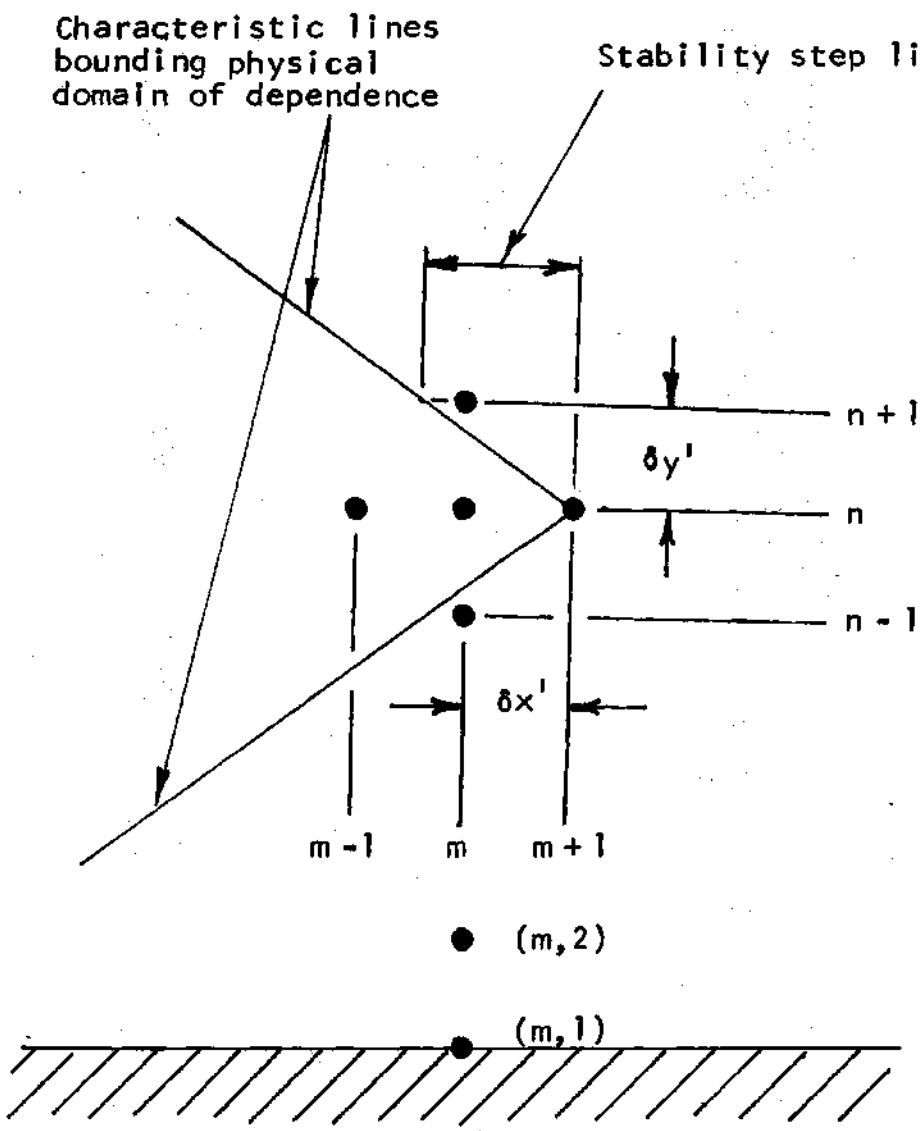

Figure 7. The Finite Difference Grid

system of equations can then be written as

$$\begin{bmatrix} 1 - M_\infty^2 & M_\infty^2 k\delta x' \\ - M_\infty^2 k\delta x' & 1 - M_\infty^2 \end{bmatrix} \begin{bmatrix} \psi_{R_{m+1,n}} \\ \psi_{I_{m+1,n}} \end{bmatrix} = \begin{bmatrix} B_1 \\ B_2 \end{bmatrix} \tag{83}$$

where

$$B_1 = \left[2(1-M_\infty^2) + 2\lambda^2 - k^2 M_\infty^2 \delta x'^2\right] \psi_{R_{m,n}} \tag{84}$$

$$- \lambda^2(\psi_{R_{m,n+1}} + \psi_{R_{m,n-1}}) + M_\infty^2 k\delta x' \psi_{I_{m-1,n}}$$

$$- (1 - M_\infty^2)\, \psi_{R_{m-1,n}}$$

$$B_2 = \left[2(1-M_\infty^2) + 2\lambda^2 - k^2 M_\infty^2 \delta x'^2\right] \psi_{I_{m,n}} \tag{85}$$

$$- \lambda^2(\psi_{I_{m,n+1}} + \psi_{I_{m,n-1}}) - M_\infty^2 k\delta x' \psi_{R_{m-1,n}}$$

$$- (1-M_\infty^2)\, \psi_{I_{m-1,n}}$$

and

$$\lambda = \frac{\delta x'}{\delta y'} \tag{86}$$

Solving Equation (83) gives

$$\psi_{R_{m+1,n}} = \left[B_1(1-M_\infty^2) - B_2 M_\infty^2 k\delta x' \right] \tag{87}$$

$$/\left[(1-M_\infty^2)^2 + M_\infty^4 k^2 \delta x'^2 \right]$$

and

$$\psi_{I_{m+1,n}} = \left[B_2(1-M_\infty^2) + B_1 M_\infty^2 k\delta x' \right] \tag{88}$$

$$/\left[(1-M_\infty^2)^2 + M_\infty^4 k^2 \delta x'^2 \right]$$

For stability reasons, it is necessary that the Courant-Friedricks-Lewy [26] step criterion be observed; i.e.

$$\lambda \leq \sqrt{M_\infty^2 - 1} \tag{89}$$

Referring again to Figure 7 the above restriction on λ assures that the Mach wedge, which defines the physical domain of dependence for the point (m + 1, n), is contained within the numerical domain of dependence, which is bounded by the two rear diagonal rows of nodes passing through the point (m + 1, n). It is interesting to note that for the special case of zero frequency oscillation, the governing equation becomes the spatial wave equation and Hildebrand [26] shows that solution of the corresponding difference equation represents an exact solution if λ

assumes the equality in Equation (89).

A first order difference representation for Equations (40) and (42) give the airfoil surface boundary conditions (only the lower surface is given here; the upper surface is obtained in a symmetrical manner) for rotational oscillation as

$$\psi_{R_{m,1}} = \psi_{R_{m,2}} - 2k^2(x'-b)\,\delta y \tag{90}$$

$$\psi_{I_{m,1}} = \psi_{I_{m,2}} + 4k\,\delta y \tag{91}$$

and for translational oscillation

$$\psi_{R_{m,1}} = \psi_{R_{m,2}} - 2k^2\,\delta y \tag{92}$$

$$\psi_{I_{m,1}} = \psi_{I_{m,2}} \tag{93}$$

Now if Cauchy type data [23] is given along a non-characteristic line somewhere upstream of the blade channel shown in Figure 2, then Equations (87) and (88) may be used, along with the periodicity and blade boundary conditions to advance the solution from upstream through the entire domain. The discussion in Chapter II indicated that no such initial data is known and that periodic solutions might not exist for arbitrarily chosen data. The proper posing of this initial value problem, however,

demands that the solution begin with established initial data.

The choice of the hypothetical upstream boundaries of the domain shown in Figure 2 was arbitrary. A more convenient choice for purposes of numerical calculation is shown in Figure 8.

The boundary conditions along the hypothetical upstream and downstream boundaries follow from the periodicity condition, Equation (39) as

$$C_p^*\Big|_{0,y'} = e^{i\beta}\, C_p^*\Big|_{s'\sin\theta,\ y' + s'\cos\theta} \tag{94}$$

and

$$\frac{\partial C_p^*}{\partial x'}\Big|_{0,y'} = e^{i\beta}\, \frac{\partial C_p^*}{\partial x'}\Big|_{s'\sin\theta,\ y' + s'\cos\theta} \tag{95}$$

for the inlet and

$$C_p^*\Big|_{1,y'} = e^{i\beta}\, C_p^*\Big|_{1 + s'\sin\theta,\ y' + s'\cos\theta} \tag{96}$$

and

$$\frac{\partial C_p^*}{\partial x'}\Big|_{1,y} = e^{i\beta}\, \frac{\partial C_p^*}{\partial x'}\Big|_{1 + s'\sin\theta,\ y' + s'\cos\theta} \tag{97}$$

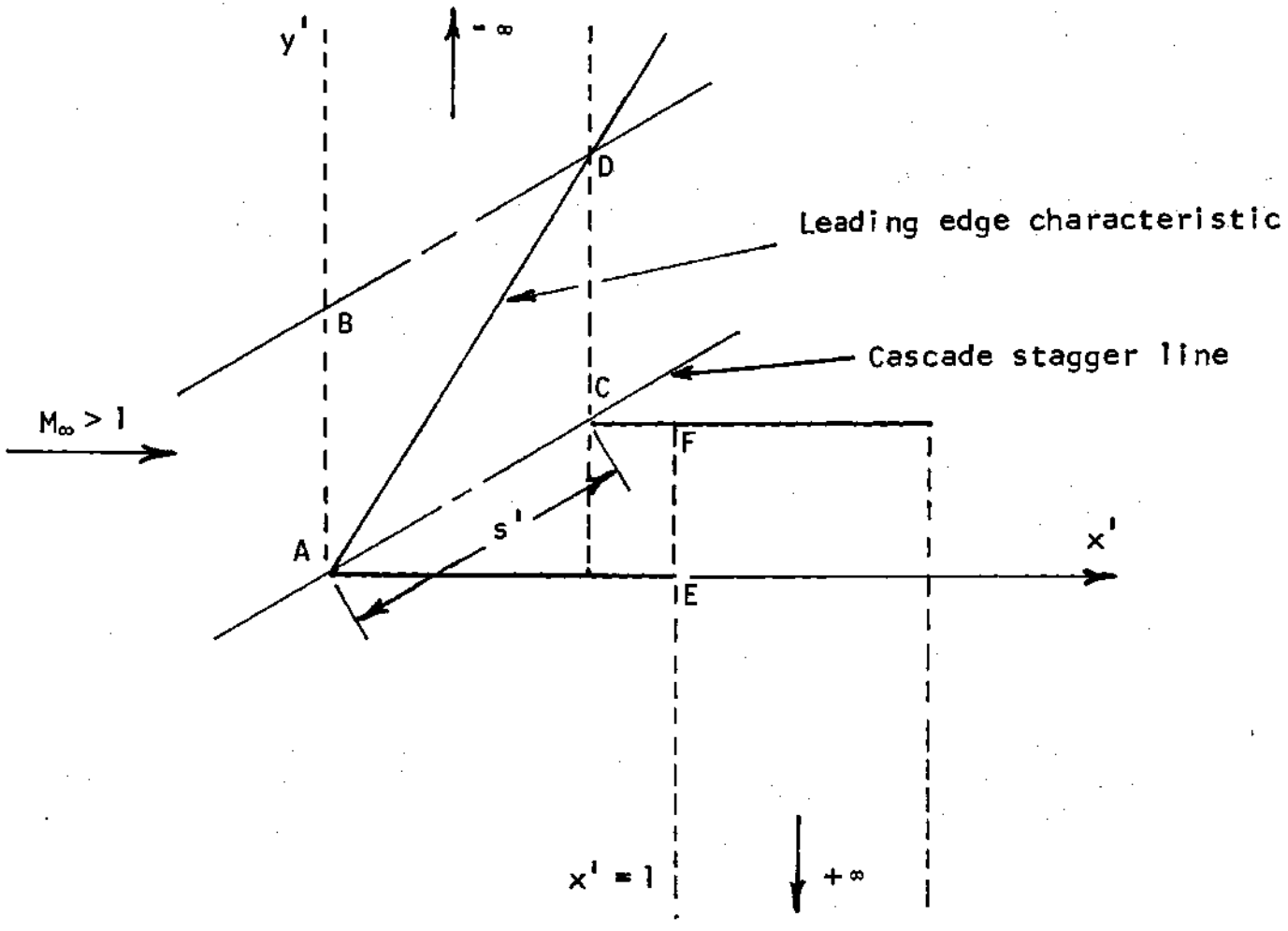

Figure 8. The Computational Domain

for the exit.

Considering the inlet region, initial data is sought along the line $x' = 0$ above the leading edge of the lower blade such that the resulting solution along the line $x' = s'\sin\theta$ satisfies Equations (94) and (95). Suppose that the disturbance pressure and derivative are initially zero along $x' = 0$. Then Equations (87) and (88) along with the lower surface boundary condition may be used to march the solution along x' to produce a nonzero solution along segment C-D of the line $x' = s'\sin\theta$ bounded by the leading edge of the upper blade and the leading edge characteristic of the lower blade. Notice that the numerical calculation need only be performed for the domain below the upper bounding characteristic since above it the solution remains identically zero. Since the periodicity requirement demands that this solution along C-D be related only by a phase shift to the solution along segment A-B, it is clear that this condition is violated. If the initial data along A-B is replaced with the solution along C-D and shifted by the appropriate phase angle, then an iteration is defined which proceeds as follows:

(1) Choose initial data long line $x' = 0$ arbitrarily (for reasons that will be made apparent, zero is a good choice).

(2) Generate the solution along line $x' = s'\sin\theta$ by using Equations (87) and (88) along with the lower blade surface boundary conditions to march from the initial data line.

(3) Replace the initial data along $x' = 0$ with the resulting solution along $x' = s'\sin\theta$ and shift in phase by the interblade phase angle (i.e. use Equations (94) and (95) to obtain the new initial data).

(4) Repeat steps (2) and (3) until convergence is reached in some sense.

From the previous argument on the existence of periodic solutions of this problem, there is no guarantee that the above iteration can converge in the sense of producing a solution which is periodic within an arbitrarily small tolerance all the way to infinity. Instead, solutions are sought which converge to a periodic solution in the "vicinity" of the reference blade channel. Some confidence as to the convergence of the iteration in the latter sense can be gained on physical grounds.

If the initial data is taken as zero, as suggested in step one, then it is easily ascertained that the first step corresponds to the solution of a two blade cascade. A close examination of the iteration procedure along with Figure 9 reveals that each step in the iteration corresponds

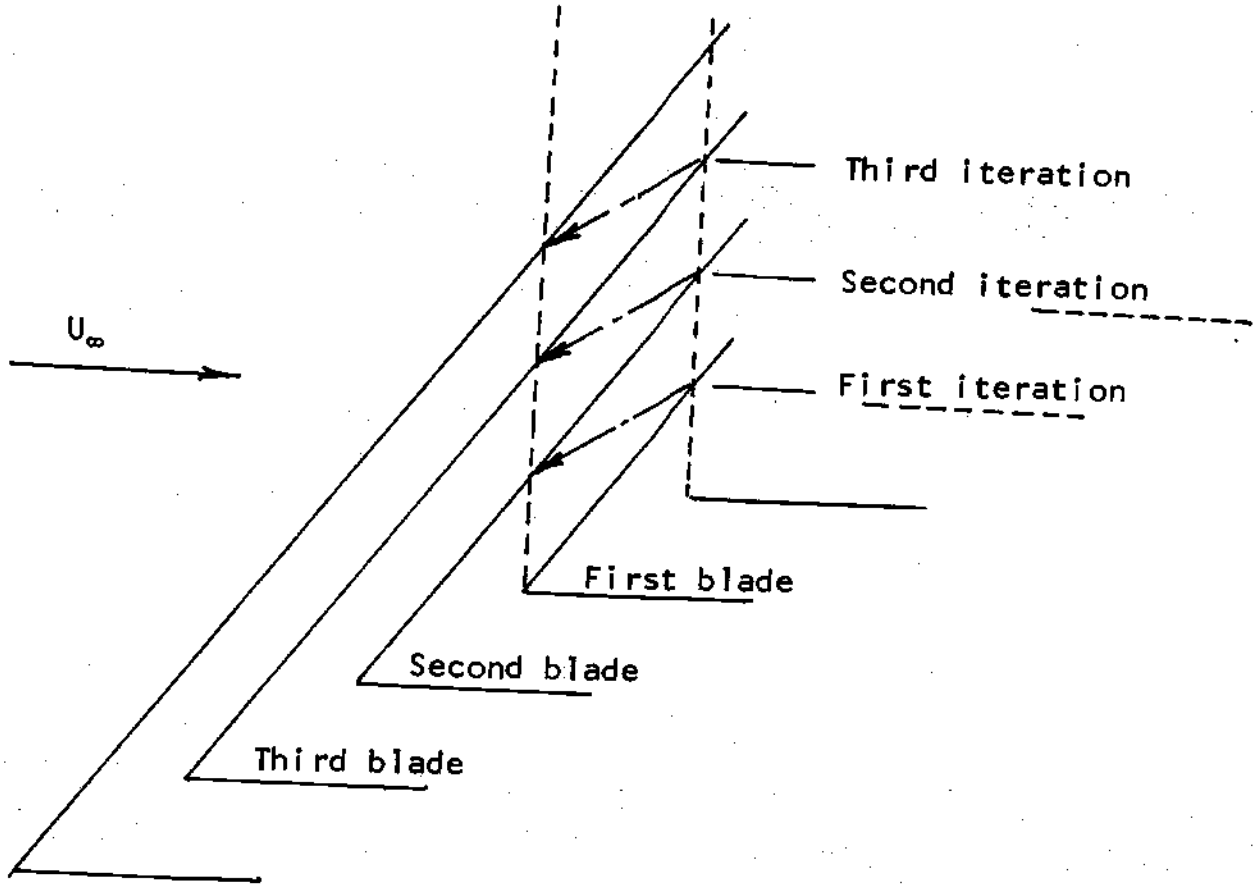

Figure 9. The Finite Cascade

precisely to adding an additional blade to the cascade. Convergence in the physical sense occurs if the solution for C_p^* on the first blade surface approaches a limit as the number of blades in the cascade approaches infinity. With the expectation that this process does physically converge in the above sense for all but a finite number or range of cases, then this criterion is also taken as the definition of the convergence of the iteration. The convergence of this process was investigated numerically and the results are discussed in Chapter IV.

The introduction of the pressure amplitude function, as discussed earlier, leads to a considerable simplification in the exit field calculation due to its continuity through the exit field wakes. The inlet field calculation, however, becomes slightly more complicated because local velocity information is lost through the introduction of C_p^* and this information is needed to calculate the jump discontinuity in C_p^* across the airfoil leading edges. Explicit enforcement of jump conditions is not required for the velocity potential formulation due to the continuity of ϕ^* across the leading edge characteristics. Since ϕ^* is continuous through the leading edge characteristics, the jump in C_p^* may be related to the jump in $u^* = \frac{\partial \phi^*}{\partial x'}$, through Equation (34) as

$$\Delta C_p^* = -2\Delta u^* \tag{98}$$

The hodograph characteristic equation [25] (sometimes called the compatibility relation) may be used to relate Δu^* to Δv^* across the left and right leading edge characteristics. Splitting this equation into its real and imaginary parts gives

$$\left.\frac{\Delta v_R}{\Delta u_R}\right|_{L,R} = \mp\sqrt{M_\infty^2-1} - (2M_\infty^2 k u_I + M_\infty^2 k^2 \phi_R)\left.\frac{\Delta y}{\Delta u_R}\right|_{L,R} \tag{99}$$

and

$$\left.\frac{\Delta v_I}{\Delta u_I}\right|_{L,R} = \mp\sqrt{M_\infty^2-1} + (2M_\infty^2 k u_R - M_\infty^2 k^2 \phi_I)\left.\frac{\Delta y}{\Delta u_I}\right|_{L,R} \tag{100}$$

Recognizing that

$$\Delta y \to 0$$

while Δu^* remains finite across the leading edge characteristic lines then

$$\left.\frac{\Delta v_R}{\Delta u_R}\right|_{L,R} = \mp\sqrt{M_\infty^2 - 1} \tag{101}$$

and

$$\left.\frac{\Delta v_1}{\Delta u_1}\right|_{L,R} = \mp \sqrt{M_\infty^2 - 1} \tag{102}$$

so that

$$\left.\Delta C_p^*\right|_{L,R} = \left(2 \Big/ \pm \sqrt{M_\infty^2 - 1}\right) \left.\Delta v^*\right|_{L,R} \tag{103}$$

which gives the jump in the pressure amplitude function as a function of the jump in normal velocity at the airfoil leading edge. This condition is a more general form of the result given by Miles [27] that the pressure and phase at the leading edge of an isolated airfoil oscillating in supersonic flow may be calculated from quasi-steady considerations.

Equation (34) may be differentiated with respect to y' to obtain

$$ikv^* + \frac{\partial v^*}{\partial x'} = -\frac{1}{2}\frac{\partial C_p^*}{\partial y'} \tag{104}$$

which may be integrated with respect to x' at constant y' from an upstream reference point x_r' to give

$$v^*(x') = v^*(x_r') e^{ik(x_r' - x')} - \frac{1}{2} e^{-ikx'} \int_{x_r'}^{x'} \frac{\partial c_p^*}{\partial y'} e^{ikx} \, dx \quad (105)$$

Equation (105) may now be used to evaluate v^* just ahead of an airfoil leading edge and v^* at the leading edge is given by the velocity boundary condition, Equation (26). The difference between the two gives Δv^* and Equation (103) now determines the jump in c_p^*. The evaluation of Equation (105) in terms of successive iterations is given in Appendix D.

The inlet region calculation just described may easily be continued through the blade passage with the aid of the upper and lower blade surface boundary conditions to provide initial data along segment E-F of the exit field initial data line, $x' = 1$. Initial data for the remainder of this line for the first exit iteration is obtained from an isolated airfoil solution on the bottom side of the lower blade. The solution then proceeds as in the inlet region with the solution being generated at the aft boundary of the exit region and then used to replace the initial data via Equations (96) and (97).

Acoustic Resonance

Depending on the Mach number, stagger angle, blade

spacing, and interblade phase angle, the acoustic disturbances created by the vibrating cascade may either decay or propagate undiminished to infinity. Any point along the boundary separating these two regimes is called an acoustic cutoff or resonance point. A detailed discussion and derivation of this condition for cyclindrical ducts with no through flow is given by Tyler and Sofrin [12]. The convergence of the iteration described in the last section is greatly influenced by the proximity of the case under consideration to the cutoff point. Since this condition may actually be encountered at some section along the rotor blade span, it is necessary to know where it occurs, the effect it has on the solution at the point itself, and more importantly, the behavior of the solution in the neighborhood of the point.

The following derivation for the cutoff condition in two dimensions for the case with flow proceeds on the basis of the physical condition that cutoff occurs when the pressure disturbance pattern created at the inlet of the vibrating cascade travels at Mach one relative to the approaching flow (Figure 10). Then at cutoff

$$(U_\theta + V_p)^2 + (U_\infty \cos\theta)^2 = a^2 \qquad (106)$$

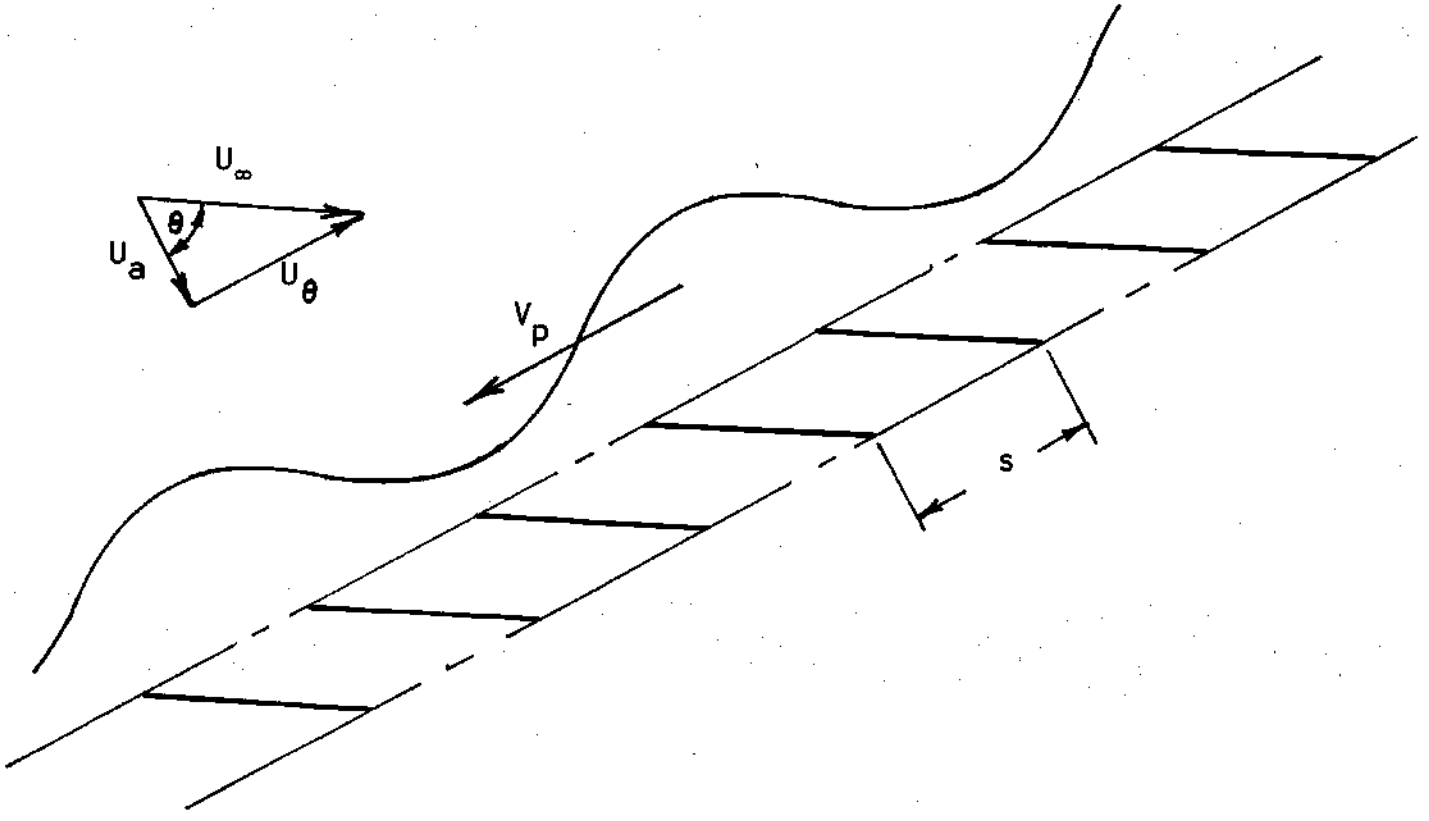

Figure 10. Traveling Pressure Wave at Cascade Inlet

The phase velocity along the cascade, V_p, may also be written as

$$V_p = - U_\infty k/\sigma(\beta \pm 2n\pi) \tag{107}$$

where σ is introduced as the blade chord to spacing ratio or solidity, β is the interblade phase angle, defined as positive for the lower blade leading the upper, n is an arbitrary integer and k is the previously defined reduced frequency parameter. Substituting Equation (107) into (108) gives

$$\beta \pm 2n\pi = k/\sigma \left[\sin\theta \pm \frac{1}{M_\infty} \sqrt{1-M_\infty^2 \cos^2\theta} \right]^{-1} \tag{108}$$

For supersonic flow the right hand side of Equation (108) is always positive for all real values of the radical (subsonic leading edge) since

$$\sin\theta \geq \frac{1}{M_\infty} \sqrt{1 - M_\infty^2 \cos^2\theta}$$

This means that both the cutoff phase angles given by Equation (108) correspond to backward traveling waves (i.e. opposite to the direction of rotor rotation as measured in rotor fixed coordinates). In stationary or engine fixed coordinates choice of the minus sign gives a forward rotating wave and the plus gives a counter

rotating wave at the same speed; i.e.

$$V_{p_{abs.}}^{+} = - V_{p_{abs.}}^{-} = a_\infty \sqrt{1 - M_\infty^2 \cos^2\theta} \qquad (109)$$

Then for

$$M_\infty < 1/\cos\theta$$

there exist two distinct cutoff points for a given cascade geometry and blade frequency parameter so that for the range of interblade phase angles

$$k/\sigma \left[\sin\theta + \frac{1}{M_\infty}\sqrt{1 - M_\infty^2 \cos^2\theta}\right]^{-1} < \beta \pm 2n\pi \qquad (110)$$

$$< k/\sigma \left[\sin\theta - \frac{1}{M_\infty}\sqrt{1 - M_\infty^2 \cos^2\theta}\right]^{-1}$$

the disturbances decay away from the cascade and outside of this range the disturbances propagate to infinity. For the special case

$$M_\infty = 1/\cos\theta$$

which corresponds to the case when the leading edge Mach wave is coincident with the cascade stagger line, then there exists only one cutoff point. If the Mach number is increased further so that

$$M_\infty > 1/\cos\theta$$

the leading edge Mach wave is swept inside the cascade, and disturbances created by the cascade can no longer exist upstream of the cascade stagger line.

To understand a little more clearly how the cutoff condition might affect the solution of the cascade problem, consider a pressure disturbance generated at the leading edge of the lower airfoil in Figure 11 at time, t_o, when the blade is at some reference phase angle.

Now assume that this disturbance arrives at the leading edge of the above blade Δt later so that this blade is again at the reference phase angle (i.e. the disturbance arrives in phase). The time required for the disturbance to reach the leading edge of the second blade is given by

$$\Delta t = \frac{s}{a_\infty (M_\infty^2 - 1)} \left[M_\infty \sin\theta \pm \sqrt{1 - M_\infty^2 \cos^2\theta} \right] \qquad (111)$$

but also

$$\Delta t = (\beta \pm 2n\pi)\ C/kU_\infty \qquad (112)$$

where n is chosen so that

$$\beta \pm 2n\pi > 0$$

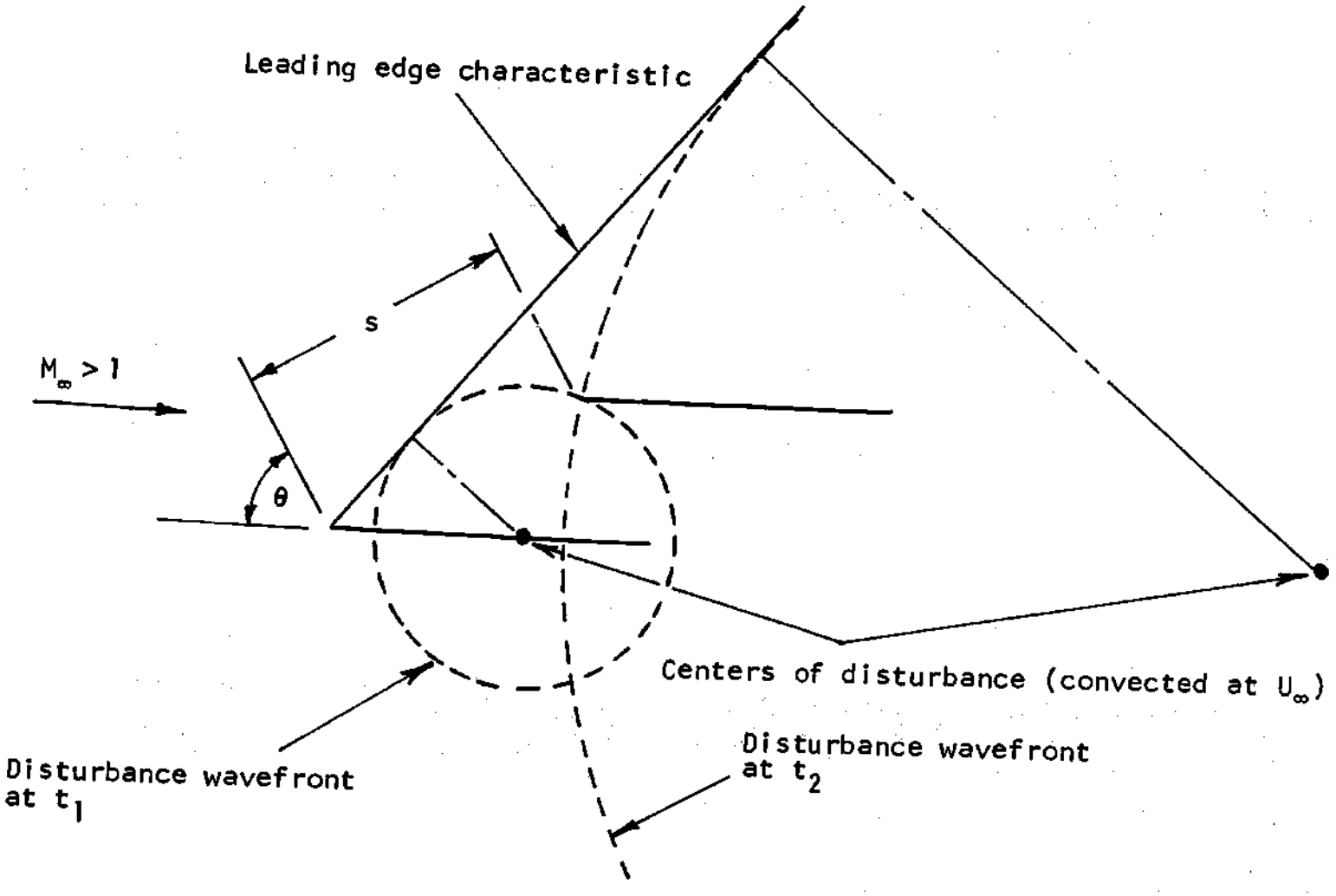

Figure 11. Propagation of the Leading Edge Disturbance in a Supersonic Cascade

Equating times then gives

$$\beta \pm 2n\pi = \frac{kM_\infty}{\sigma(M_\infty^2 - 1)} \left[M_\infty \sin\theta \pm \sqrt{1 - M_\infty^2 \cos^2\theta} \right] \qquad (113)$$

or equivalently

$$\beta \pm 2n\pi = k/\sigma \left(\sin\theta \pm \frac{1}{M_\infty} \sqrt{1 - M_\infty^2 \cos^2\theta} \right)^{-1} \qquad (114)$$

which is identical with the expression derived for the cutoff condition, Equation (108). Choice of the plus sign now corresponds to the front of the wave arriving in phase at t_1 and the minus corresponds to the back of the wave arriving in phase at larger time, t_2. The disturbances created by successive blades may thus interfere constructively at the cutoff points. It was found numerically that convergence of the solution method described in the first section of this chapter is greatly affected by this condition. The results of this numerical investigation are presented and discussed in the following chapter.

CHAPTER IV

DISCUSSION

Results of the Numerical Computations

A computer program was written following the solution method presented in Chapter III and the results thus obtained are compared to some existing solutions for special cases and to some very recently published results using different methods. The program has also been used to perform parametric studies, and these results are presented in this section. The convergence of the method, both near and away from resonance points, is numerically investigated.

In Figure 12 the present numerical method is compared to the isolated supersonic airfoil results of Garrick and Rubinow [28]. The comparisons are made in terms of the Garrick and Rubinow parameters CM_α and $\bar{\omega}$ where

$$CM_\alpha = (8/\pi k^2)\ C_{m_\alpha}$$

and

$$\bar{\omega} = k M_\infty^{\ 2} / (M_\infty^{\ 2} + 1)$$

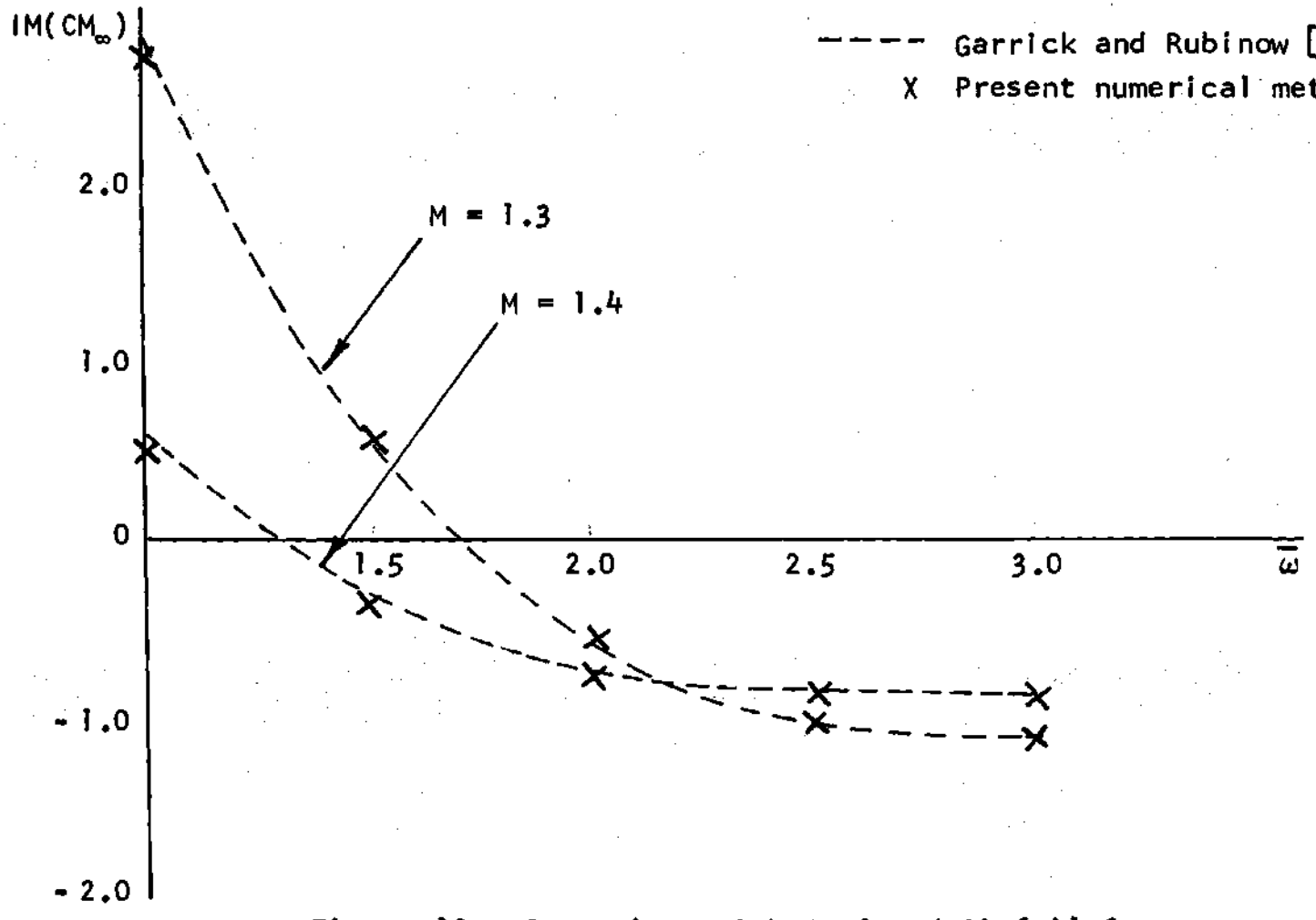

Figure 12. Comparison with Isolated Airfoil for Rotational Oscillation About Quarter-Chord

The out of phase component of the moment coefficient for rotational oscillation is presented for Mach numbers of 1.3 and 1.4 and the results are seen to be in virtually perfect agreement with the Garrick and Rubinow results. Although not presented here, this same excellent agreement was typical of the lift and moment results over a wide Mach number and frequency range for both translational and rotational oscillations.

The method presented is valid for both the supersonic and subsonic leading edge problem. The iteration method described in the previous chapter for enforcing the upstream periodicity condition converges in a single step for the supersonic leading edge case since the Mach wave from the lower blade is swept inside the cascade stagger line, thus leaving the upstream flow undisturbed. Figure 13 shows the out of phase component of the pressure coefficient along the lower surface of the supersonic leading edge cascade depicted in Figure 14 for rotational oscillations about the leading edge. The predicted pressure distribution shows excellent agreement with Chalkley's [29] method of characteristics solution. The observed discontinuities in the pressure distribution correspond to the reflection points of the leading edge bow waves in Figure 14.

Figure 15 compares the present method with

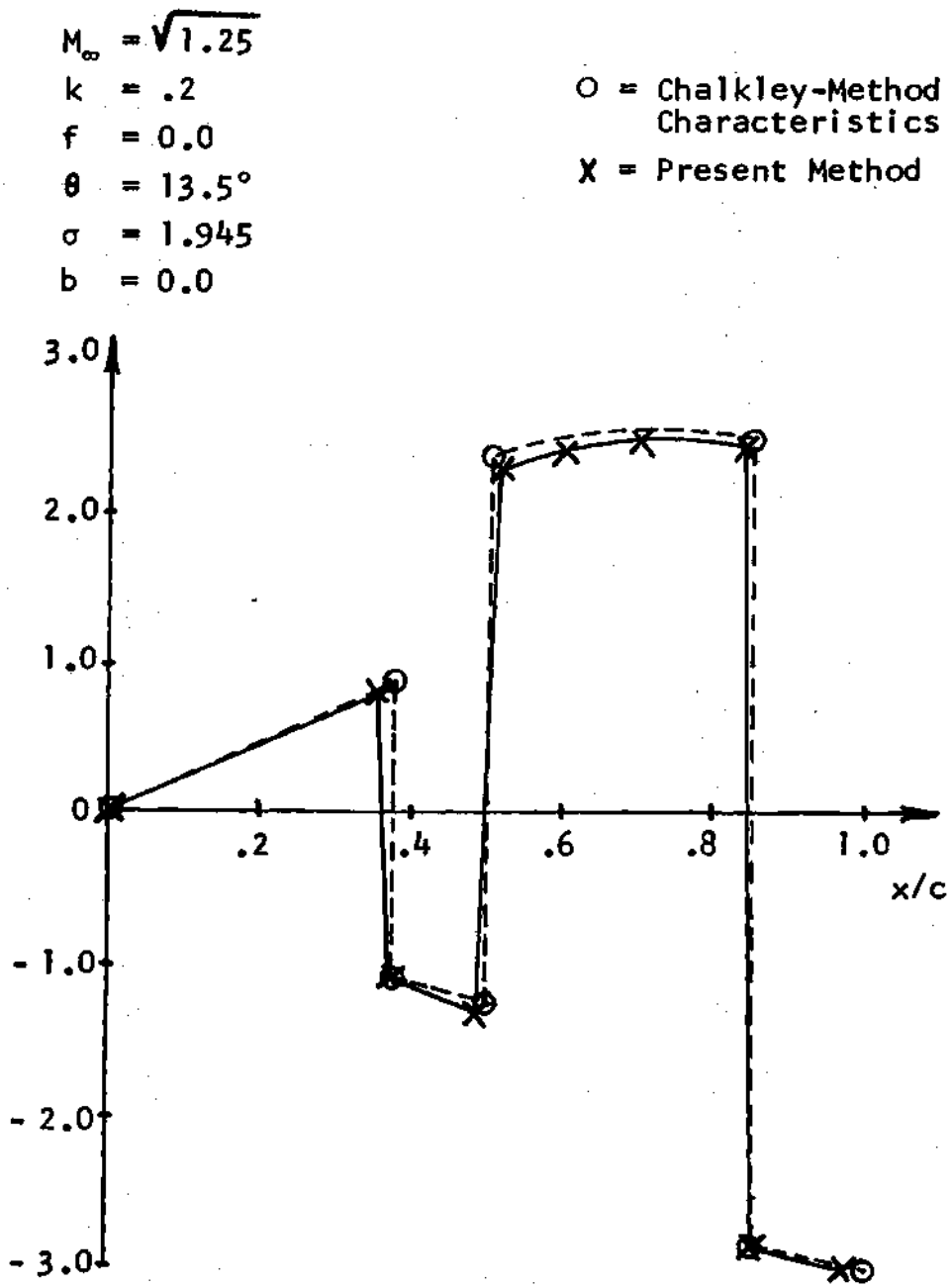

Figure 13. Out of Phase Pressure Distribution - Cascade A

$M_\infty = \sqrt{1.25}$
$\theta = 13.5$
$\sigma = 1.945$

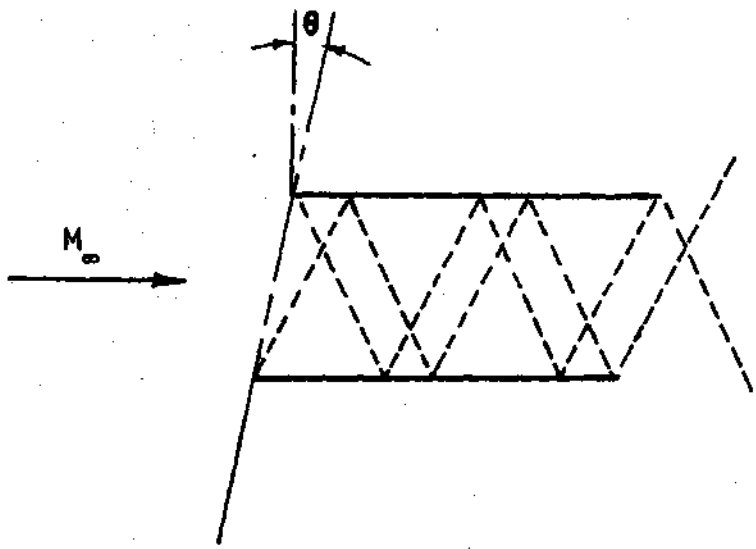

Figure 14. Cascade A

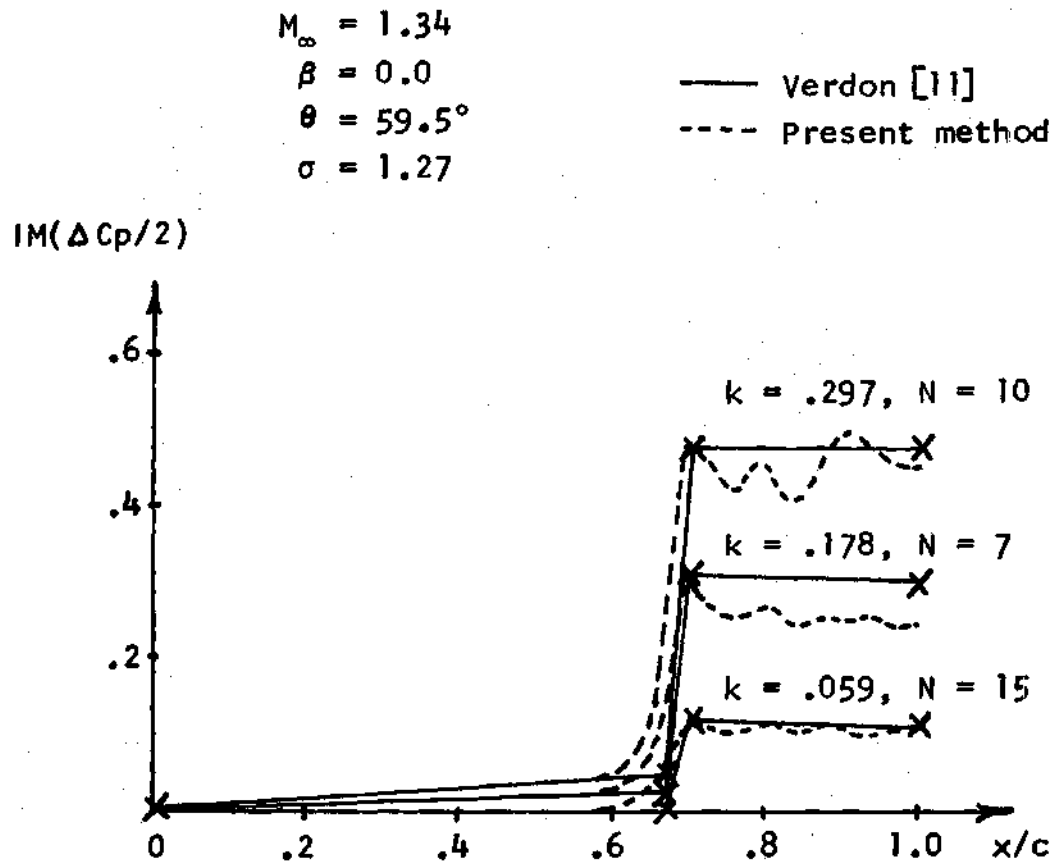

Figure 15. Out of Phase Pressure Difference Distributions for Translational Oscillations of Cascade B

Verdon's [11] results for translational (or bending) oscillations of Cascade B Figure 16. The results, in the form of pressure difference distributions, show very good agreement for several frequencies, except over the last third of the airfoil chord where Verdon's results show considerable irregularity. This irregularity is due to improper numerical reflection of the characteristic discontinuities from the wake surfaces and is not, as suggested by Verdon and McCune [14] , attributable to the inherent "waviness" of the finite difference approximation in the immediate vicinity of finite discontinuities. The magnitude of this characteristic waviness in the present method was typically less than five percent of the maximum pressure amplitude and was always very rapidly damped with distance away from the discontinuity. The basic finite difference method presented here was also programmed in terms of the velocity potential with the wake treated explicity as outlined in Chapter II by requiring continuity of the pressure and normal velocity across the wake. The resulting pressure distributions calculated by this method (see Figure 17) exhibit the same irregularity as Verdon's method over the portion of the blade surface which is within the domain of influence of the wake. Careful tracking of the discontinuities during the exit field iteration process revealed that the local irregular

$M_\infty = 1.34$
$\theta = 59.5°$
$\sigma = 1.27$

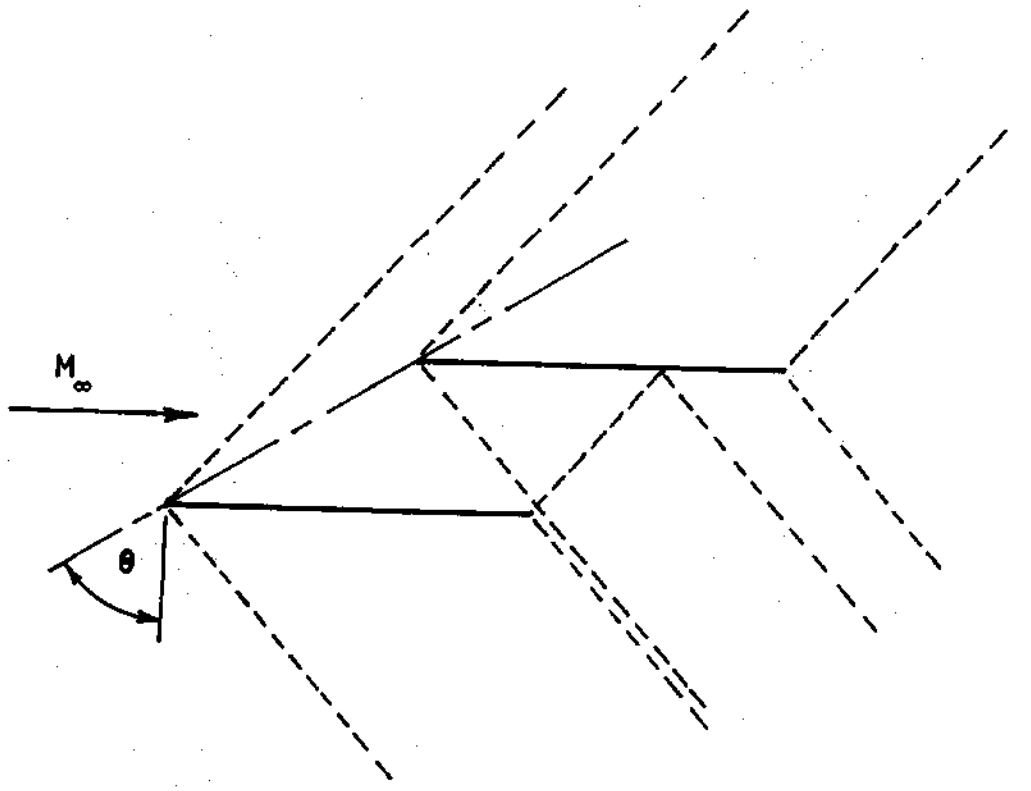

Figure 16. Cascade B

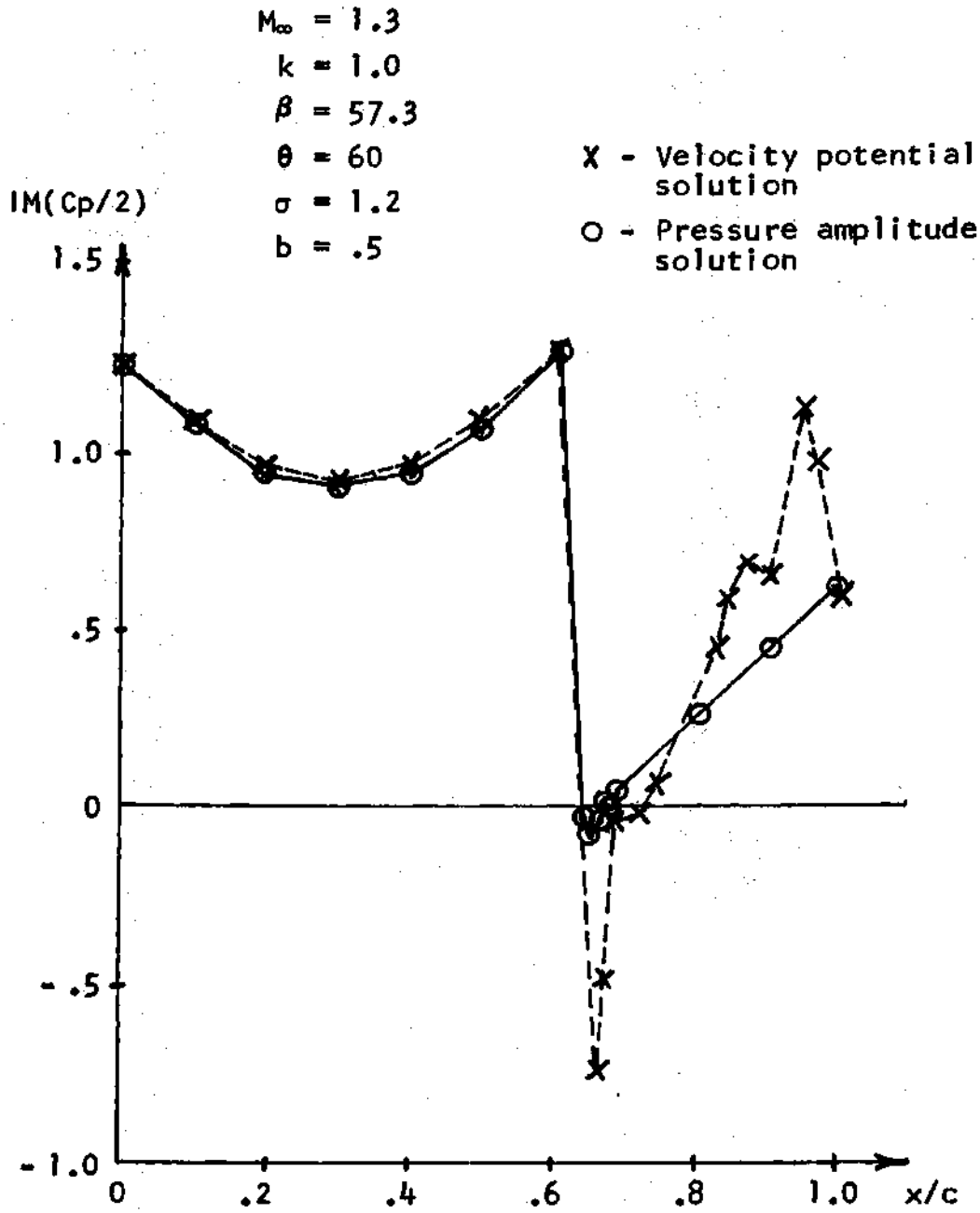

Figure 17. Comparison of Velocity Potential and Pressure Amplitude Solutions for Cascade C

spikes in the pressure distribution corresponded to the location of multiply reflected leading and trailing edge characteristics from the wake surfaces. The introduction of the pressure coefficient amplitude function, C_p^*, as the primary dependent variable eliminated both the need for explicit numerical consideration of the wake and the undesirable wake reflections obtained with the velocity potential method. The relatively small oscillations through the discontinuity produced by the pressure amplitude method (indicated by the solid line in Figure 17) are the ones characteristic of finite difference methods and can in no way account for the large undamped oscillations observed in the velocity potential-finite difference method.

Further comparisons of the present method with Verdon's results are shown in Figure 18 for rotational oscillations of Cascade B. Again excellent agreement is obtained except over the aft third of the blade. The effect of interblade phase angle on the out of phase pressure distribution for this case is shown in Figure 19 for the case of translational oscillation.

The characteristic method developed by Platzer and Chalkley [9] for the supersonic leading edge problem has been extended to treat the subsonic leading edge problem by Platzer and Brix [17]. A comparison of the present

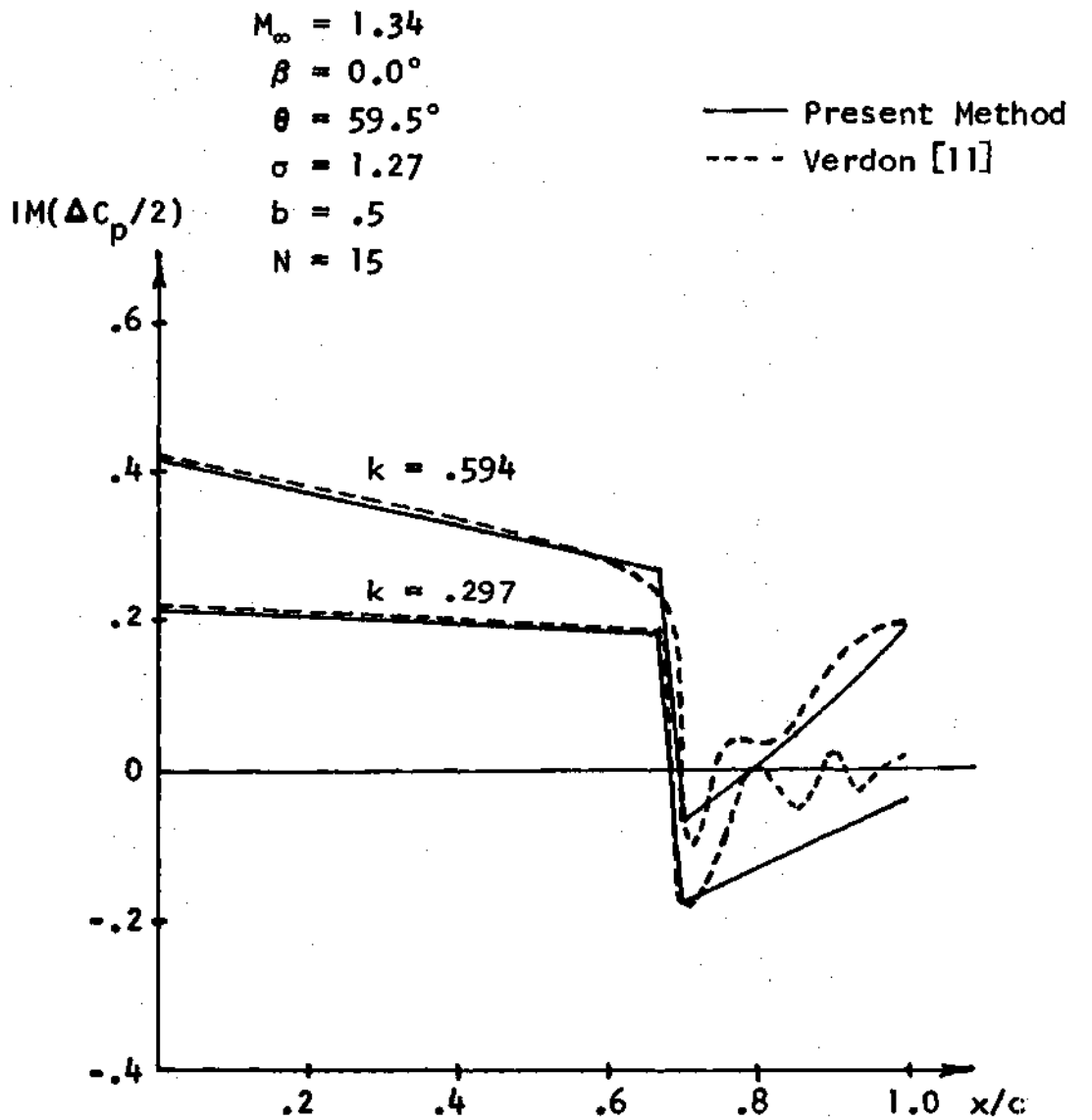

Figure 18. Out of Phase Pressure Difference Distribution for Rotational Oscillations of Cascade B

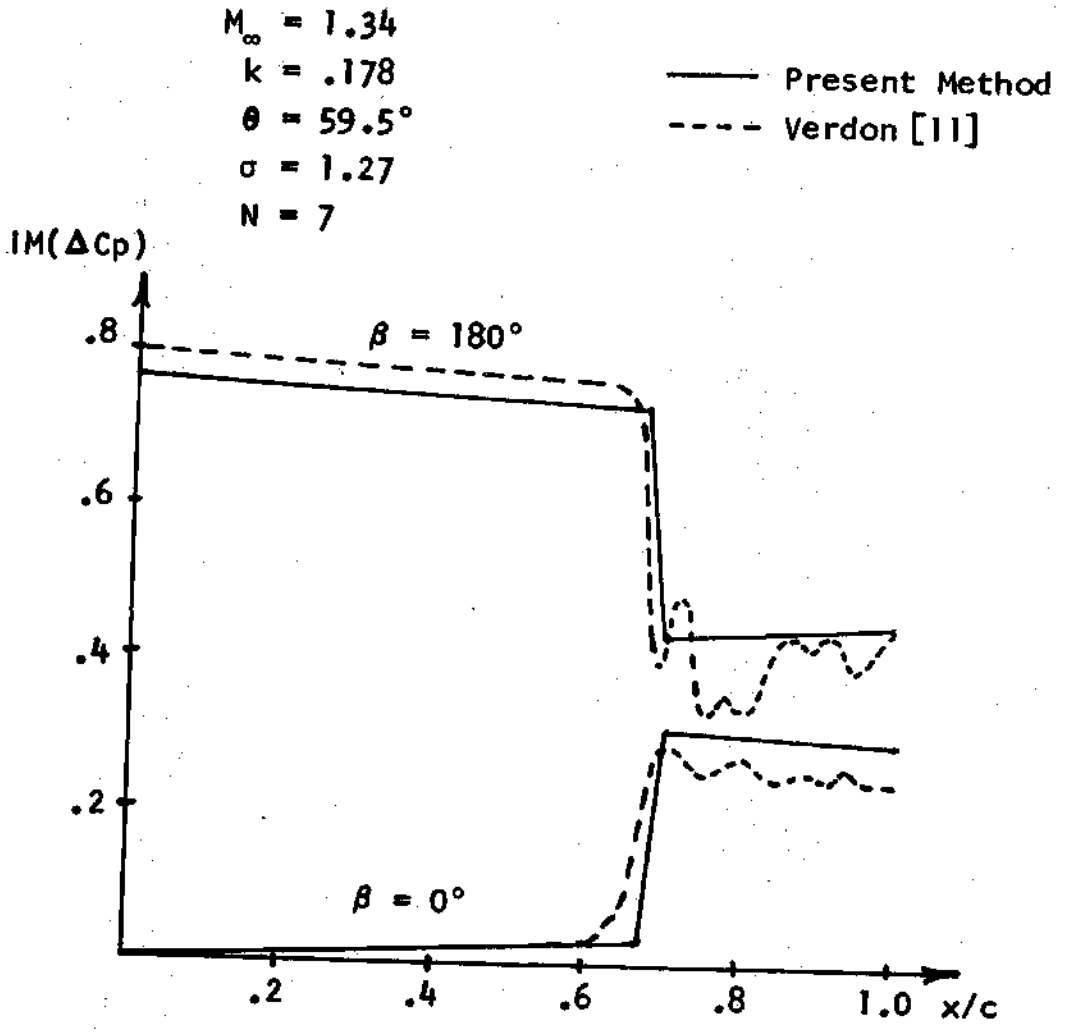

Figure 19. Out of Phase Pressure Difference Distributions - Effect of Interblade Phase Angle - Cascade B

method with the characteristics method for torsional oscillation of cascade B is presented in Figure 20. The agreement is seen to be excellent for a fifteen blade simulation with neither method exhibiting irregular pressure distributions over the aft part of the blade.

Using Verdon's analysis, Snyder and Commerford [30] have presented complex moment coefficients for a typical turbofan cascade (Cascade C of Figure 21) for a range of interblade phase angles at several different values of the frequency parameter. Figure 22 gives a comparison of these results with those produced by the present method. All points for the present method were produced using a ten blade simulation. The number of blades used by Snyder and Commerford is not known, however, with the exception of the points near the unusual loop of the lowest frequency case, all points were reasonably well converged and compare favorably. The origin of the loop for the lowest frequency case is unknown, but it is approximately centered about an acoustic resonance point occurring at an interblade phase angle of 128.9 degrees. The convergence of the method was also found to be very slow in this region although it is not known whether or not this is directly associated with the resonance condition. The failure to observe this loop at the other resonance point for this frequency and the absence of similar loops near the

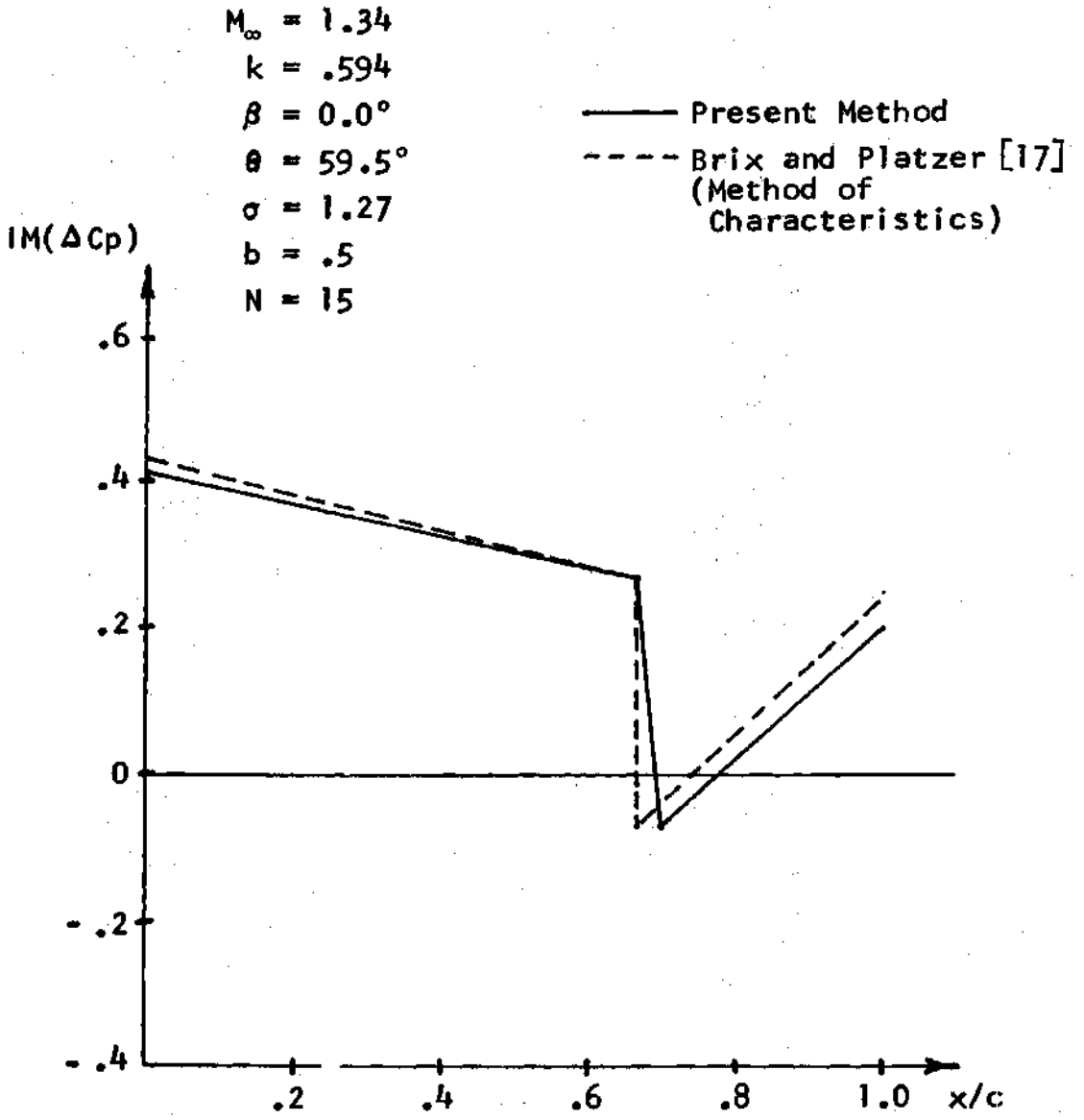

Figure 20. Comparison of Out of Phase Pressure Difference Distribution with a Method of Characteristics Solution for Rotational Oscillation of Cascade B

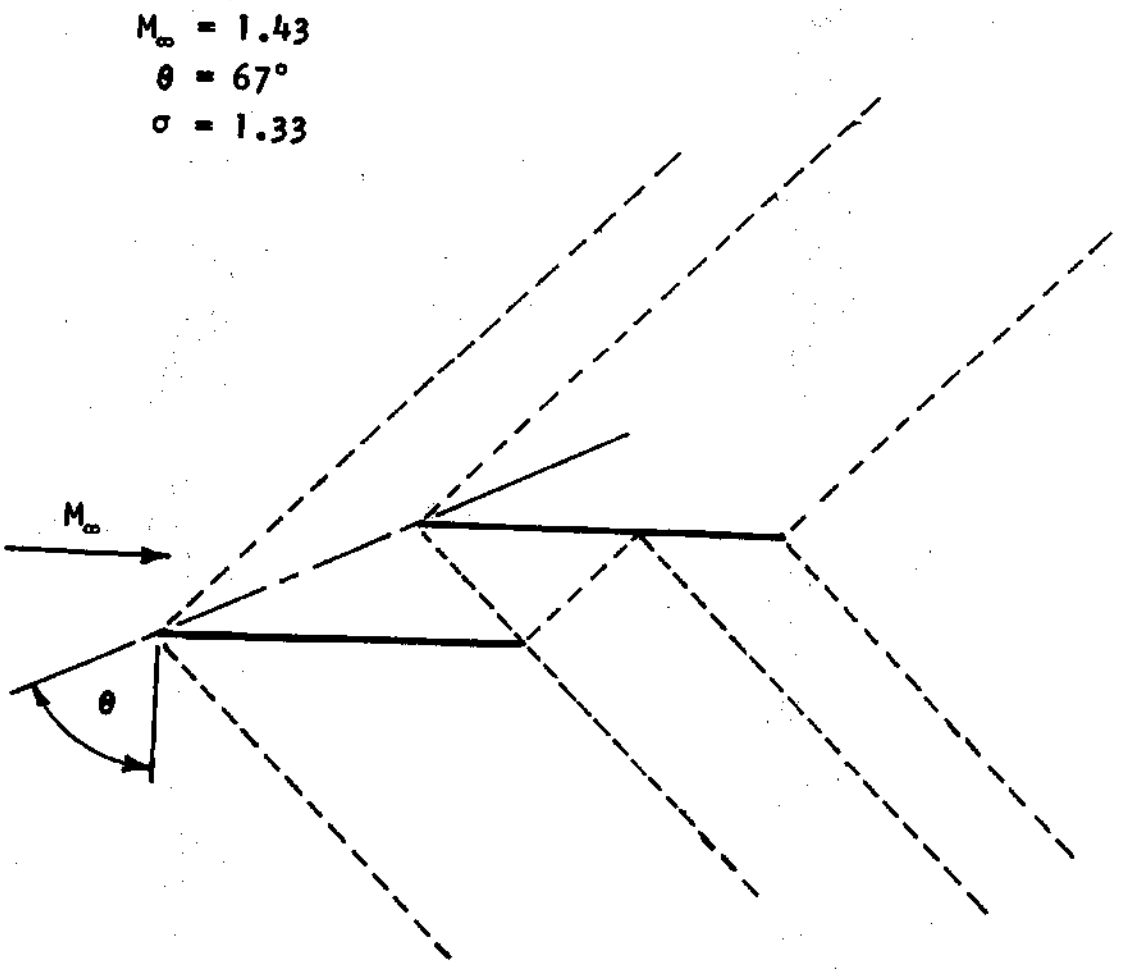

Figure 21. Cascade C

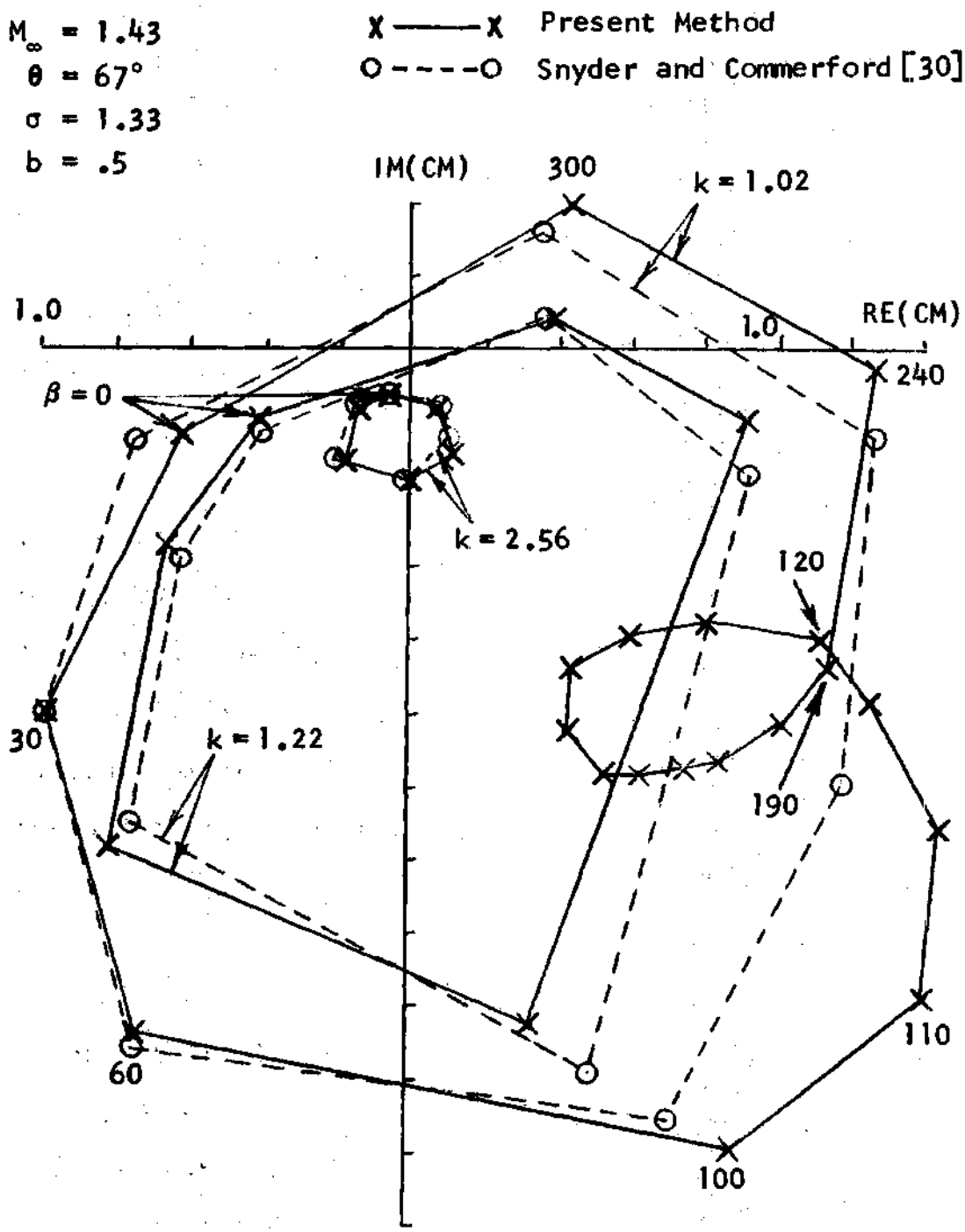

Figure 22. Effect of Interblade Phase Angle on the Moment Coefficient for Rotational Oscillation of Cascade C

resonance points at the other frequencies investigated would indicate that the occurrence of the observed loop is only coincidentally related to the actual occurrence of resonance. The absence of this loop in the Snyder-Commerford presentation is probably due simply to an inadequate number of points within this phase angle range to properly identify the loop.

The convergence of the iteration (recall from the discussion in Chapter III that each iteration corresponds to adding a blade to a finite cascade) is investigated in Figure 23 for interblade phase angles falling within the loop of Figure 22. In each case, the most rapidly changing component of the complex moment coefficient is displayed. At the resonance phase angle of 128.9 degrees the solution, after twenty iterations, still continues to climb giving no indication that an asymtotic value might be achieved by continuing the iteration (i.e. by adding more blades). Two other points, away from the resonance point but still within the loop, are also shown. These cases, especially the interblade phase angle of 100.0 degrees, exhibit an oscillatory behavior although the magnitude of the oscillation appears to decay as the iteration continues. A similar behavior is observed at resonance for a higher reduced frequency of 1.588 (Figure 24). Only 15.6 degrees away from the resonance in this

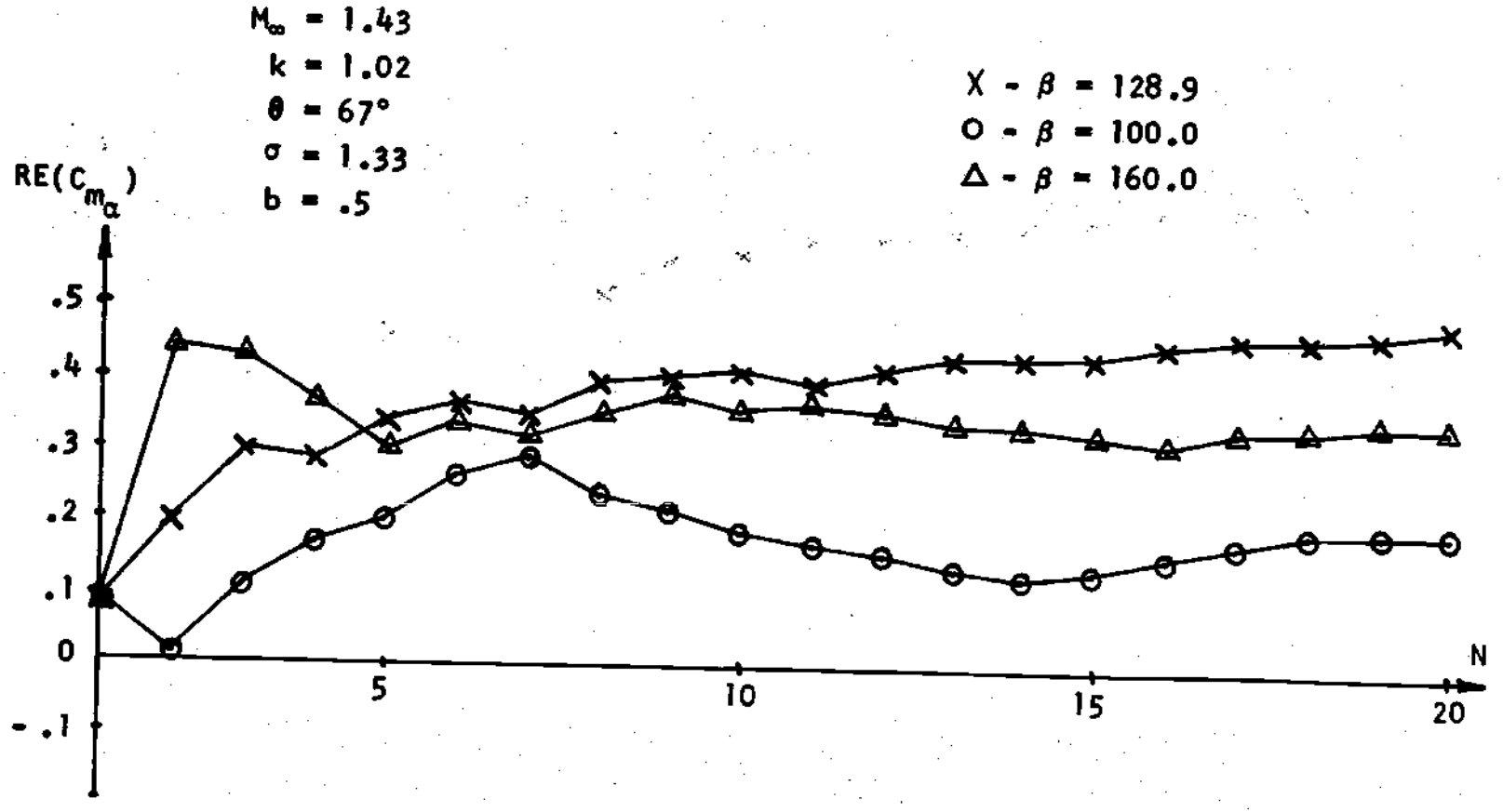

Figure 23. Convergence Near Resonance - Case 1

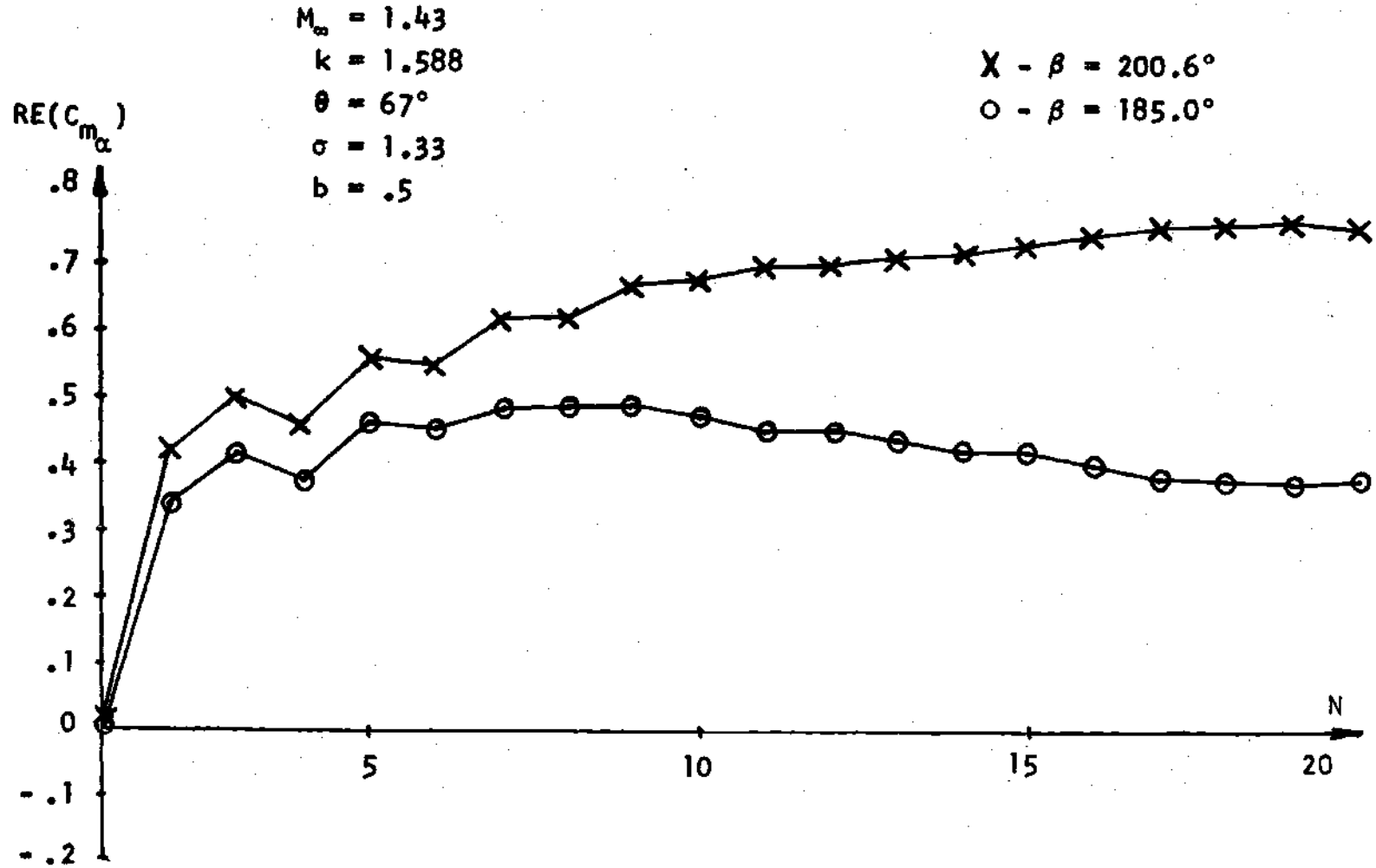

Figure 24. Convergence Near Resonance - Case 2

case, the behavior of the solution for large N is seen to be markedly different. The variation of the solution with frequency through resonance for the above two cases is shown in Figures 25 and 26. Ten iterations were performed to produce the solution for each point. No large changes are noted at the resonance frequencies of the two cases presented, however, at the resonance points the solution is far from convergence at ten iterations and does not appear to oscillate about any apparent mean value as do the nonresonance cases.

A more typical convergence behavior is illustrated in Figure 27 for two cases well away from their resonance phase angles. In both cases the solution is observed to rise very quickly and then oscillate at low amplitude about an apparent mean value. As shown, the oscillation in the lower frequency case is of larger amplitude and more persistent than the higher frequency case. The larger and more slowly damped oscillation of the lower frequency cases was consistently observed in all the cascade configurations and Mach numbers studied. This fact is of practical importance in determining the number of iterations required for a particular case to establish a representative solution.

Although the convergence of this method has not been proved, the observed behavior of the solution over

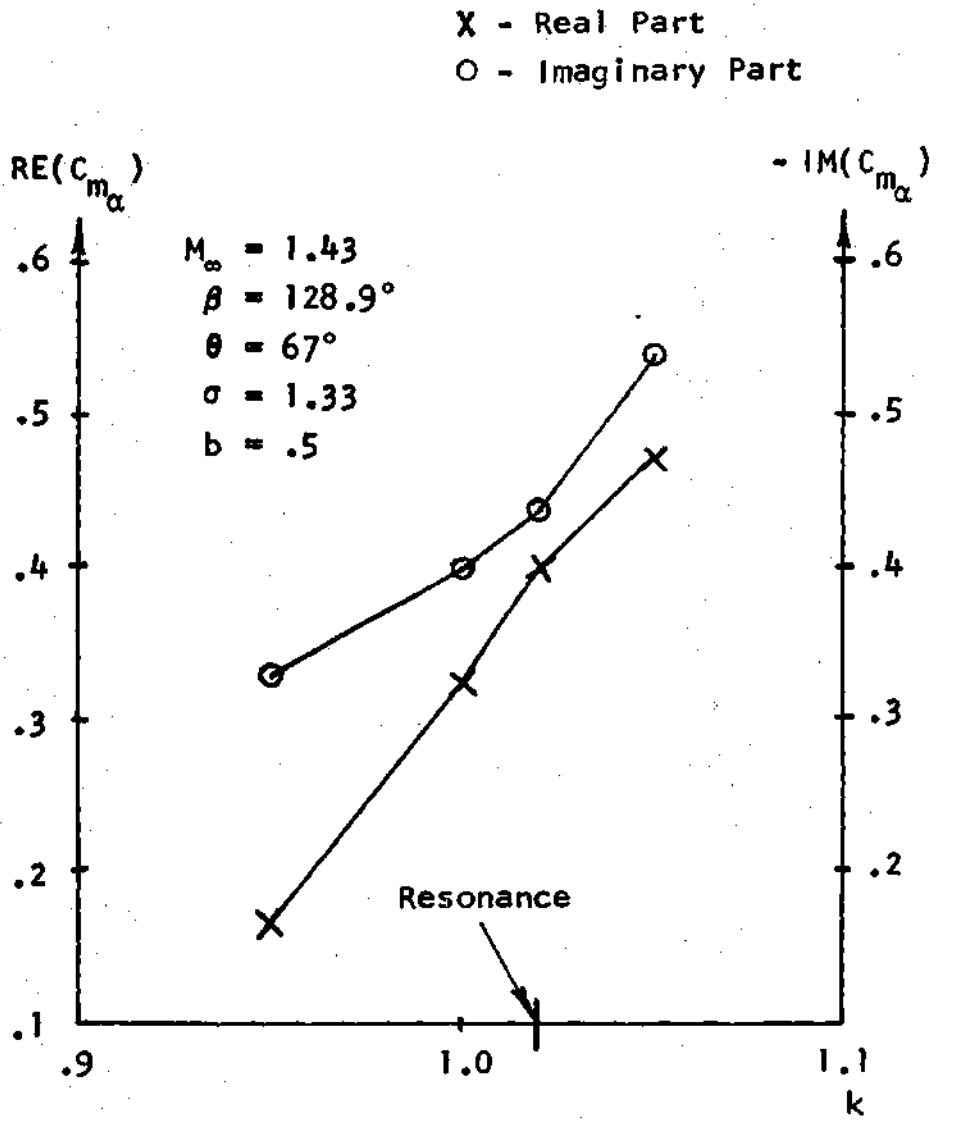

Figure 25. Behavior of the Solution Near Resonance Frequency - Case I

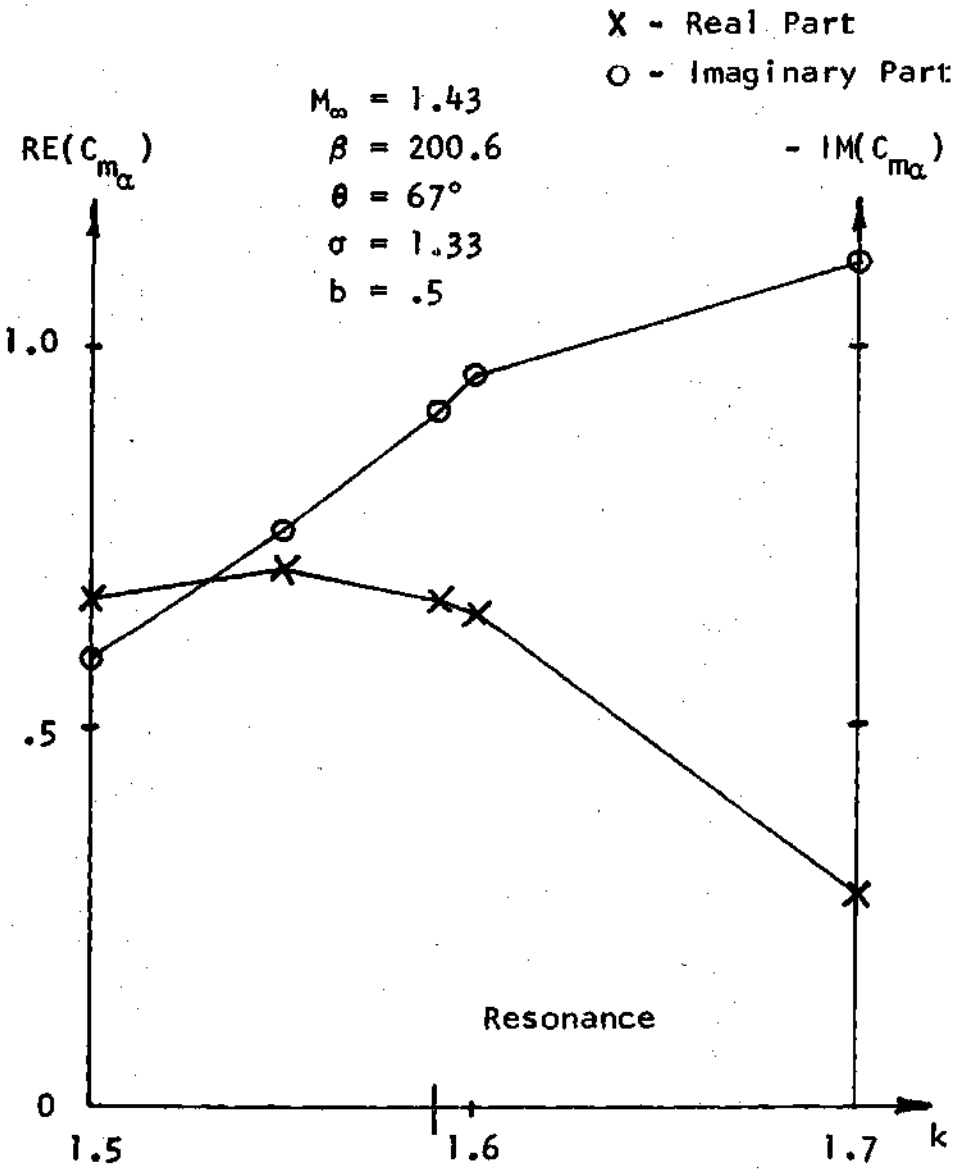

Figure 26. Behavior of the Solution Near Resonance Frequency - Case 2

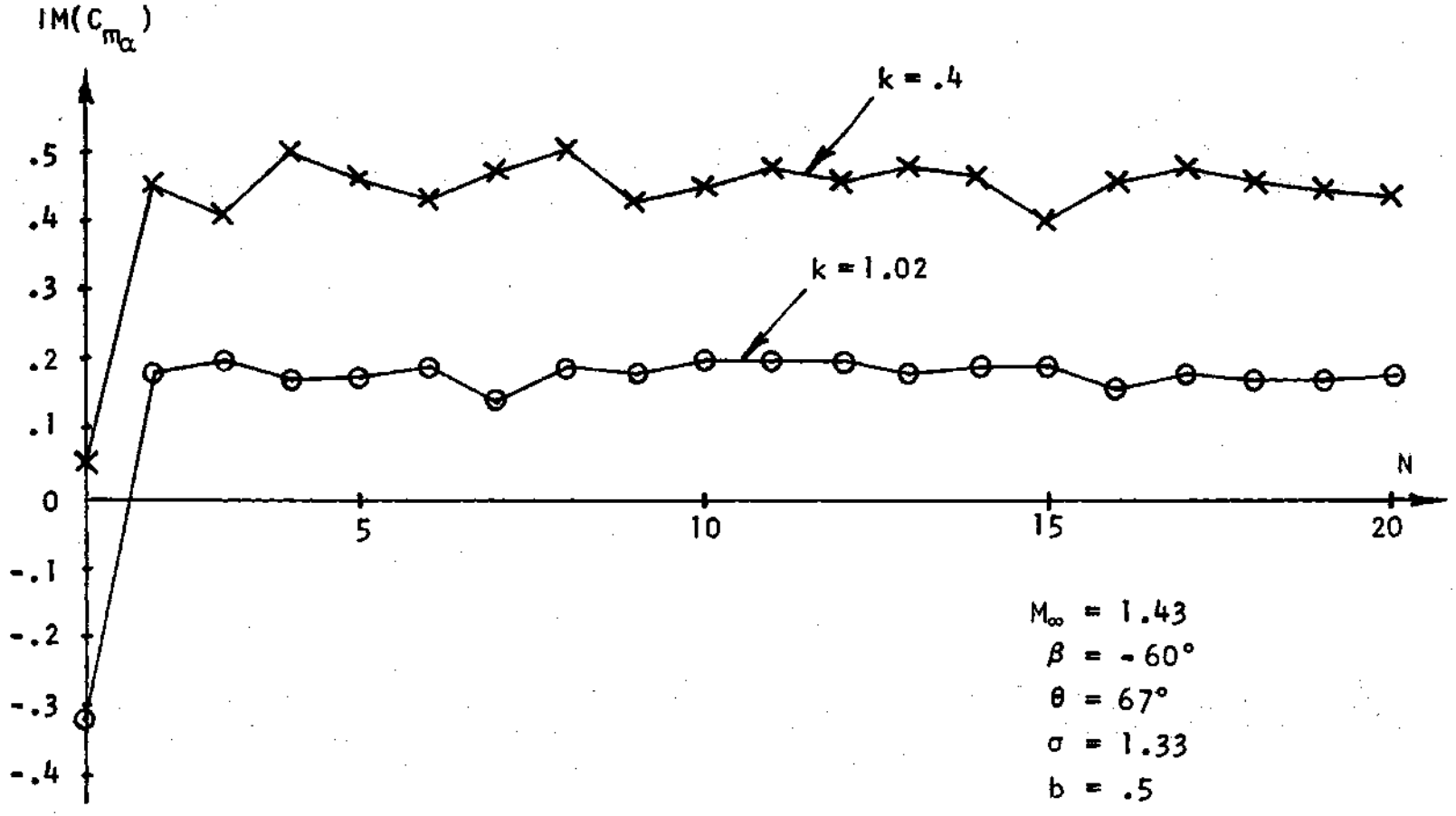

Figure 27. Convergence of the Method

a significantly large number of iterations would seem to indicate that with the exception of the resonance points, the solution is at least bounded as $N \to \infty$ and oscillates about some mean value. At best, the oscillation damps as $N \to \infty$ and the solution approaches a limiting value. In either case a solution which approaches a limit as $N \to \infty$ can be given by

$$\bar{S} = 1/(N-N_1 + 1) \sum_{n=N_1}^{N} S_n \qquad (115)$$

where S_n is the solution at the n^{th} iteration, N is the total number of iterations performed and N_1 is selected, based on experience, to obtain the best sample for the data set considered. Choice of N_1 beyond the first local maximum of the solutions plotted in Figure 27, for example, would yield a better solution for relatively small N.

In Figures 28 and 29 detailed pressure coefficient distributions are given for two different cascade configurations (shown in Figures 16 and 30 respectively) operating at different Mach number and reduced frequency conditions. The results after only ten iterations compare very favorably with an infinite cascade solution recently given for these cascades by Verdon and McCune [14]. The excellent agreement thus obtained helps to dispel concern

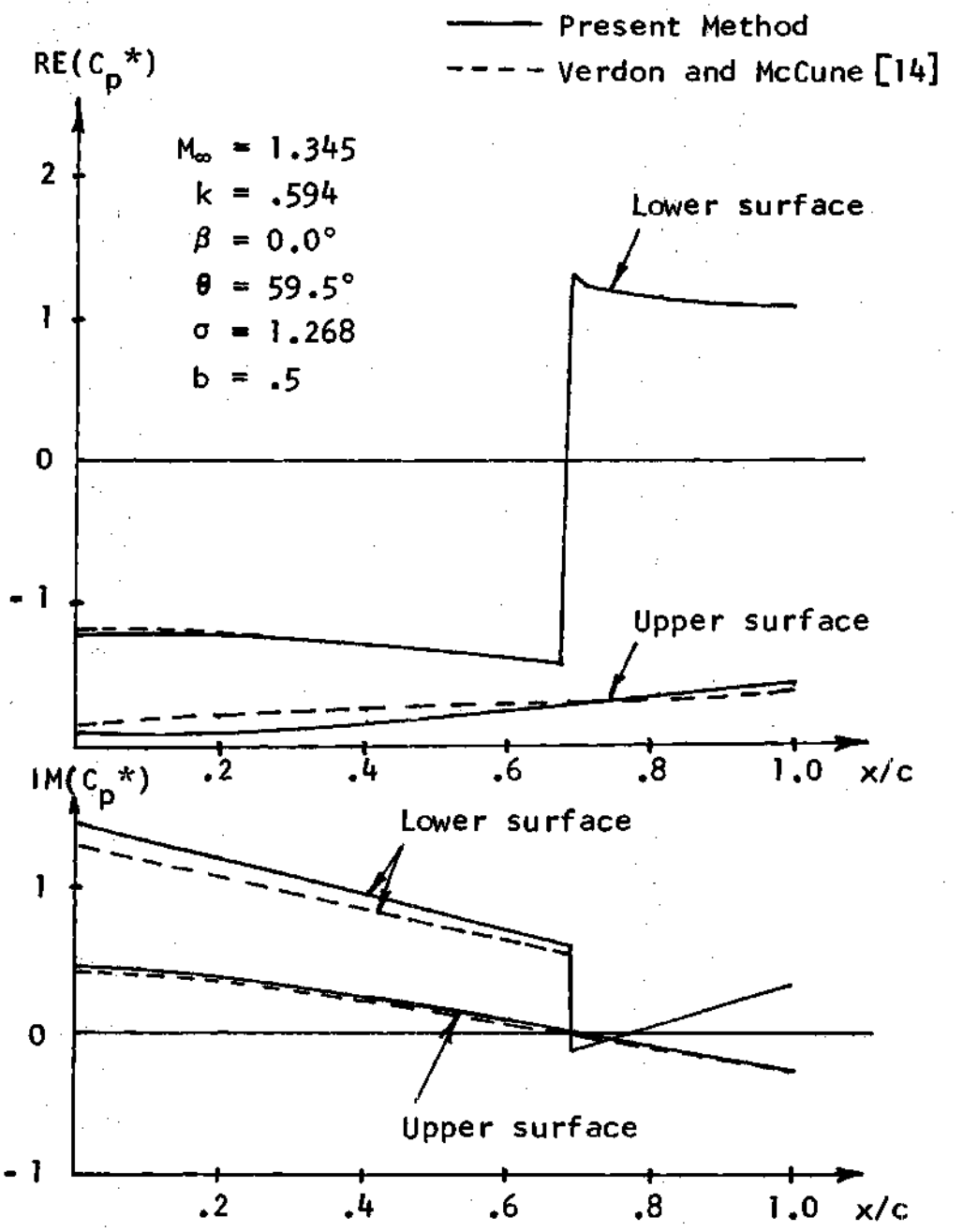

Figure 28. Surface Pressure Distributions for Cascade B (Rotational Oscillation)

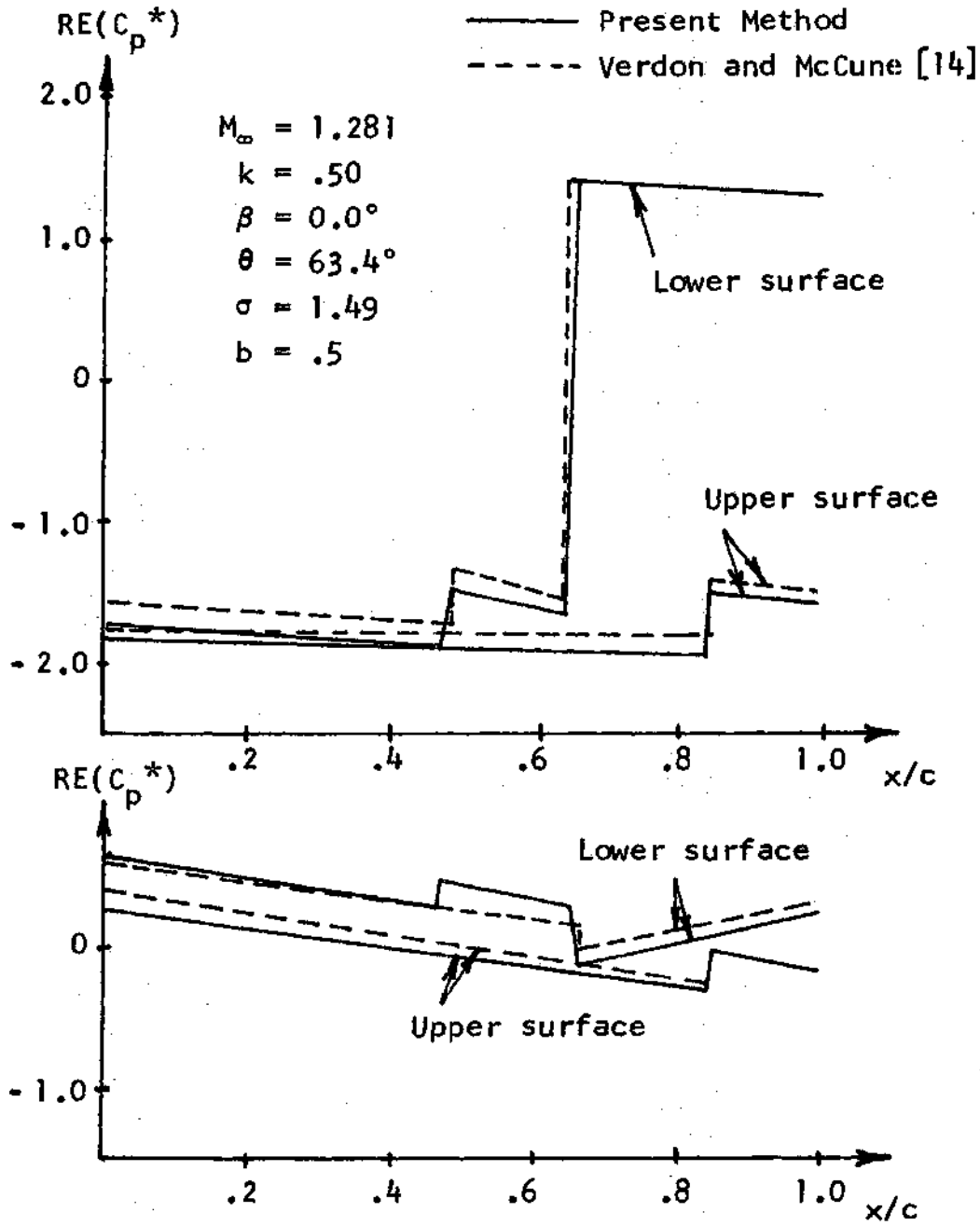

Figure 29. Surface Pressure Distributions of Cascade D (Rotational Oscillation)

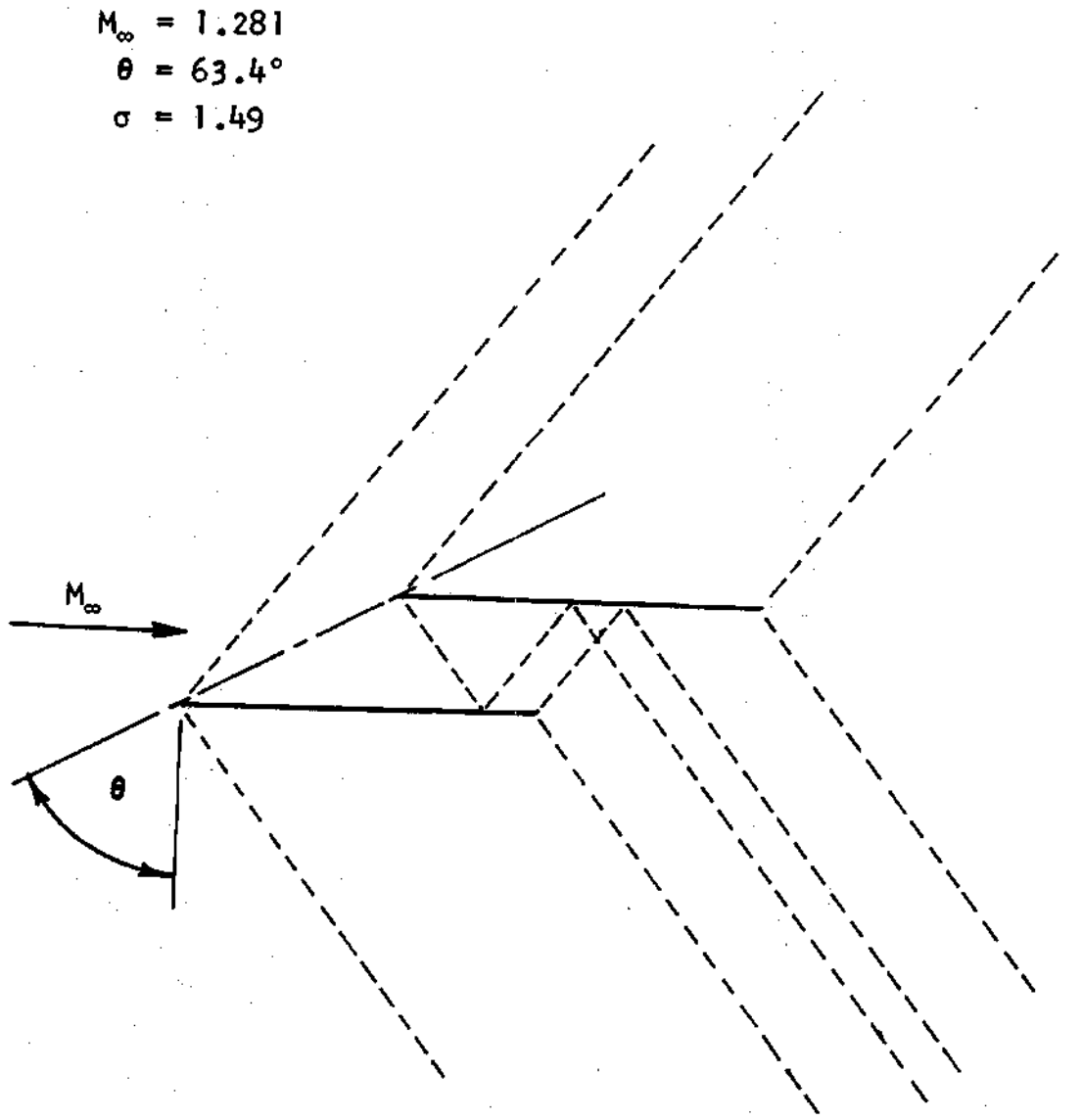

Figure 30. Cascade D

over the convergence of the present method, although it is pointed out that the Verdon-McCune method itself fails to converge over a wide range of interblade phase angles. The method presented here shows no unusual behavior over the same interblade phase angle range.

A brief parametric study is given below over a range of parameters considered typical of tip region sections of modern supersonic turbofan rotors. The parameters varied are Mach number, reduced frequency parameter, cascade stagger angle, blade chord to spacing ratio (cascade solidity) and interblade phase angle. The computer program output consists of complex unsteady lift and moment coefficients for both rotational and translational oscillation. For pure rotational and pure translational motion, the aerodynamic work/cycle is proportional to the out of phase component of the moment and lift respectively. Since this aerodynamic work/cycle determines the stability of the cascade under the assumed motion, the out of phase (imaginary) component can be considered indicative of the cascade stability. For the cases presented a positive imaginary component indicates work transferred from the air to the cascade (unstable) and a negative component indicates work from the cascade to the air (stable). Arbitrary simple harmonic rigid body cascade motion can be obtained by superposition of the separate rotational

and translational solutions. The general aerodynamic work/cycle expression for coupled bending and rotational oscillation is derived in Appendix E.

Generally, it is necessary for the actual dynamic stability analysis of a fan rotor to seek the most unstable interblade phase angle. Figure 22 shows the dramatic variation with interblade phase angle of the moment coefficient for midchord torsional oscillation of Cascade C (Figure 21) for several values of reduced frequency. It is noted that in each case the most unstable phasing occurs for phase angles between zero and -120.0 degrees. The most unstable phase angle, of course, depends on the particular cascade configuration, Mach number, and reduced frequency. The following parametric studies for Cascade E (shown in Figure 31) are performed for an interblade phase angle of -60.0 degrees.

Figure 32 shows the variation with reduced frequency of the out of phase pitching moment for midchord rotational oscillation of Cascade E. The results, presented for a range of Mach numbers, show a universal tendency toward increased stability with increasing reduced frequency. The particular interblade phase angle for which this study was performed shows the lowest Mach number to be the least stable over nearly all of the unstable low frequency range. It should be noted, however,

$M_\infty = 1.4$
$\theta = 60°$
$\sigma = 1.2$

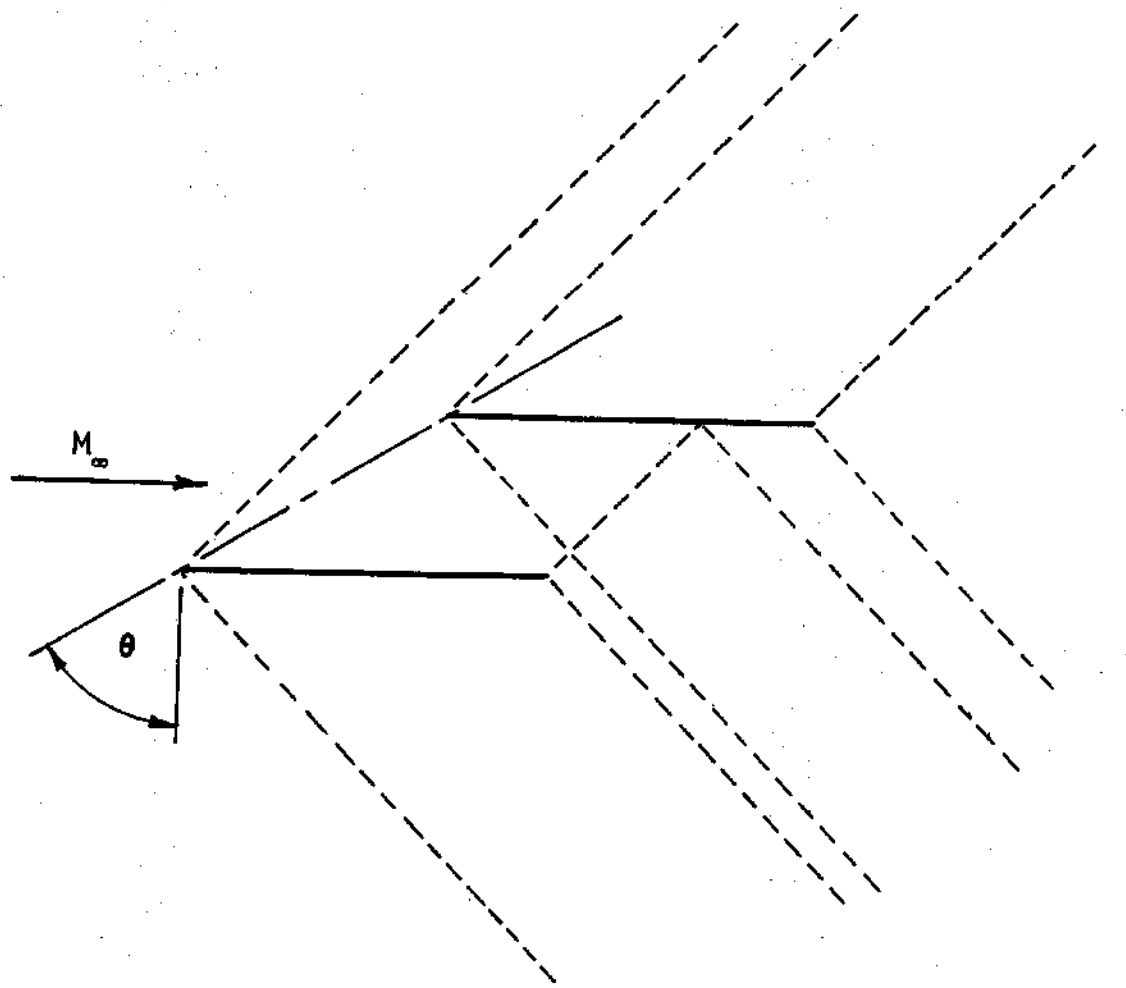

Figure 31. Cascade E

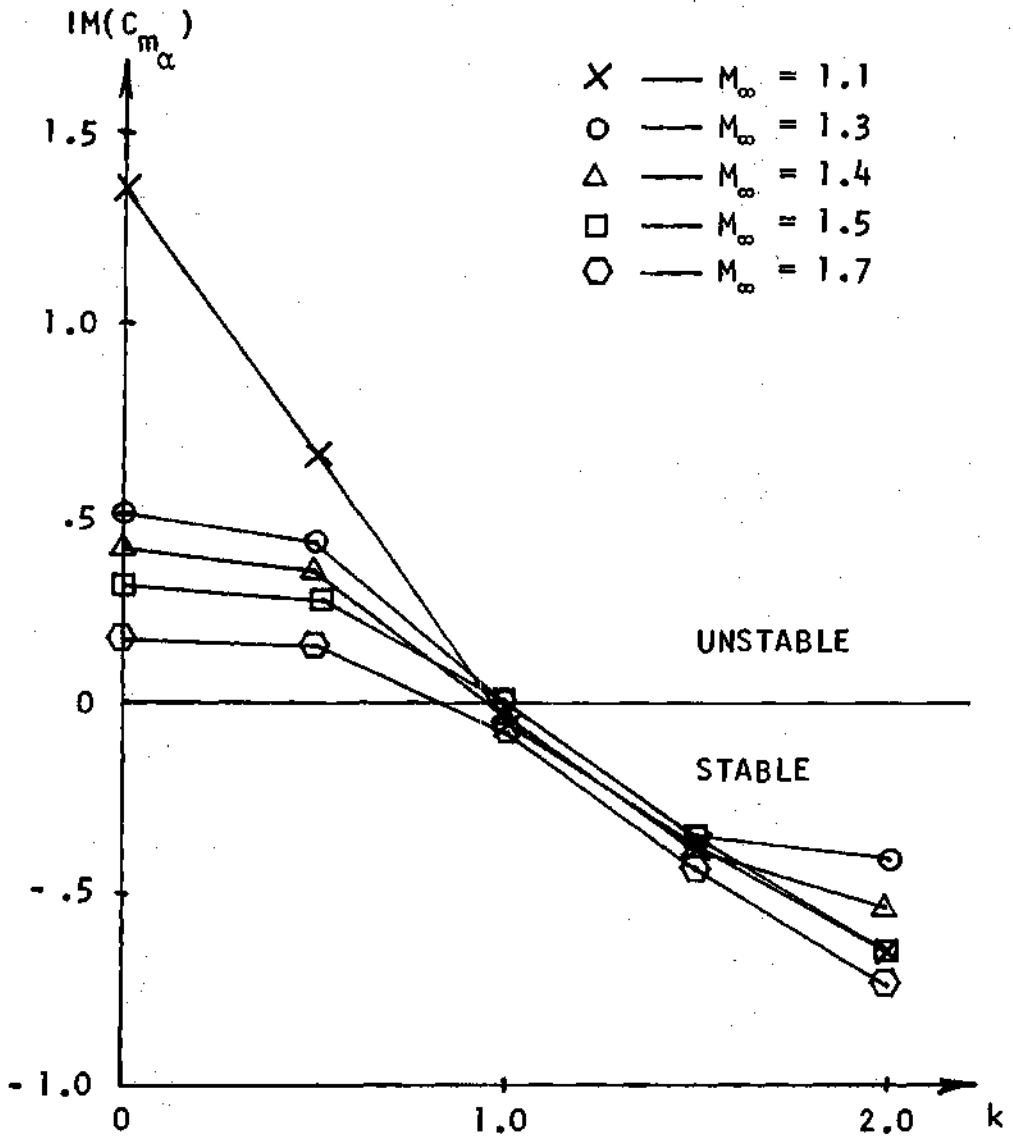

Figure 32. Effect of Reduced Frequency on the Out of Phase Moment Coefficient at Various Mach Numbers (Midchord Rotational Oscillation of Cascade E)

that the least stable interblade phase angle differs for each Mach number and reduced frequency point. In interpreting the results, it should be noted that, for a given rotor, the blade reduced frequency (based on the natural frequency*) and relative inlet Mach number are not independent but are both functions of the compressor rotational speed (RPM). Then with increasing RPM, the reduced frequency drops as the Mach number increases giving an overall decrease in stability with increased rotor speed. The results of an actual blade/wheel system flutter analysis using the present aerodynamic analysis to provide the needed unsteady lift and moment coefficients are given in Figure 33. The results are presented in terms of the system mechanical damping required for stability versus compressor RPM. The above discussed decrease in stability with RPM is clearly demonstrated. The predicted flutter RPM is obtained as the intersection of the damping available line with the damping required curve.

The out of phase component of the lift coefficient for translational oscillation (normal to the airfoil chord)

---

*It has been found that the flutter frequencies and mode shapes are generally very close to the natural frequencies and mode shapes for typical fan and compressor rotors. This result is counter to that observed in aircraft wing flutter due to the greatly increased density of the blade relative to the density of the surrounding air.

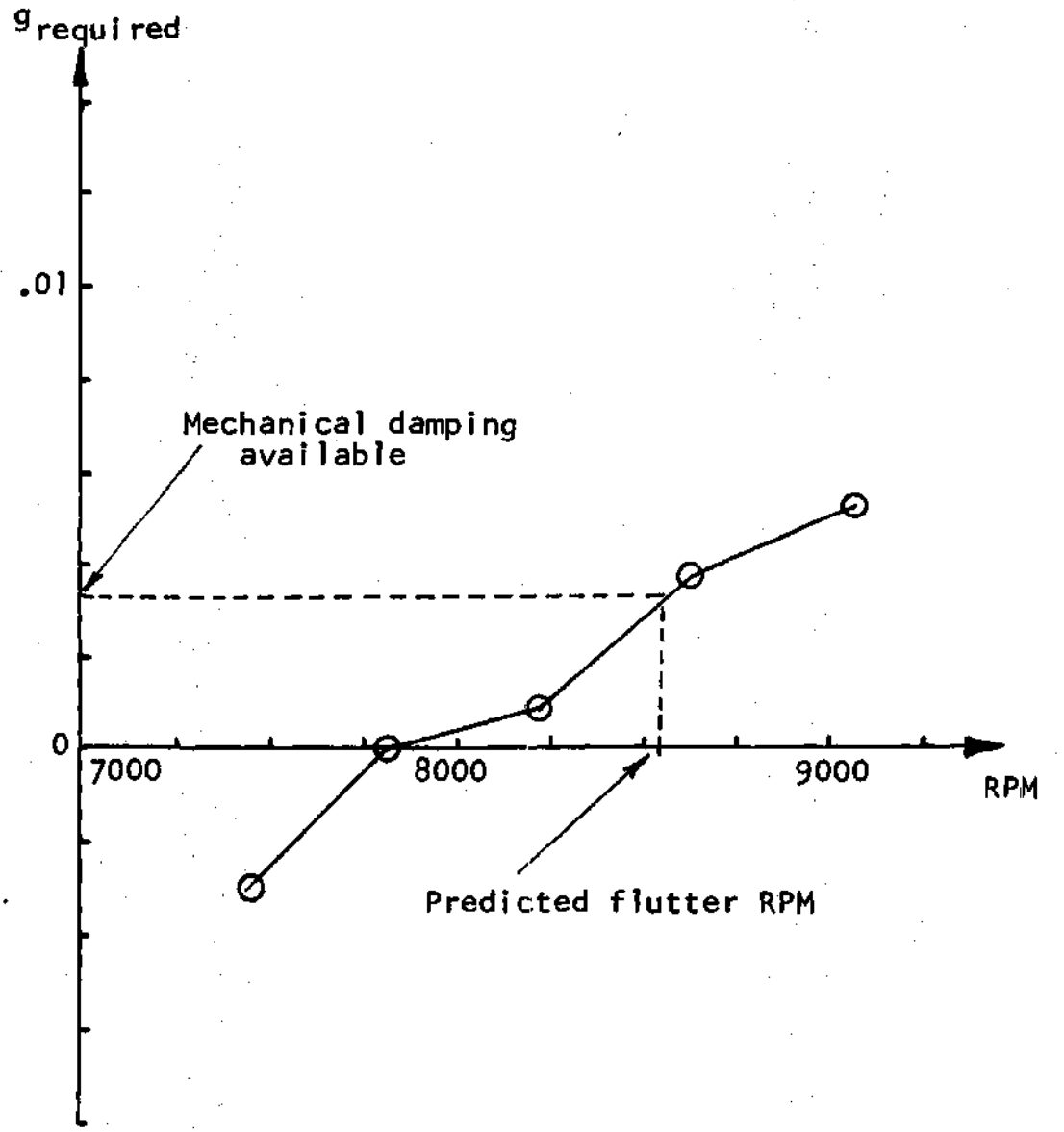

Figure 33. Damping Required for Stability as a Function of Compressor RPM for a Typical Turbofan Rotor

is shown in Figure 34. The results show that this type of oscillation is stable for all Mach number and reduced frequency combinations at the chosen phasing. These results are also plotted versus Mach number at selected frequencies in Figures 35 and 36. The lower frequency case is shown here to be more sensitive to changes in Mach number.

The very dramatic effects of changes in the cascade stagger angle are shown in Figures 37 and 38. The rotational oscillation case is seen to go from a stable situation at the lower stagger angles to an unstable situation at the higher stagger angles. One reason for such large changes in stability with change in stagger angle should be obvious from examination of the calculated pressure distributions for any of the presented cascades. The location of discontinuities in the pressure distributions is highly dependent on the cascade stagger angle. It follows that the lift and moment coefficients are also strongly influenced. The out phase component of the lift coefficient is also seen to be greatly affected by changes in cascade stagger angle, although for pure translational oscillation the cascade remains stable over the entire stagger angle range presented.

The effect of cascade solidity (chord to spacing ratio) on the moment coefficient for midchord rotational

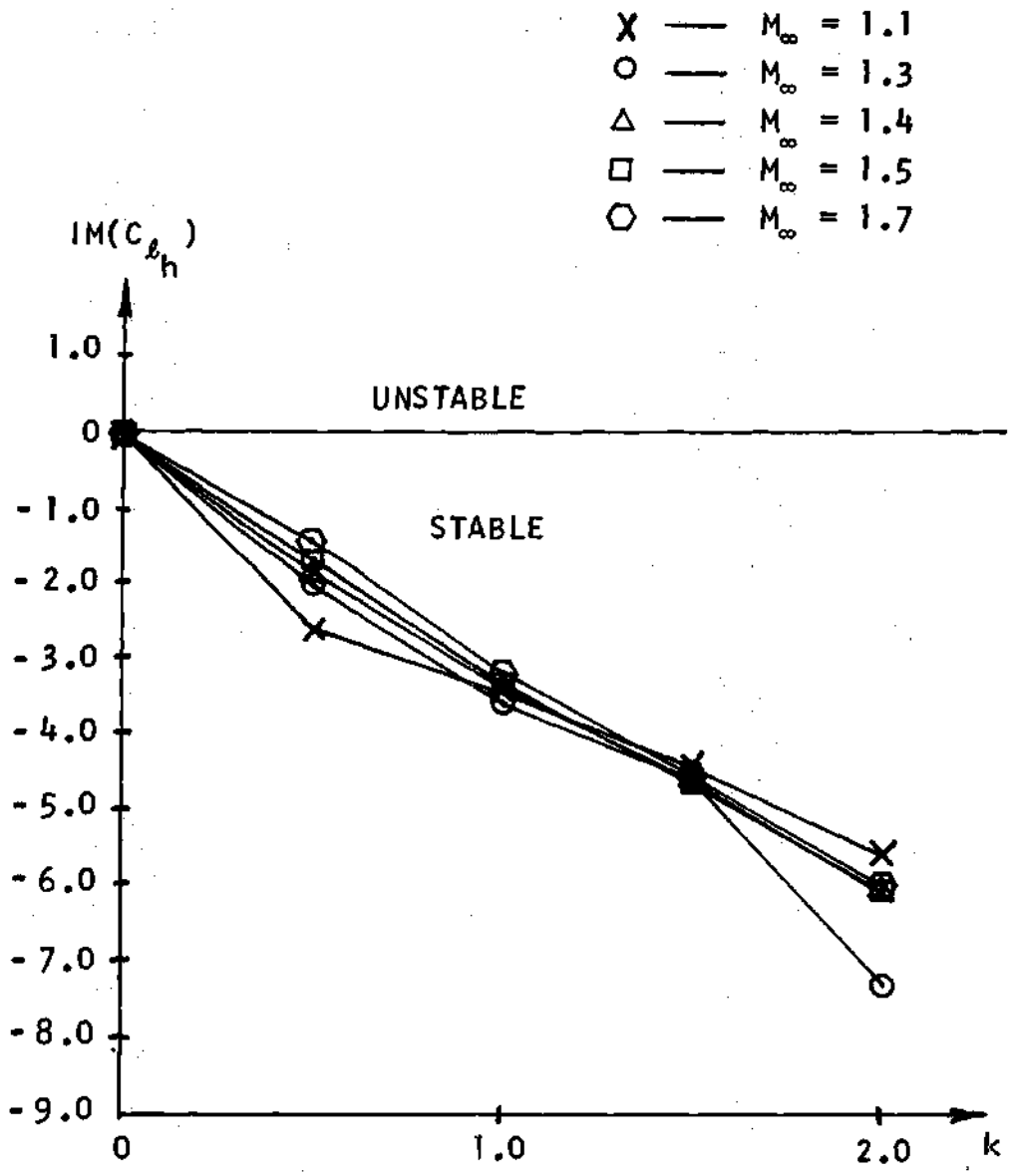

Figure 34. Effect of Reduced Frequency on the Out of Phase Lift Coefficient at Various Mach Numbers (Translational Oscillation of Cascade E)

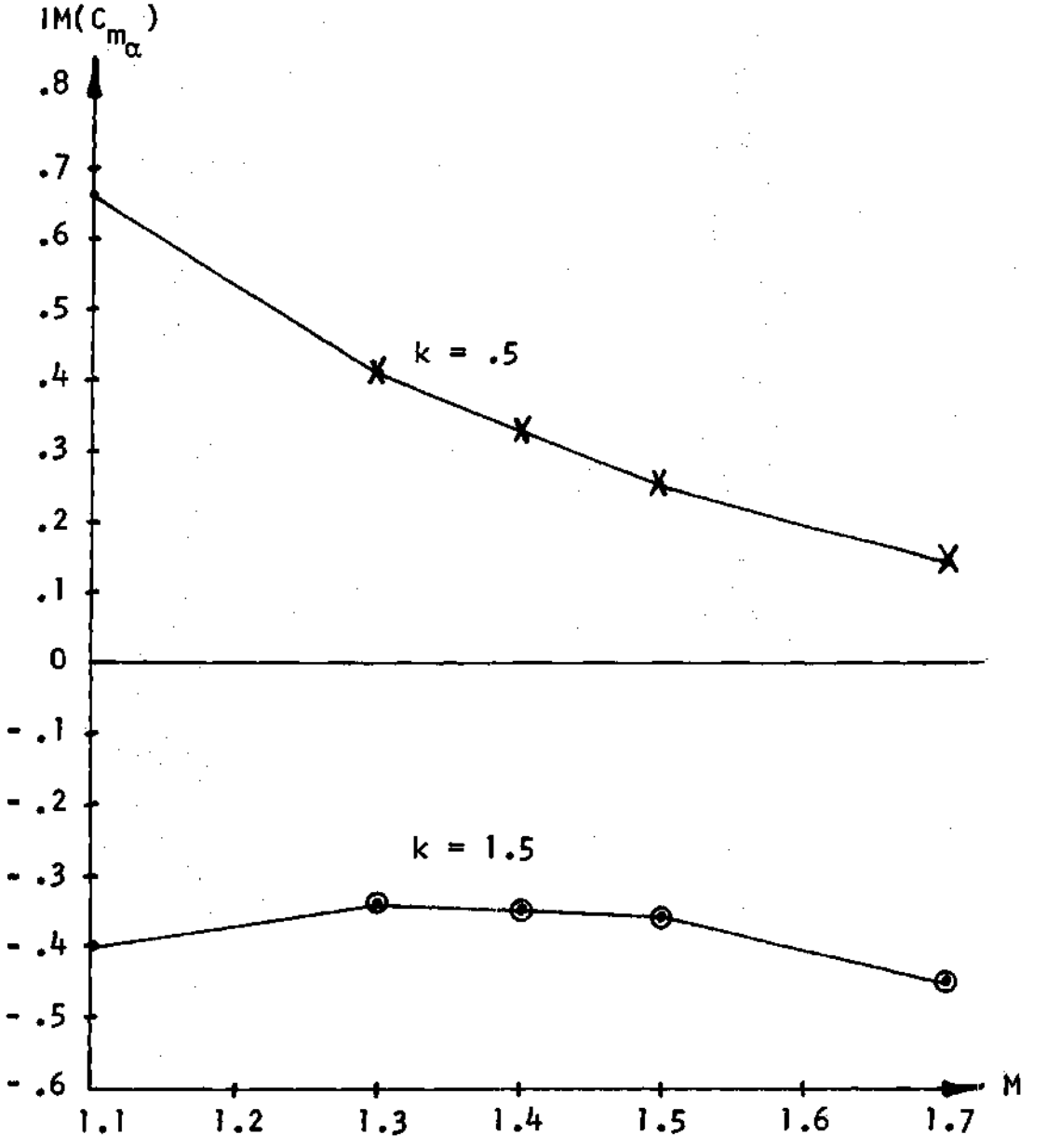

Figure 35. Effect of Mach Number on Out of Phase Moment Coefficient (Rotational Oscillation of Cascade E)

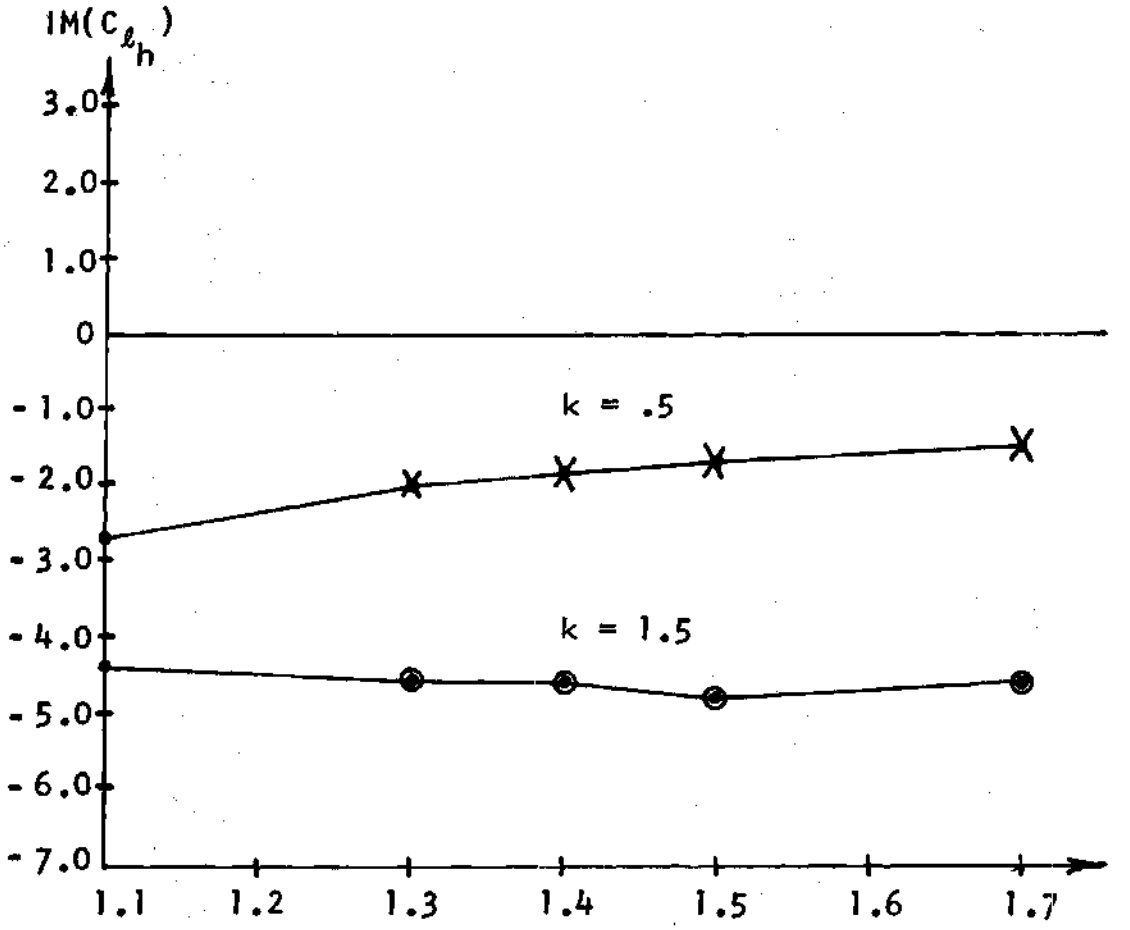

Figure 36. Effect of Mach Number on Out of Phase Lift Coefficient (Translational Oscillation of Cascade E)

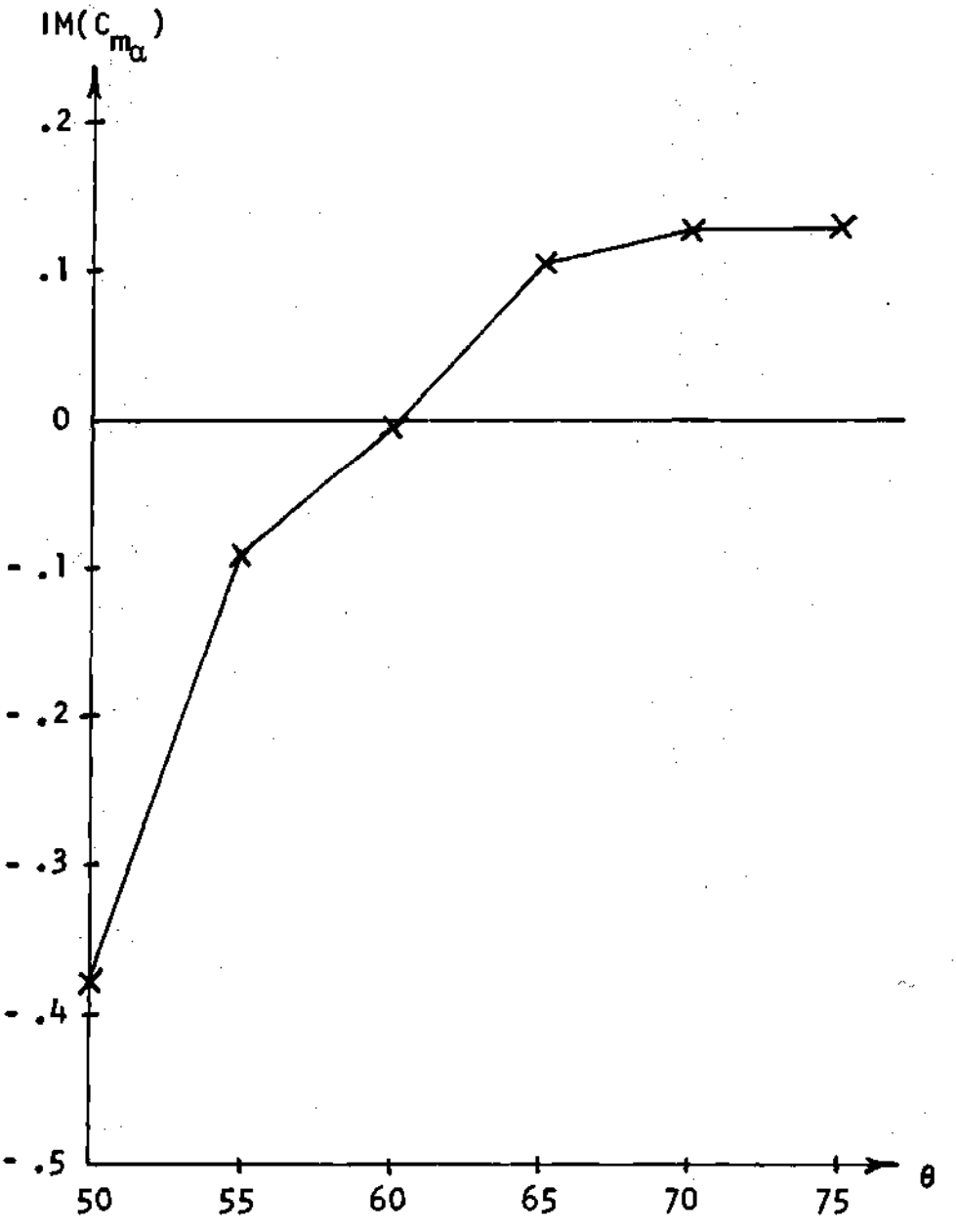

Figure 37. Effect of Stagger Angle on Out of Phase Moment Coefficient (Rotational Oscillation of Cascade E)

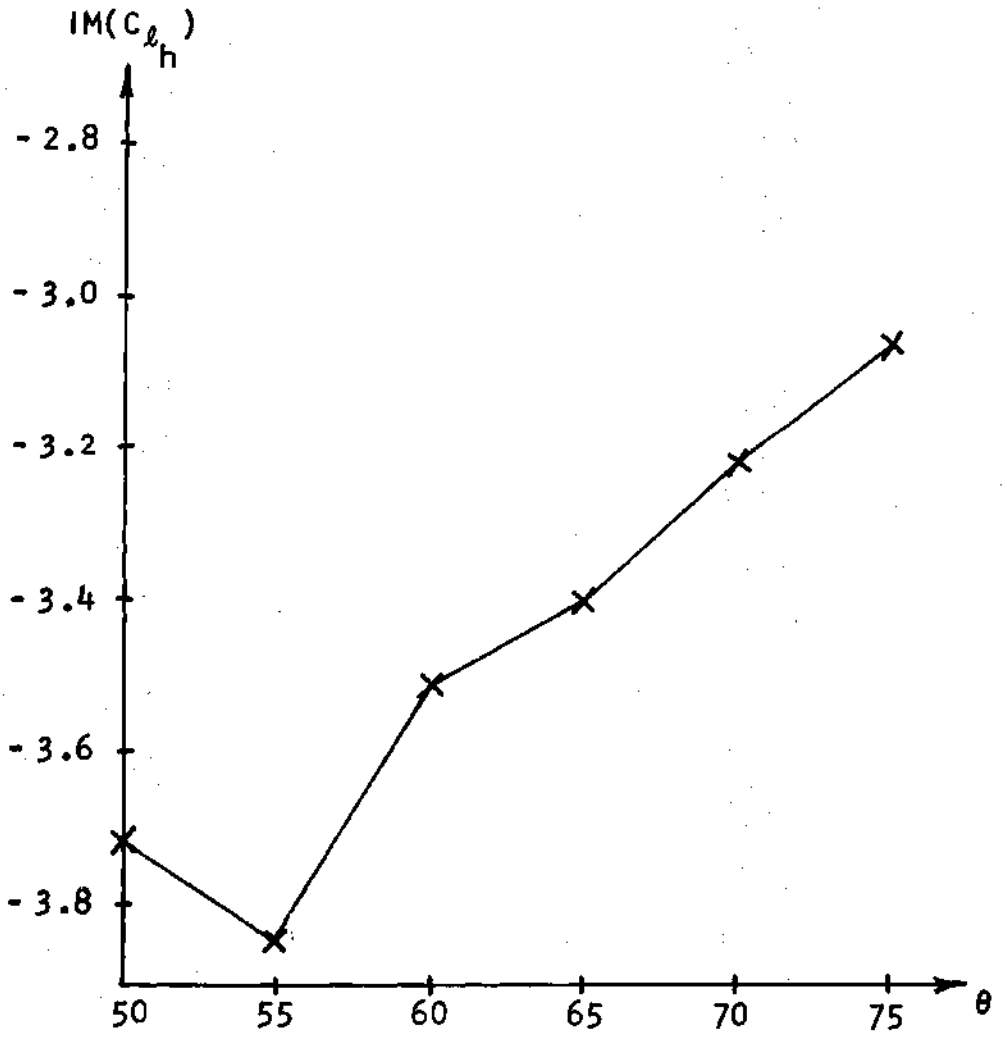

Figure 38. Effect of Stagger Angle on Out of Phase Lift Coefficient (Translational Oscillation of Cascade E)

oscillation is presented in Figure 39. The influence of changes in cascade solidity is also seen to be quite strong over the range of solidities given, however, typical supersonic fan designs usually fall in a narrower solidity range of 1.0 to 1.4 over which the changes are seen to be nominal.

A comparison of predicted pressure distributions with recently obtained low frequency unsteady cascade data is presented in Reference 31.

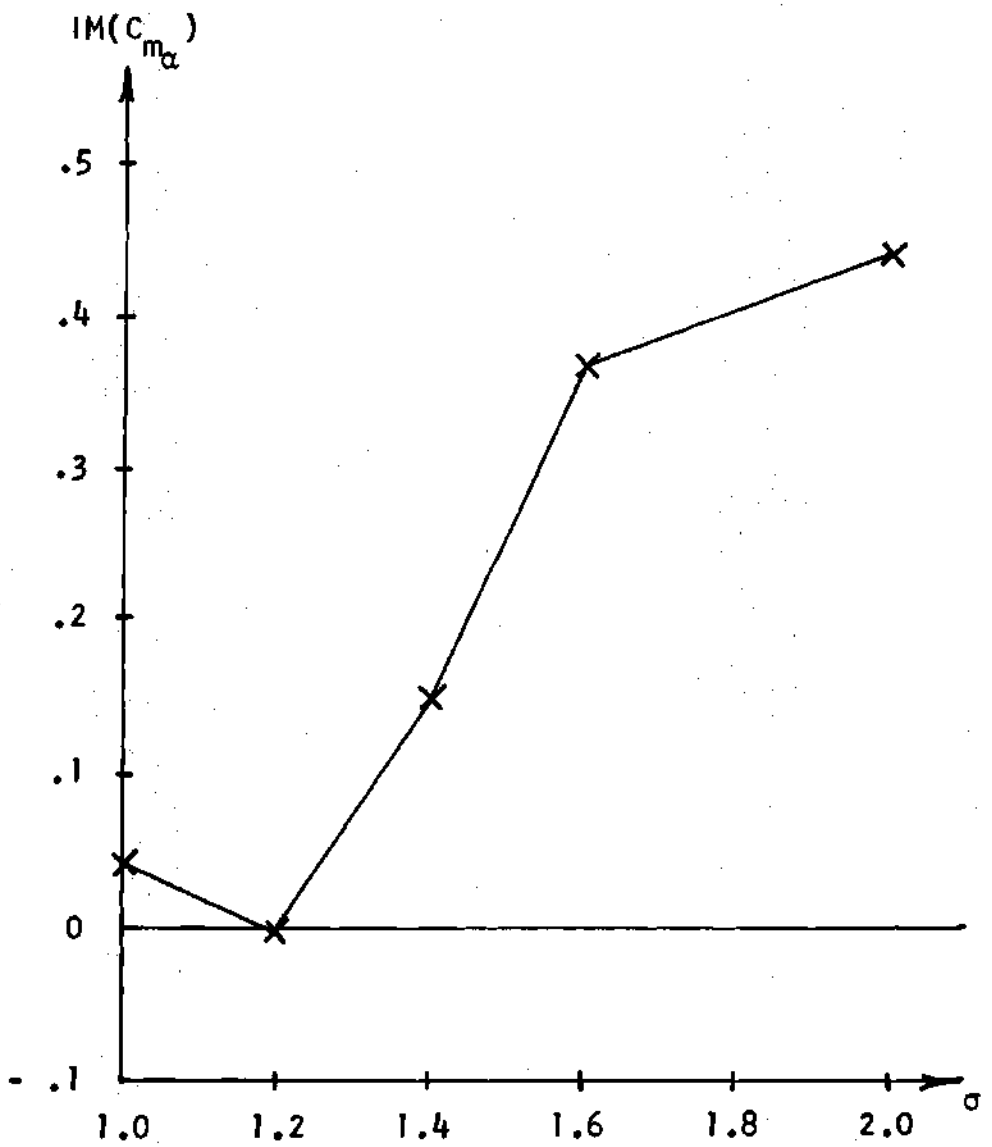

Figure 39. Effect of Cascade Solidity on Out of Phase Moment Coefficient (Rotational Oscillation of Cascade E)

CHAPTER V

CONCLUSIONS AND RECOMMENDATIONS

Conclusions

A solution to the supersonic cascade problem using a finite difference-pressure amplitude function method has been obtained. Solutions obtained using this method have been compared to some existing solutions in the limiting cases and to some very recently published results using different methods. Excellent agreement is obtained in all the limiting cases and any discrepancies in the cascade results (which also show generally good agreement) are explained. The convergence of the method was numerically investigated both in the neighborhood of and away from the resonance points. The influences of the various governing parameters on the solution are demonstrated in a brief parametric study of a typical cascade configuration.

The equations and boundary conditions for unsteady perturbations about a non-uniform steady flow are developed in natural orthogonal curvilinear coordinates. Physical interpretations are given for the new equations and boundary conditions.

The primary conclusions drawn from the present study are summarized as follows:

(1) The agreement of the finite difference-pressure amplitude method presented in this study with a variety of special cases and different methods establishes it as a viable solution method.

(2) The introduction of the pressure amplitude function as the primary independent variable rather than the velocity potential allows the exit region to be calculated without explicit consideration of the wake.

(3) The irregular pressure distributions over the aft portion of the upper blade surface obtained by Verdon's method are due to improper numerical reflection of characteristic discontinuities from the wake surface and are not inherent in the finite difference method. This same behavior was obtained when the present method was programmed in terms of the velocity potential, but is completely eliminated by reformulation in terms of the pressure amplitude function.

(4) The iterative method used in this analysis to enforce the periodicity conditions corresponds

precisely to adding one blade at a time to a finite cascade.

(5) The convergence of this method is in doubt at the resonance points. More importantly, however, the convergence in the neighborhood of resonance appears to be at least "convergent" in the sense of a mean although convergence is slow. Away from resonance, the iteration converged relatively quickly, although the convergence was still a function of frequency and interblade phase angle with the lower frequency and counter-rotating waves generally converging more slowly.

(6) The influence of non-uniform steady flow on the small perturbation unsteady cascade flow may be included within the limits of linear theory. The choice of the natural orthogonal curvilinear coordinate system allows the perturbation equation to be written in a form very similar to that for uniform steady flow in a rectangular Cartesian system.

(7) An additional term arises in the unsteady boundary conditions for the case of non-uniform steady flow which is needed to account for the displacement of the airfoil from its mean position in the non-uniform steady flow field.

Recommendations

At present, there is very little detailed experimental information with which the theoretical results may be compared. The data presented in Reference 31 compares favorably with the results obtained using the present analysis. The reduced frequencies of these experiments, however, are too low (less than .3) to be taken as representative of typical blade frequencies which are on the order of 1.0. Experimental verification is therefore needed in the higher reduced frequency ranges. The results of Reference 31 were obtained in a stationary linear cascade and are thus as nearly two-dimensional as possible. Detailed measurements of this kind are also needed in actual rotating blade rows to substantiate the two-dimensional assumption and thus validate (or invalidate) the strip theory approach to analysis of unsteady rotor flows.

The basic theoretical groundwork has been laid for the solution of the unsteady cascade problem under non-uniform steady flow conditions. The governing equations have been developed in such a way as to make the finite difference solution procedure used in the uniform steady flow case applicable to the non-uniform case with only minor modifications as long as the steady flow remains supersonic. Programming of this procedure would allow evaluation of moderate thickness, camber, and compression

ratio effects on the stability of supersonic cascades.

In order to analyze the unsteady supersonic cascade under high loading conditions (high compression ratio) a generalized perturbation analysis should be formulated and a solution method obtained which is applicable to rotational and mixed subsonic supersonic unsteady flows. This is due to the occurrence of strong inter-passage shocks which invalidates the assumptions of the present method as well as the spatial forward marching solution technique. The time marching solution techniques, developed for solving mixed steady flow problems, offer a possible approach to this problem, either by direct solution of the nonlinear unsteady equations or by solution of a generalized perturbation model.

APPENDICES

APPENDIX A

PERTURBATION OF THE SOUND SPEED

For isentropic flow

$$a/A = (P/\bar{P})^{\frac{\gamma-1}{2\gamma}} \tag{A-1}$$

where A and $\bar{P}$ are local steady values of the sound speed and static pressure. Expand a(P) in a Taylor's series to obtain

$$a(P) = A + \frac{\gamma-1}{2\gamma}\frac{A}{\bar{P}}(P-\bar{P}) + \ldots + \left[0\right](P-\bar{P})^2 \tag{A-2}$$

Then if

$$P' = P-\bar{P}$$

is a small perturbation in pressure, then a(P) is given to first order in the perturbation pressure as

$$a(P) = A + \frac{\gamma-1}{2\gamma}\frac{A}{\bar{P}}P' \tag{A-3}$$

so

$$a' = a - A = \frac{(\gamma-1)A}{2\gamma \bar{P}} P' = \frac{\gamma-1}{2\bar{\rho}A} P' \qquad (A-4)$$

In terms of the perturbation potential Equation (B-9) yields

$$a' = -\frac{\gamma-1}{2A}\left[\frac{\partial \phi'}{\partial t} + q_s \frac{\overline{\partial \phi'}}{\overline{\partial \ell}}\right] \qquad (A-5)$$

where the streamwise velocity perturbation, $\tilde{u}$, has been replaced by the streamwise derivative of the perturbation velocity potential. That is

$$\frac{\overline{\partial \phi'}}{\overline{\partial \ell}} = \tilde{u}$$

For uniform steady flow Equation (A-5) reduces to

$$a' = -\frac{\gamma-1}{2A}\left[\frac{\partial \phi'}{\partial t} + U_\infty \frac{\partial \phi'}{\partial x}\right] \qquad (A-6)$$

Assuming a simple harmonic time variation and defining

$$a^* = a' e^{-i\omega t} \Big/ a_\infty \delta$$

and

$$\hat{a} = A/a_\infty$$

then, using the notation of Chapter II,

$$a^* = -\frac{(\gamma-1)M_\infty^2}{2\hat{a}}\left[ik\phi^* + \tilde{q}\,\frac{\bar{\partial}\phi^*}{\bar{\partial}\ell'}\right] \qquad \text{(A-7)}$$

APPENDIX B

LINEARIZATION OF THE PRESSURE COEFFICIENT

Kelvin's equation is

$$\frac{\partial \phi}{\partial t} + q^2/2 + \int_{P_\infty}^{P} \frac{dP}{\rho} = f(t) \qquad \text{(B-1)}$$

Evaluation at upstream infinity where the flow is considered undisturbed gives

$$f(t) = U_\infty{}^2/2 \qquad \text{(B-2)}$$

so that

$$\int_{P_\infty}^{P} \frac{dP}{\rho} = -\left[\frac{\partial \phi}{\partial t} + \frac{1}{2}\left(q^2 - U_\infty{}^2\right)\right] \qquad \text{(B-3)}$$

Now let P' be an unsteady pressure perturbation from the local steady value $\overline{P}$ and let $\tilde{u}$ and $\tilde{v}$ be unsteady velocity perturbations along and normal to the steady flow streamline. Equation (B-3) can then be expressed as

$$\int_{P_\infty}^{\overline{P}} \frac{dP}{\rho} + \int_{\overline{P}}^{\overline{P}+P'} \frac{dP}{\rho} = -\left[\frac{\partial(\phi_s + \phi')}{\partial t} + \frac{1}{2}\left((q_s + \tilde{u})^2 + \tilde{v}^2 - U_\infty{}^2\right)\right] \qquad \text{(B-4)}$$

where

$$\phi = \phi_s + \phi' \qquad \left| \nabla\phi' \right| << \left| \nabla\phi_s \right|$$

$$q^2 = (q_s + \tilde{u})^2 + \tilde{v}^2 \qquad \left| \tilde{u} \right|, \left| \tilde{v} \right| << \left| q_s \right|$$

Noting that

$$\frac{\partial \phi_s}{\partial t} \equiv 0$$

and from steady flow that

$$\int_{P_\infty}^{P} \frac{dP}{\rho} = -\frac{1}{2}\left(q_s^2 - U_\infty^2\right) \tag{B-5}$$

then to first order in perturbation quantities Equation (B-4) gives

$$\int_{\bar{P}}^{\bar{P}+P'} \frac{dP}{\rho} = -\left[\frac{\partial \phi'}{\partial t} + q_s \tilde{u}\right] \tag{B-6}$$

Now since the flow has been assumed isentropic let

$$1/\rho = F(P)$$

be expanded in a Taylor's series about $P = \bar{P}$.

$$F(P) = F(\bar{P}) + F'(\bar{P})(P-\bar{P}) + \ldots + \left[0\right](P-\bar{P})^2 \tag{B-7}$$

then

$$\int_{\bar{P}}^{\bar{P}+P'} \frac{dP}{\rho} = \int_{\bar{P}}^{\bar{P}+P'} F(\bar{P}) + F'(\bar{P})(P-\bar{P}) + \ldots + \left[0\right] (P-\bar{P})^2 \quad dP \tag{B-8}$$

$$= F(\bar{P})P' + F'(\bar{P}) \frac{P'^2}{2} + \ldots + \left[0\right] P'^3$$

so that to first order in perturbation quantities Equation (B-6) becomes

$$P'/\bar{\rho} = -\left[\frac{\partial \phi'}{\partial t} + q_s \tilde{u}\right] \tag{B-9}$$

which for a simple harmonic time variation gives

$$P'^*/\bar{\rho} = -\left[i\omega t \bar{\phi} + q_s \frac{\bar{\partial \phi}}{\bar{\partial \ell}}\right] \tag{B-10}$$

where

$$P' = P'^* e^{i\omega t}$$

and

$$\tilde{u} = \frac{\bar{\partial \phi}'^*}{\bar{\partial \ell}} e^{i\omega t}$$

Introducting the normalized parameters

$$C_p^* = p'^* / \tfrac{1}{2} \rho_\infty U_\infty^2 \delta$$

$$\hat{\rho} = \bar{\rho} / \rho_\infty$$

$$\hat{q} = q_s / U_\infty$$

$$\phi^* = \phi'^* / U_\infty C \delta$$

$$\ell' = \ell / c$$

then the equation for the normalized perturbation pressure coefficient amplitude becomes

$$C_p^* = - 2\hat{\rho} \left[ik\phi^* + \hat{q} \frac{\partial \phi^*}{\partial \ell'} \right] \qquad \text{(B-11)}$$

APPENDIX C

DERIVATION OF THE POTENTIAL EQUATION IN ORTHOGONAL CURVILINEAR COORDINATES

Let q_Γ and q_χ be the velocity components along the orthogonal curvilinear coordinates (Γ,χ) of Figure 5. Also let θ_c be the local slope of the Γ coordinate line (measured to horizontal). Then

$$q_y = q_\chi \cos\theta_c + q_\Gamma \sin\theta_c \qquad (C\text{-}1)$$

and

$$q_x = q_\Gamma \cos\theta_c - q_\chi \sin\theta_c \qquad (C\text{-}2)$$

The two-dimensional continuity equation in rectangular Cartesian coordinates is

$$\frac{\partial \rho}{\partial t} + \frac{\partial \rho q_x}{\partial x} + \frac{\partial \rho q_y}{\partial y} = 0 \qquad (C\text{-}3)$$

Substituting for q_x and q_y from Equations (C-1) and (C-2), expanding the partial derivatives, and collecting terms gives

$$\frac{\partial \rho}{\partial t} + \left(\frac{\partial (\rho q_\Gamma)}{\partial x} \cos\theta_c + \frac{\partial (\rho q_\Gamma)}{\partial y} \sin\theta_c \right) \qquad \text{(C-4)}$$

$$+ \left(- \frac{\partial (\rho q_\chi)}{\partial x} \sin\theta_c + \frac{\partial (\rho q_\chi)}{\partial y} \cos\theta_c \right)$$

$$+ \rho q_\Gamma \left(- \frac{\partial \theta_c}{\partial x} \sin\theta_c + \frac{\partial \theta_c}{\partial y} \cos\theta_c \right)$$

$$+ \rho q_\chi \left(\frac{\partial \theta_c}{\partial x} \cos\theta_c + \frac{\partial \theta_c}{\partial y} \sin\theta_c \right) = 0$$

or

$$\frac{\partial \rho}{\partial t} + \frac{\bar{\partial}(\rho q_\Gamma)}{\bar{\partial} \ell} + \frac{\bar{\partial}(\rho q_\chi)}{\bar{\partial} n} + \rho q_\Gamma \frac{\bar{\partial} \theta_c}{\bar{\partial} n} + \rho q_\chi \frac{\bar{\partial} \theta_c}{\bar{\partial} \ell} = 0 \qquad \text{(C-5)}$$

where $\frac{\bar{\partial}}{\bar{\partial} \ell}$ and $\frac{\bar{\partial}}{\bar{\partial} n}$ are the total derivatives with respect to arc length along Γ and χ respectively given by

$$\frac{\bar{\partial}}{\bar{\partial} \ell} = \cos\theta_c \frac{\partial}{\partial x} + \sin\theta_c \frac{\partial}{\partial y} \qquad \text{(C-6)}$$

and

$$\frac{\bar{\partial}}{\bar{\partial} n} = - \sin\theta_c \frac{\partial}{\partial x} + \cos\theta_c \frac{\partial}{\partial y} \qquad \text{(C-7)}$$

Equation (C-5) can be expanded and written in the form

$$\frac{1}{\rho}\frac{\partial \rho}{\partial t} + \left(\frac{\bar{\partial} q_T}{\bar{\partial} \ell} + \frac{\bar{\partial} q_X}{\bar{\partial} n} \right) + \bar{q} \cdot \frac{1}{\rho} \nabla_c \rho \qquad \text{(C-8)}$$

$$+ q_T \frac{\bar{\partial} \theta_c}{\bar{\partial} n} - q_X \frac{\bar{\partial} \theta_c}{\bar{\partial} \ell} = 0$$

where

$$\nabla_c = \hat{\ell} \frac{\bar{\partial}}{\bar{\partial} \ell} + \hat{n} \frac{\bar{\partial}}{\bar{\partial} n} \qquad \text{(C-9)}$$

Assuming isentropic and irrotational flow then

$$\bar{q} = \nabla_c \phi \qquad \text{(C-10)}$$

and Kelvin's equation may be written as

$$\int_{P_\infty}^{P} \frac{dP}{\rho} = -\left[\frac{\partial \phi}{\partial t} + \frac{1}{2} (q^2 - U_\infty{}^2) \right] \qquad \text{(C-11)}$$

Taking the partial time derivative of Equation (C-3) gives

$$\frac{\partial}{\partial t} \int_{P_\infty}^{P} \frac{dP}{\rho} = -\left[\frac{\partial^2 \phi}{\partial t^2} + \frac{1}{2} \frac{\partial}{\partial t} (q^2) \right] \qquad \text{(C-12)}$$

but for any barotropic flow

$$P = P(\rho)$$

so that

$$\frac{\partial}{\partial t}\int_{P_\infty}^{P}\frac{dP}{\rho} = \frac{\partial}{\partial t}\int_{P_\infty}^{P} f(P)\,dP = \frac{\partial}{\partial t}F(P) \qquad (C\text{-}13)$$

$$= \frac{dF(P)}{dP}\frac{\partial P}{\partial t} = f(P)\frac{dP}{d\rho}\frac{\partial \rho}{\partial t} = \frac{1}{\rho}\frac{dP}{d\rho}\frac{\partial \rho}{\partial t}$$

then Equation (C-4) and (C-5) yield

$$\frac{1}{\rho}\frac{\partial \rho}{\partial t} = -\,1/a^2\left(\frac{\partial^2 \phi}{\partial t^2} + \frac{1}{2}\frac{\partial}{\partial t}q^2\right) \qquad (C\text{-}14)$$

Taking the gradient of Kelvin's equation likewise gives

$$\frac{1}{\rho}\nabla_c \rho = -\,1/a^2\left(\frac{\partial \bar{q}}{\partial t} + \frac{1}{2}\nabla_c q^2\right) \qquad (C\text{-}15)$$

Substituting Equations (C-14) and (C-15) into Equation (C-8) and remembering that

$$q_T = \frac{\partial \bar{\phi}}{\partial \ell}$$

and

$$q_\chi = \frac{\partial \bar{\phi}}{\partial n}$$

gives finally

$$\frac{\partial^2 \phi}{\partial \ell^2} + \frac{\partial^2 \phi}{\partial n^2} + \frac{\partial \phi}{\partial \ell} \frac{\partial \theta_c}{\partial n} - \frac{\partial \phi}{\partial n} \frac{\partial \theta_c}{\partial \ell} \tag{C-16}$$

$$= 1/a^2 \left(\frac{\partial^2 \phi}{\partial t^2} + \frac{\partial q^2}{\partial t} + \bar{q} \cdot \nabla_c q^2/2 \right)$$

APPENDIX D

EVALUATION OF EQUATION (105) IN TERMS OF SUCCESSIVE ITERATIONS

The geometry of the inlet solution domain (Figure 8) and the nature of the periodicity iteration are such that Equation (105) may not be directly evaluated at a particular iteration from flow field information generated during that iteration alone.

Let

$$\Delta x = s' \sin\theta$$

and

$$\Delta y = s' \cos\theta$$

Equation (105) written for the vertical velocity just ahead of the upper blade leading edge for the m^{th} iteration is then

$$v_m^*(0,\Delta y) = v_m^*(-\Delta x,\Delta y)e^{-ik\Delta x} - \frac{1}{2}\int_{-\Delta x}^{0} \frac{\partial}{\partial y'}\left(C_p^*(x',\Delta y)\right) e^{ikx'} dx' \qquad (D\text{-}1)$$

Now define

$$I_{m,n} = -\frac{1}{2}\int_{-\Delta x}^{0} \frac{\partial}{\partial y'}\left(C_p^*(x', n\Delta y)\right) e^{ikx'}\, dx' \qquad (D\text{-}2)$$

so that

$$v_m^*(0,\Delta y) = v_m^*(-\Delta x,\Delta y)\, e^{-ik\Delta x} + I_{m,1} \qquad (D\text{-}3)$$

but $v_m^*(-\Delta x,\Delta y)$ is obtained by applying the periodicity condition to the previous iteration. Therefore, using Equation (12)

$$v_m^*(-\Delta x,\Delta y) = e^{i\beta} v_{m-1}^*(0,2\Delta y) \qquad (D\text{-}4)$$

but

$$v_{m-1}^*(0,2\Delta y) = v_{m-1}^*(-\Delta x,2\Delta y) - \frac{1}{2}\int_{-\Delta x}^{0} \frac{\partial}{\partial y'}\left(C_p^*(x', 2\Delta y)\right) e^{ikx'}\, dx'$$

$$= v_{m-1}^*(-\Delta x,2\Delta y) + I_{m-1,2} \qquad (D\text{-}5)$$

Then substituting Equations (D-4) and (D-5) into Equation (D-3) gives

$$v_m^*(0,\Delta y) = e^{i(\beta - k\Delta x)}\left[v_{m-1}^*(-\Delta x,2\Delta y) + I_{m-1,2}\right] + I_{m,1} \qquad (D\text{-}6)$$

Replacing $v^*_{m-1}(-\Delta x, 2\Delta y)$ in like manner gives

$$v_m^*(0,\Delta y) = e^{i(\beta - k\Delta x)}\left[e^{i(\beta - k\Delta x)}\cdot\right. \tag{D-7}$$

$$\left.\left(v^*_{m-2}(-\Delta x, 3\Delta y) + I_{m-2,3}\right) + I_{m-1,2}\right]$$

$$+ I_{m,1}$$

Repeating this process m times and recognizing that

$$v_o^*(-\Delta x, m\Delta y) = 0 \tag{D-8}$$

then the result is generalized as

$$v_m^*(0,\Delta y) = \sum_{j=1}^{m} a_j I_{m+1-j,j} \tag{D-9}$$

where a_j is defined by

$$a_j = e^{i(j-1)(\beta - k\Delta x)} \tag{D-10}$$

APPENDIX E

AERODYNAMIC WORK CALCULATION FOR ARBITRARY AIRFOIL MOTION

It is easily verified by direct substitution into Equation (11) that either the real or the imaginary part of $\phi^* e^{i\omega t}$ satisfies the original time dependent equation subject to the actual airfoil motion given respectively as either the real or imaginary part of the complex boundary condition, Equation (26). The actual corresponding unsteady lift and moment are thus given by either the real or imaginary parts of their complex representations. The aerodynamic work/cycle, defined as positive for work transferred from the air to the blade, may be calculated by integrating the actual moment through the actual angle plus the actual lift through the actual normal displacement over a cycle of the oscillation. The aerodynamic work/cycle can thus be calculated using either the real or imaginary components. Choosing the real part and letting

$$\tau = \omega t$$

the aerodynamic work/cycle is given as

$$W_a = \int_0^{2\pi} RE(M^*) \cdot RE(\frac{d\tilde{\alpha}}{d\tau})\, d\tau \qquad (E\text{-}1)$$

$$+ \int_0^{2\pi} RE(L^*) \cdot RE(\frac{d\tilde{h}}{d\tau})\, d\tau$$

Now let the translational oscillation lag the rotational oscillation by the phase angle, θ_b. Also let

$$\tilde{\alpha} = \alpha e^{i\tau}$$

$$\tilde{h} = h e^{i\tau} = ch' e^{i\tau} = c\bar{h}' e^{-i\theta_b} e^{i\tau}$$

The work expression can then be written as

$$W_a = \tfrac{1}{2}\rho_\infty U_\infty{}^2 c^2 \int_0^{2\pi} RE\left[(C_{m_\alpha}\alpha + C_{m_h}\bar{h}' e^{-i\theta_b}) e^{i\tau}\right] \alpha \sin\tau d\tau \qquad (E\text{-}2)$$

$$- \tfrac{1}{2}\rho_\infty U_\infty{}^2 c^2 \int_0^{2\pi} RE\left[(C_{\ell_\alpha} e^{i\theta_b}\alpha + c_{\ell_h}\bar{h}') e^{i\tau}\right] \bar{h}' \sin\tau d\tau$$

Taking the appropriate real parts of the integrand, integrating and collecting terms gives

$$W_a = \tfrac{1}{2}\rho_\infty U_\infty{}^2 c^2 \pi \left\{ IM(C_{m_\alpha})\, \alpha^2 + \right. \qquad (E\text{-}3)$$

$$\left[\left[\left(IM(C_{m_h}) + IM(C_{\ell_\alpha})\right)\cos\theta + \left(RE(C_{\ell_\alpha}) - RE(C_{m_h})\right)\sin\theta\right]\alpha\bar{h}' + IM(C_{\ell_h})\,\bar{h}'^2\right\}$$

BIBLIOGRAPHY

1. Whitehead, D. S., "Torsional Flutter of Unstalled Cascade Blades at Zero Deflection," British Aeronautical Research Council, London, R. and M. No. 3429, 1964.

2. Smith, S. N., "Discrete Frequency Sound Generation in Axial Flow Turbomachines," British Aeronautical Research Council, London, R. and M. No. 3709, 1972.

3. Whitehead, D. S., "The Effect of Compressibility on Unstalled Torsional Flutter," Cambridge University Engineering Department Report A-Turbo/TR51, August 1973.

4. Kaji, S. and Okazaki, T., "Propagation of Sound Waves Through a Blade Row," Journal of Sound and Vibration, Vol. 11, P. 355, 1970.

5. Snyder, L. E., "Supersonic Torsional Flutter in Cascades," Pratt and Whitney Aircraft Report No. PWA TM-4701, April, 1973.

6. Carta, F. O., "Coupled Blade-Disc-Shroud Flutter Instabilities in Turbojet Engine Rotors," American Society of Mechanical Engineers, Winter Annual Meeting and Energy Systems Exposition, New York, New York, November 27 - December 1, 1966, Paper No. 66-WA/GT-6.

7. Fleeter, S., "Aeroelasticity in Turbomachines," Proceedings of a Workshop held at Detroit Diesel Allison, Indianapolis, June 1-2, 1972, Project Squid, Office of Naval Research.

8. Lane, F., "Supersonic Flow Past an Oscillating Cascade with Supersonic Leading Edge Locus," Journal of the Aeronautical Sciences, Vol. 24, January 1957. pp. 65-66.

9. Platzer, M. F. and Chalkey, H. G., "Theoretical Investigation of Supersonic Cascade Flutter and Related Interference Problems," AIAA Paper No. 72-377, April 1972.

10. Platzer, M. F. and Pierce, C. V., "Theoretical Investigation of Wind Tunnel Interference Effects Upon Fluttering Panels and Airfoils in Low Supersonic Flow," Proc. of AIAA/ASME 11th Structures, Structural Dynamics and Materials Conference, Denver, Colorado, April 1970.

11. Verdon, J. M., "The Unsteady Aerodynamics of a Finite Supersonic Cascade with Subsonic Axial Flow," Transactions of ASME, Series E, Journal of Applied Mechanics, Vol. 40, No. 3, September 1973, pp. 667-671.

12. Tyler, J. M. and Sofrin, T. G., "Axial Compressor Noise Studies," SAE Trans., Vol. 70, 1962.

13. Samoylovich, G. S., Unsteady Flow Around and Aeroelastic Vibration in Turbomachine Cascades, translated by Translation Division Foreign Technology Division, WPAFB, Ohio, February 1971.

14. Verdon, J. M. and McCune, J. E., "The Unsteady Supersonic Cascade in Subsonic Axial Flow," AIAA Paper No. 75-22, presented at the AIAA 13th Aerospace Sciences Meeting, Pasadena, California, January 20-22, 1975.

15. Kurosaka, M., "On the Unsteady Supersonic Cascade with a Subsonic Leading Edge — An Exact First Order Theory: Parts 1 and 2," Transactions of ASME, Series A, Journal of Engineering for Power, Vol. 96, No. 1, January 1974, pp. 13-31.

16. Nagashima, T. and Whitehead, D. S., Aerodynamic Forces and Moments for Vibrating Supersonic Cascade Blades," Cambridge University Engineering Department Report A-Turbo/TR59, 1974.

17. Brix, C. W. and Platzer, M. F., "Theoretical Investigation of Supersonic Flow Past Oscillating Cascades with Subsonic Leading Edge Locus," AIAA Paper No. 74-14 presented at the AIAA 12th Aerospace Sciences Meeting, Washington, D. C., January 1974.

18. Jay, R. L., "Effect of TF41-A2 Fan Rotor Speed Increase and Afterburner Operation on the Dynamics of the LP2 and LP3 Blades," Detroit Diesel Allison Internal Report No. AF.0222-069, December 1973.

19. Ni, R., "Nonstationary Aerodynamics of Arbitrary Cascades in Compressible Flow," Ph.D. thesis, Stevens Institute of Technology, Hoboken, New Jersey, June 1974.

20. Fung, Y. C., An Introduction to the Theory of Aeroelasticity, Dover Publications Inc., New York, 1945.

21. Bisplinghoff, R. L., Ashley, H., and Halfman, R. L., Aeroelasticity, Addison - Wesley Publishing Company Inc., Reading, Massachusetts, 1955.

22. Lamb, H., Hydrodynamics, Dover Publications, New York, 6th edition, 1932.

23. Morse, P. M., and Feshbach, H., Methods of Theoretical Physics, McGraw-Hill, New York, Toronto, London, Volume 1, 1953.

24. Lichtfuss, H. J., and Starken, H., "Supersonic Cascade Flow," From Progress in Aerospace Science, Volume 15, Oxford, New York: Pergamon Press Ltd., 1974.

25. Shapiro, A. H., The Dynamics and Thermodynamics of Compressible Fluid Flow, Ronald Press Co., New York, Vol. 1, 1953.

26. Hildebrand, J. B., Finite Difference Equations and Simulations, Prentice - Hall Inc., Englewood, Cliffs, New Jersey, 1968.

27. Miles, J. W., The Potential Theory of Unsteady Supersonic Flow, Cambridge University Press, 1959.

28. Garrick, J. E., and Rubinow, S. J., "Flutter and Oscillating Air Force Calculations for an Airfoil in Two-Dimensional Supersonic Flow," NACA Report 846, 1946.

29. Chalkley, H. G., "A Study of Supersonic Cascade Flutter," Aeronautical Engineers Thesis, Naval Postgraduate School, Monterey, California, June, 1972.

30. Synder, L. E., and Commerford, G. L., "Supersonic Unstalled Flutter in Fan Rotors; Analytical and Experimental Results," ASME Paper No. 74-GT-40, November 1973.

31. Fleeter, S., Novick, A. S., Riffel, R. E., and Caruthers, J. E., "An Experimental Determination of the Unsteady Aerodynamics in a Controlled Oscillating Cascade," ASME Paper No. 76-GT-17, December 1975.

VITA

John Everett Caruthers was born in West Point, Georgia on September 19, 1945. His parents are Lester Everett Caruthers, originally from Fredricktown, Missouri, and Jewel Evelyn (Bishop) Caruthers, originally from Wingate, Texas.

He was raised in Lanett, Alabama where he attended the public school system and where he graduated from Lanett High School in 1963. He enrolled at Auburn University fall quarter 1963 where he received a B.S. degree in Aerospace Engineering in 1967. He immediately entered the Graduate School in Aerospace Engineering under a National Science Foundation Fellowship.

In 1969 he was employed by the Mathematical Sciences group of Allison Division of General Motors. He completed his M.S. degree while employed there in 1970. He was transferred to the Compressor Aerodynamics group in the Research Department in 1970 where he remained until enrolling in the Graduate School at Georgia Tech in the fall quarter of 1973.

John has been married since August 1, 1970 to Linda Susan (Norred) Caruthers and they have a son, Brian Everett Caruthers, born May 26, 1976. He also

has a brother, Robert Lester Caruthers of Atlanta, Georgia and a sister, Judith Ann Caruthers of New Orleans, Louisiana.